Universidade de Aveiro
2020

Elisa Alexandra Gonçalves Martins

Hidrogéis derivados de membrana coriónica humana como uma plataforma inovadora para cultura celular 3D

Hydrogels derived from human chorionic membrane as an innovative platform for 3D cell culture

Universidade de Aveiro
2020

Elisa Alexandra Gonçalves Martins

Hidrogéis derivados de membrana coriónica humana como uma plataforma inovadora para cultura celular 3D

Hydrogels derived from human chorionic membrane as an innovative platform for 3D cell culture

Dissertação apresentada à Universidade de Aveiro para cumprimento dos requisitos necessários à obtenção do grau de Mestre em Materiais e Dispositivos Biomédicos, realizada sob a orientação científica da Doutora Catarina de Almeida Custódio, Investigadora Júnior do Departamento de Química da Universidade de Aveiro.

o júri

presidente

Professora Doutora Maria Helena Figueira Vaz Fernandes
Professora Associada da Universidade de Aveiro

Doutor António José Braga Osório Gomes Salgado
Investigador Principal Com Agregação no ICVS-Instituto de Investigação em Ciências da Vida e Saúde da Universidade do Minho

Doutora Catarina de Almeida Custódio
Investigadora Júnior da Universidade de Aveiro

agradecimentos

Em primeiro lugar agradeço ao professor João Mano por me ter dado a oportunidade de fazer a dissertação neste grupo de investigação. Foi um gosto poder trabalhar nesta área tão fascinante.

Gostaria de fazer um agradecimento especial à minha orientadora, Dra Catarina Custódio por todas as vezes que o trabalho correu menos bem, me ter ajudado e motivado para que corresse o melhor possível. Agradeço também por se demonstrar sempre disponível.

Também quero deixar um sincero agradecimento aos restantes membros da "equipa de orientação" que não oficialmente também participou em parte nesse cargo: em especial à Inês Deus, que me ensinou e ajudou desde o primeiro dia, à Cátia Monteiro e à Sara Santos por todos os conselhos, disponibilidade e boa vontade em ajudar.

Um agradecimento aos restantes membros do COMPASS RG que também me ajudaram. Agradeço também aos colegas de tese pela partilha de experiências e por tornarem os dias mais divertidos.

Sem esquecer quem me acompanhou ao longo do percurso académico. Apesar de ultimamente já não convivermos tanto, obrigada por terem tornado o percurso da licenciatura ou mestrado mais especiais.

Por último, mas o mais importante, um agradecimento muito especial à minha família. Ao meu marido, Daniel por fazermos esta caminhada juntos, por estares sempre presente, por me apoiares e motivares a ultrapassar todos os momentos mais difíceis. Agradeço muito aos meus pais e irmãs, pois sem eles nada disto seria possível, obrigada por todo o apoio desde sempre, motivação e confiança.

Foi sem dúvida a etapa académica mais desafiante e enriquecedora do meu percurso universitário.

palavras-chave

Membrana coriónica, matriz extracelular, engenharia de tecidos cardíacos, tridimensional, hidrogel, placenta, medicina personalizada.

resumo

A medicina regenerativa e a engenharia de tecidos surgiram como alternativas às terapias atualmente usadas no tratamento e substituição de tecidos ou órgãos danificados, pois o corpo humano tem capacidade muito limitada de regeneração. Esta área combina a cultura de células em biomateriais com biomoléculas sinalizadoras. No tecido nativo, as células estão envolvidas por matriz extracelular (ECM) composta por diversas proteínas, glicosaminoglicanos e fatores solúveis. A ECM é muito importante na resposta celular, pois tem influência em processos com a migração, proliferação e diferenciação. Assim, tem sido feito um esforço para criar materiais que mimetizem essa função.

A placenta humana trata-se uma fonte de ECM virtualmente ilimitada, sem questões éticas associadas, imunoprivilegiada devido à falta de expressão de antigénios, possui elevada biocompatibilidade, propriedades imunossupressoras, anti-inflamatórias e regenerativas. Para além disso, está reportado na literatura o sucesso do uso de membranas fetais como aloenxerto e mais recentemente a membrana coriónica foi descrita como eficaz na regeneração periodontal. Para além do material base, também é importante a morfologia usada.

Os hidrogéis são uma classe única de materiais relativamente à capacidade de mimetizar a ECM. São redes poliméricas hidrofílicas 3D capazes de captar grandes quantidades de água, permitindo a fixação e migração celular, trocas de nutrientes, oxigénio e resíduos celulares. No entanto, a maioria dos hidrogéis produzidos a partir de ECM descelularizada, tem reduzidas propriedades mecânicas e pouca estabilidade *in vitro*. Assim, o objetivo deste trabalho é produzir, pelo que sabemos, pela primeira vez, hidrogéis derivados de membrana coriónica (CM) humana foto-reticuláveis com propriedades mecânicas ajustáveis, para a cultura de células 3D. Neste trabalho foram produzidos pré-polímeros de CM através da reação com metacrílico anidrido, com dois graus de modificação: um de menor grau (CMMA100) e outro com maior grau de modificação (CMMA250). Ao adicionar um fotoiniciador a estes pré-polímeros e na presença de luz com comprimento de onda específico é possível produzir hidrogéis. A quantificação de DNA permitiu verificar uma descelularização eficiente da CM, enquanto que as quantificações de algumas das mais importantes proteínas da ECM permitiram verificar a sua retenção no material obtido. A avaliação das propriedades mecânicas permitiu perceber que foi possível produzir hidrogéis robustos e cuja rigidez e capacidade de absorção de água são ajustáveis. Para além disso foi possível verificar que os hidrogéis permitem a cultura de células, que proliferaram e mantiveram-se viáveis por pelo menos 7 dias. Os resultados obtidos até agora sugerem que estes hidrogéis baseados em CMMA têm potencial para cultura de células 3D.

keywords

Chorionic membrane, extracellular matrix, cardiac tissue engineering, three-dimensional, hydrogel, placenta, personalized medicine.

abstract

Regenerative medicine and tissue engineering have emerged as alternatives to therapies currently used in the treatment and replacement of damaged tissues or organs, due to the very limited capacity of the human body to regenerate. This area combines the culture of cells in biomaterials and the presence of signals. In native tissue, cells are surrounded by an extracellular matrix (ECM) composed of several proteins, glycosaminoglycans and soluble factors. ECM is very important in the cellular response, as it influences processes such as migration, proliferation and differentiation. Thus, an effort has been made to create materials that mimic this function.

The human placenta is a virtually unlimited source of ECM, without associated ethical issues, immunoprivileged, biocompatible and capable of healing. In addition, the successful use of fetal membranes as an allograft has been reported in the literature and more recently the chorionic membrane has been described as effective in periodontal regeneration. In addition to the base material, the used morphology is also important.

Hydrogels are a unique class of materials in terms of their ability to mimic ECM. They are 3D hydrophilic polymeric networks capable of capturing large amounts of water, allowing cell fixation and migration, exchange of nutrients, oxygen and cellular waste. However, most hydrogels produced from decellularized ECM have low mechanical properties, since these must mimic the native tissue. Thus, the objective of this work is to produce, as far as we know, for the first time, hydrogels derived from photocrosslinkable human chorionic membrane (CM) with adjustable mechanical properties, for the 3D culture of cells. In this work, CM prepolymers were produced by the addition of methacrylic anhydride, with two degrees of modification: one with a lower degree (CMMA100) and another with a higher degree of modification (CMMA250). By adding a photoinitiator to these prepolymers and in the presence of light with a specific wavelength it is possible to produce hydrogels. Quantifications of some of the most important ECM proteins allowed to verify their retention in the obtained material. The evaluation of the mechanical properties allowed to realize that it was possible to produce robust hydrogels and whose mechanical properties and water absorption capacity vary with their concentration and which are in the range of most human tissue elastic modulus. Moreover, it was possible to verify that CMMA hydrogels allowed the culture of cells that proliferated and remained viable for at least 7 days. The results obtained so far suggest that these CMMA-based hydrogels have potential for 3D cell culture.

Contents

I. Background 2

Abstract 2

1. Tissue engineering (TE) 2
2. Biomaterial 3
3. Human perinatal tissues 4
4. Cell culture platforms 6
5. References 8

II. Extracellular matrix scaffolds for Cardiac Tissue Engineering 12

Abstract 12

1. Introduction 12
2. Cardiac tissue 14
3. Mechanisms of cardiac repair process 16
4. Scaffolds for Cardiac Tissue Engineering 17
5. 3D ECM-based structures for cardiac tissue engineering and regenerative medicine 19
   - 5.1. Decellularized whole organs 22
   - 5.2. Injectable Hydrogels 25
   - 5.3. Patches 30
     - 5.3.1. Decellularized tissue patches 31
     - 5.3.2. Smooth hydrogel patches 32
     - 5.3.3 Topographical hydrogel patches 33
       - 5.3.3.1. Microcontact printing 33
       - 5.3.3.2. 3D Bioprinting 34
6. ECM derived hydrogels in clinical trials 35
7. Typical cell sources for cardiac TERM 36
8. Conclusion and future perspectives 37
9. References 39

III. Materials and Methods 49

1. Placenta collection 49
2. Chorionic membrane (CM) isolation and decellularization 49

3. dCM solubilization 52
4. dCM proteins functionalization 54
5. Characterization of CMMA degree of modification 55
5.1. Proton nuclear magnetic resonance (^{1}H NMR) 55
5.2. TNBSA (2,4,6-Trinitrobenzene Sulfonic Acid) 55
6. Biochemical characterization of CMMA100 and CMMA250 56
6.1. Total protein quantification 56
6.2. Collagen quantification 56
6.3. Laminin quantification 57
6.4. Sulfated proteoglycans and glycosaminoglycans (GAGs) quantification 57
7. Preparation of CMMA hydrogels 58
8. Characterization of CMMA hydrogels 59
8.1. Mechanical properties 59
8.2. Water content 59
9. Cell culture and hydrogels biological response 60
9.1. Top seeding 60
9.2. Encapsulation 61
9.2.1. Cell viability analysis 61
9.2.2. Cell morphology analysis 61
10. Statistical analysis 62
11. References 63
IV. Chorionic membrane derived hydrogels as an innovative human based platform for 3D cell culture 67
Abstract 67
1. Introduction 68
2. Materials and methods 69
2.1. Placenta collection 69
2.2. Chorionic membrane (CM) isolation and decellularization 69
2.3. dCM solubilization 70
2.4. dCM proteins functionalization 71
2.5. Characterization of CMMA degree of modification 71
2.5.1. Proton nuclear magnetic resonance (^{1}H NMR) 71

2.5.2. TNBSA (2,4,6-Trinitrobenzene Sulfonic Acid) 71
2.6. Biochemical characterization of CMMA100 and CMMA250 72
2.6.1. Total protein quantification 72
2.6.2. Collagen quantification 72
2.6.3. Laminin quantification 72
2.6.4. Sulfated proteoglycans and glycosaminoglycans (GAGs) quantification 73
2.7. Preparation of CMMA hydrogels 73
2.8. Characterization of CMMA hydrogels 73
2.8.1. Mechanical properties 73
2.8.2. Water content 74
2.9. Cell culture and hydrogels biological response 74
2.9.1. Top seeding 75
2.9.2. Encapsulation 75
2.9.3. Cell viability analysis 75
2.9.4. Cell morphology analysis 75
2.10. Statistical analysis 76
3. Results and discussion 76
3.1. CM isolation, decellularization and solubilization 76
3.2. Characterization of CMMA degree of modification 78
3.3. Biochemical characterization of dCM and CMMA 80
3.3.1. Total protein quantification 81
3.3.2. Laminin quantification 81
3.3.3. Collagen quantification 81
3.3.4. Sulphated GAGs quantification 82
3.4. Preparation of CMMA hydrogels 82
3.4.1. Characterization of CMMA hydrogels: mechanical properties and water content 83
3.5. Cell culture and hydrogels biological response 85
4. Conclusions and future perspectives 87
5. References 88
V. Conclusion and Future Perspectives 92

List of Figures

Figure I.1. Schematic representation of the human placenta, highlighting the amniotic and chorionic membrane composition. 5

Figure II.1. The main cardiac cell types that provide contraction power, vascular stability, produce ECM and that potentiate inflammation and arteriogenesis..... 15

Figure II.2. Ischemic cascade that leads to myocardial scar production. At left is represented the homeostasis state and at the right, all the steps that occur after injury. The myocardium cross three different phases, each with different time consumption and the relative number of injured cells. Are highlighted the immunologic response, the fibroblast activity and it is also represented the myocardium aspect over time. Adapted from Forte et al [29]..... 17

Figure II.3. Rat heart decellularization through 1% SDS perfusion; A) During decellularization, the heart becomes completelly translucent where B) no intact cells or nuclei are visible in H&E staining of a thin section [40]. C) CaiT mapping of a recellularized heart. I) Asynchronized region, that re-synchronizes under electrical stimulation. II) Synchronized region. [41] 23

Figure II.4. Physical aspect of human AM during the processing. A) Fresh AM, before decellularization. B) Decellularized AM. C) Solubilized and lyophilized AM. D) Gelation of decellularized AM matrix at 37 °C. E) Representative images of Masson trichrome-stained rat heart sections of adult myocardial regeneration after MI at 5 weeks after AM matrix or PBS injection. Scale bars = 4 mm. F) Measurement of infarcted size at 5 weeks after AM matrix or PBS injection analyzed by Masson trichrome staining. n = 5 for each group, *p < 0.05. Adapted from Henry et al [53]..... 29

Figure II.5. A) Three dispensing modules used for cardiac tissue constructs printing; B) Basic motion program; C) String form; D) Progress of tissue over 4 weeks (left) and plotting of spontaneous beating based on bright-field video over the same time (right); E) Rapid increase in α-actinin positive cell area, cardiomyocyte perimeter and alignment of muscle fibers. Adapted from Wang *et al* [64]. 35

Figure II.6. Diagram of pluripotent stem cells sources, namely Embryonic Stem Cells (ESCs) and human induced Pluripotent Stem cells (iPSCs) that have self-renewal capacity and are able to differentiate in almost all cell types of the body. 37

Figure III.1. Schematic image of methods employed in this work. 53

Figure III.2 Schematic representation of the methacrylation reaction of dCM derived proteins. dCM proteins are dissolved in PBS and reacted with methacrylic anhydride at pH controlled to 8-9 producing methacrylate and methacrylamide groups. 54

Figure III.3 Scheme of CMMA hydrogel production when dCM derived proteins methacrylated (CMMA) are irradiated in the presence of a photoinitiator. 59

Figure IV.1.Steps from isolation until solubilization of CM. A) Whole placenta with fetal side faced upward. B) Chorionic membrane. The maternal side of the CM on the side of the arrow. C) CM cut into small pieces after removing clots and blood vessels. D) Decellularized CM (dCM). E) Solubilized dCM. 77

Figure IV.2: CM decellularization: A) Representative CM section stained with DAPI and B) Representative dCM section stained with DAPI. C) Quantification of double-stranded DNA per mg of dry CM or dCM. D) Quantification of total protein in CM or dCM. 78

Figure IV.3. A) dCM modification and CMMA synthesis. B) ^{1}H NMR spectra of dCM, CMMA100, and CMMA250: 1) double-bound methacrylate and methacrylamide; and 2) CH_3 of methacrylate and methacrylamide groups. 79

Figure IV.4: Biochemical characterization of processed CMMA from both modification degrees. A) Total protein quantification. B) Laminin quantification. C) Collagen quantification. D) Sulfated GAGs quantification. 80

Figure IV.5. Hydrogels of CMMA. A) Low modification degree hydrogel with concentration of 1% (w/v) and B) Low modification degree hydrogel with concentration of 2% (w/v). High modification degree hydrogels with concentration of C) 0.25% (w/v), D) 0.5% (w/v), E) 1% (w/v) and F) 2% (w/v). Scale bar: 5 mm. 83

Figure IV.6. A) Representative compressive stress-strain curves, B) Young's modulus, C) ultimate strain, D) ultimate stress and E) water content obtained for CMMA100 and CMMA250 hydrogels. 84

Figure IV.7. Top seeding of hBM-MSCs in CMMA100 hydrogels with 0.25% (w/v), 0.5% (w/v) and 1% (w/v) of concentration: A) Live-dead staining at 24 hours, 3 and 7 days of culture. B) DAPI / Phalloidin staining at 7 days. 85

Figure IV.8. Top seeding of hBM-MSCs in 0.25% (w/v), 0.5% (w/v) and 1% (w/v) CMMA250 hydrogels: A) Live-dead staining at 24 hours, 3 and 7 days of culture. B) DAPI / Phalloidin staining at 7 days. 86

Figure IV.9. Encapsulation of hBM-MSCs in CMMA100 hydrogels with 0.25% (w/v) and 0.5% (w/v) of concentration: A) Live-dead staining at 24 hours, 3 and 7 days of culture. B) DAPI / Phalloidin staining at 7 days. 86

List of Tables

Table II-1. 3D ECM-based biomaterials explored as capable of enhancing cardiac regeneration. 20

List of Abbreviations

2D	Two-Dimensional
3D	Three-Dimensional
α-MEM	Minimum Essential Medium Alpha
AM	Amniotic Membrane
CM	Chorionic Membrane
CMMA	Decellularized Chorionic Membrane Methacrylate
CMMA100	Decellularized Chorionic Membrane Methacrylate (low-degree of methacrylation)
CMMA250	Decellularized Chorionic Membrane Methacrylate (high-degree of methacrylation)
D_2O	Deuterium Oxide
DAMPs	Damage-Associated Molecular Patterns
DAPI	4',6'-diamino-2-fenil-indol
dCM	Decellularized Chorionic Membrane
DPBS	Dulbecco's Phosphate Buffered Saline without calcium or magnesium
dsDNA	double-stranded DNA
ECM	Extracellular matrix
ESCs	Embryonic Stem Cells
GAGs	Glycosaminoglycans
GFs	Growth Factors
HA	Hyaluronic Acid
hASCs	Human-derived Adipose Stem Cells
hCPC	Human Cardiac Progenitor Cells
hiPSCs	Human Induced Pluripotent Stem Cells
hiPSC-CMs	Human Induced Pluripotent Stem Cells - Derived Cardiomyocytes
hMSCs	Human bone marrow-derived Mesenchymal Stem Cells
HUVECs	Human Umbilical Vein Endothelial Cells

IHD	Ischemic Heart Disease
LAP	Lithium phenyl-2,4,6-trimethylbenzoylphosphinate
MA	Methacrylic Anhydride
MI	Myocardial Infarction
MMPs	Matrix Metalloproteinases
MSCs	Mesenchymal Stem Cells
PBS	Phosphate Buffered Saline
PRP	Platelet-Rich Plasma
RGD	Arginine-Glycine-Aspartate
ROS	Reactive Oxygen Species
RT	Room Temperature
SDS	Sodium Dodecyl Sulfate
TE	Tissue Engineering
TERM	Tissue Engineering and Regenerative Medicine
TIMPs	Tissue Inhibitors of Metalloproteinases
TNBSA	2,4,6-Trinitrobenzene Sulfonic Acid
Tris-HCl	Trizma® hydrochloride
WHO	World Health Organization

Chapter I

Background

Background

Abstract

The increase in average life expectancy over the past century has increased by over 30 years in developed countries on account of improvement in medical care, sanitation, and lifestyle. However, associated with this, arises the growing need of therapies for patients with injuries, end-stage organ failure, or other clinical problems. Tissue Engineering and Regenerative Medicine (TERM) has emerged to address these problems by engineering biological substitutes to replace or regenerate diseased and injured tissues. In TERM, biomaterials provide mechanical support and biochemical signals for cell attachment, growth and modulate cell behavior. *In vivo*, cells reside within the extracellular matrix (ECM). Thus, ECM derived scaffolds should provide superior biocompatibility and biofunctionality.

Minimally manipulated human perinatal tissues have been used for more than a century as allogeneic biomaterials and have been clinically successful. Hence, its use as three-dimensional (3D) platforms with complex geometries for TERM applications is under investigation. Considering the human source of perinatal tissues and the possibility of including the patient's own cells, these humanized micro-tissues become possible personalized platforms for either tissue regeneration or drug screening. The aim of this master dissertation is to produce a robust hydrogel based on chorionic membrane ECM, that retains bioactivity of the original tissue. As a proof of concept, these hydrogels will be used for cardiac tissue engineering (TE).

1. Tissue engineering (TE)

TE emerged due to the limited innate capacity for self-regeneration of human tissues, the low organ donor availability and organ transplant rejection[1]. Regenerative medicine may be divided in three main strands: (i) cell therapies in which cells are injected or placed in the local to repair, (ii) gene therapies, in which the expression of a gene from a person is modified or manipulated or, by other side, alter the biological properties of living cells for therapeutic use, and (iii) tissue engineering [2,3]. TE aims to create tissue-like structures combining cells, biomaterials and signals namely biochemical (e.g., growth factors (GFs), drugs, oligonucleotides) and physical (e.g., cyclic mechanical loading) factors. Beyond the objective of repair an injury or replace the function of a failing organ, TE also has the

objective to produce specialized extracorporeal life support systems containing cells (e.g., bioartificial liver and kidney), likewise microtissues for drug screening and toxicology or as basic studies on tissue development and morphogenesis, contributing to the reduction of the need of animal models [4].

2. Biomaterial

All tissues and organs contain a mixture of cells and non-cellular components, which form well-organized networks called extracellular matrix (ECM). ECM is produced by the living cells and secreted into the surrounding medium. Beyond ECM has a structural function for cells, also regulate many cellular processes including growth, migration, differentiation, survival, homeostasis, and morphogenesis [5,6]. Thus, being an essential component in tissues and organs, the TE research aims to develop a material whose function is to mimic ECM.

A biomaterial is a biocompatible material that interfaces and interacts with biological systems and is capable to heal, enlarge, or substitute any tissue, organ or function of the body [7,8]. A biomaterial must respect some directives as for instance: (i) do not cause any inflammatory or toxic effect after implantation; (ii) its degradation rate should match the neo tissue formation; (iii) the material should have adequate mechanical properties for the purpose application and the change in mechanical properties with degradation should be compatible with the neo tissue formation; (iv) the byproducts originated from the degradation should be non-toxic, and capable to get metabolized and eliminated from the body [8]. Hence, a biomimetic biomaterial for TE is a scaffolding material that mimics one or multiple characteristics of the natural ECM [9].

A biomaterial may be classified according to its origin, being synthetic or natural. Each one has advantages and disadvantages. For instance, synthetic polymers ensure the off the-shelf availability, have high batch-to-batch consistency, have more predictable and reproducible mechanical and physical properties (e.g., tensile strength, elastic modulus, and degradation rate), and they can be manufactured with great precision. However, they are not recognized by the cells, eliciting persistent inflammatory reactions. In addition, they are unable to integrate the host tissues, being eroded [10,11]. In contrast, natural based materials, are produced by biological systems, as for instance, microorganisms, plants, and animals. Natural polymers are bioactive having specific protein binding sites and other biochemical signals that may allow cell attachment and cell-cell communication, having a higher

propensity for tissue regeneration. Moreover, their production cost is typically lower than synthetic polymers. However, they also have limitations as being generally structurally weaker, having batch-to-batch variability, being difficult control over degradation rates due to difference in host enzyme levels and also an immunogenicity issue related to allogenic or xenogeneic, where antigens such as DNA, α-Gal epitopes and damage-associated molecular pattern (DAMP) molecules are presented [10,12–14]. In this context, decellularized human derived ECM and components from ECM are promising biomaterials for TE, since they are found in native human tissue, provide ideal cues for regeneration, repair, and remodelling tissue [15]. Human allogenic decellularized tissues would be the ideal source of ECM, since xenogeneic may contain residual contamination and immunogenicity [16].

3. Human perinatal tissues

Perinatal tissues are temporary organs that forms during pregnancy to ensure fetus nourishment and development as well as prevent immune rejection. According to this biological function, ECM and cells isolated from perinatal tissues have demonstrated to retain important therapeutic properties, which mostly result from anti-microbial, anti-inflammatory and immunomodulatory activities of resident cells. Besides, as a medical waste these tissues can be readily use in clinical and commercial settings as safe and cost-effective solutions to current TERM strategies [17]. Moreover, fetal membranes are immune-privileged due to a lack of expression of antigens, have good biocompatibility, immunosuppressive and anti-inflammatory properties and healing capacity [19]. Finally, its basement membrane composed mainly by diverse types of collagen, fibronectin and laminin, GFs and proteases that also constitutes ECM from other human tissues [18,19].

The fetal membranes from placenta act as an interface between the fetus and mother during pregnancy and are comprised of two components: the amniotic membrane (AM) and chorionic membrane (CM) [18]. The AM is an avascular tissue that is most proximal to the fetus, while the CM is vascularized, surrounds the AM and firmly attach the maternal tissue, as represented in **Figure I.1**.

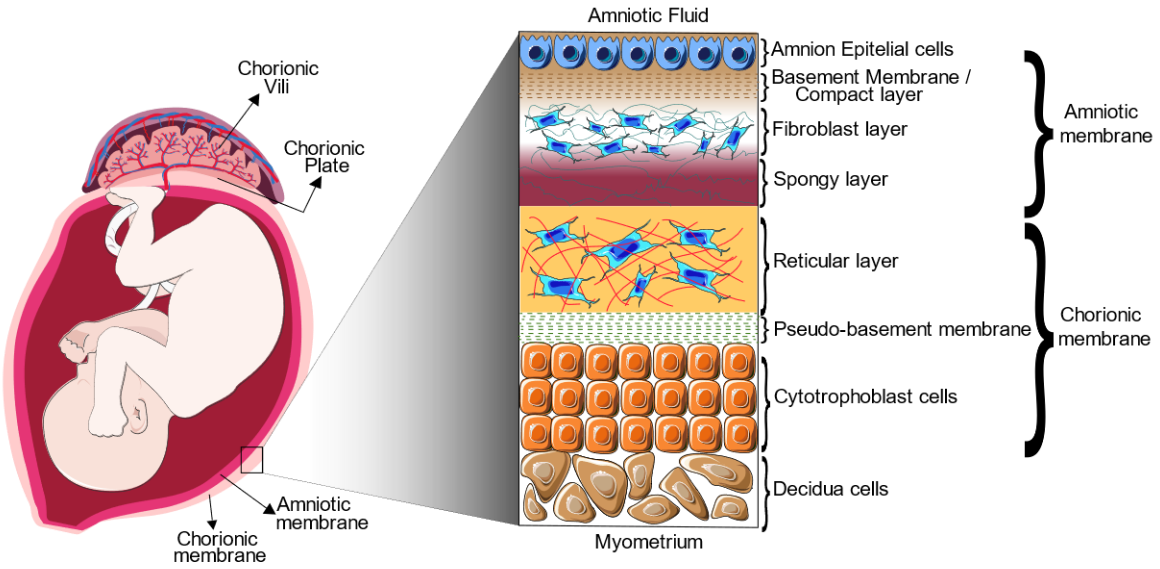

Figure I.1. Schematic representation of the human placenta, highlighting the amniotic and chorionic membrane composition.

CM adds mechanical strength to the fetal membranes, acting as a point in which the chorionic villi emerge, whose function is to carry nutrients from the maternal circulation and acts both as a physical and biomolecular barrier [20,21]. The use of AM in TE was first reported in 1910 in skin transplantation [22]. Since then, fetal membranes have been used in wound healing (e.g., burns, ulcers), in ocular, tendon and cartilage applications, otolaryngology (mucosa), periodontics, urology (e.g., bladder reconstruction), gynaecology and as a source of small diameter vessels [20,23].

Hydrogels prepared by a straightforward process of placenta decellularization followed by an enzymatic treatment and jellification at 37 °C have also proved its efficacy in treating cardiac ischemia damage in animal models [24]. Khorramirouz *et al* demonstrated the ability of decellularized AM to support stem cell differentiation into cardiomyocytes when applied as a cardiac patch for the treatment of acute myocardial infarction in rat models [25]. This study further confirmed the potential of AM-based scaffolds as support and delivery matrices for cardiac neovascularization and regeneration.

Despite the use of AM alone and conjugated with CM have been widely explored, the use of chorionic membrane alone, was much less explored. CM has been used for tooth root coverage for example due to periodontitis, as well as for enhancement of gingival demonstrating good results in terms of regeneration when applied in clinical trials [26–29]. Furthermore, previous studies that used extracts containing both AM and CM had suggested

potential ability on osteogenic differentiation of osteoblasts but was unknown which of them has more influence. To better understand which have more influence on osteogenic differentiation, Go Yoon *et al* compared CM with AM extracts and verified that CM was more effective in promoting osteogenesis [30]. In another study, decellularized CM scaffold was successfully reseeded with MSCs and induced to differentiate osteogenically [31].

In fact, has been reported that human CM has more GFs and cytokines than those present on an equal surface area of AM [30,32]. The GFs that stand out are fibroblast growth factor (FGF), endocrine gland-derived vascular endothelial growth factor (EG-VEGF), hepatocyte growth factor (HGF), insulin-like growth factor-1 (IGF-1), platelet-derived growth factor-AA and -BB (PDGF-AA and BB) and finally, tissue inhibitor of metalloproteinase (TIMP)-2 and -4 [32]. Such cytokines and GFs are immunomodulating and tissue-regenerating factors, responsible for cellular processes as migration, proliferation, differentiation and vascularization accelerating tissue repair and regeneration [32,33]. Furthermore, CM has higher antibacterial effects and higher adiponectin levels, which is a peptide with direct actions in liver, skeletal muscle, and the vasculature [32,34]. Finally, the CM multiple layers of cytotrophoblast cells contain stem cell markers, cluster of differentiation (CD) CD_{34} and CD_{45}, accentuating its hematopoietic potential, while they are not present in the AM [32,35].

Despite the CM potential for TE, the most bank tissues in the world discard it, processing only AM since it is a proven biological wound dressing, being CM quite unexplored. Taking into account the aforementioned advantages, CM is an interesting biomaterial from human origin to be explored in TE.

4. Cell culture platforms

Traditional 2D cell culture platforms have been proved to be very ineffective in mimicking the *in vivo* environment. Alternatively, 3D cell culture platforms mimic more closely the real *in vivo* microenvironment. Cells cultured in 3D platforms acquire their natural shape, interact and behave according to the mechanical cues from the surrounding environment, differentiate and have gene and protein expression levels that resemble levels found from cells *in vivo*. Moreover, they have lower drug sensitivity, approximating more to animal models [36].

These 3D cell culture platforms or scaffolds are usually highly porous with interconnected pore networks that allow nutrient and oxygen diffusion and waste removal [37]. In fact, the hydrogels are an example of 3D scaffolds. Are polymeric structures held

cohesive by: i) primary covalent crosslinks, ii) ionic forces, iii) hydrogen bonds, iv) affinity or "bio-recognition" interactions, v) hydrophobic interactions, vi) polymer crystallites, vii) physical entanglements of individual polymer chains or viii) a combination of two or more of the aforementioned interactions [38]. This is a very important and unique class of materials relative to their capacity to mimic the ECM due to their hydrophilicity and ability to uptake large amounts of water or biological fluids. They have structural similarity to the macromolecular-based components in the body, allowing cell attachment and migration, delivering and retaining cells and biochemical factors. Moreover, their interconnected pore network allows diffusion of nutrients, metabolites and wastes and their mechanical properties influence cell morphology and behaves, including proliferation and differentiation [39, 40].

In this sense, a main goal of this work is to develop a hydrogel based on CM proteins that could be used for cardiac TE.

This master dissertation is divided into the following chapters:

- Chapter 1: Background, where the contextualization and the goal of this thesis is described.
- Chapter 2: Extracellular matrix scaffolds for Cardiac Tissue Engineering, where is provided an overview of the strategies developed for cardiac tissue engineering involving decellularized tissues or components from extracellular matrix and cells.
- Chapter 3: Materials and methods.
- Chapter 4: Chorionic membrane derived hydrogels as an innovative human based platform for 3D cell culture.
- Chapter 5: Final overview, concluding remarks and future perspectives.

5. References

(1) Mhanna, R.; Hasan, A. Introduction to Tissue Engineering. In Tissue Engineering for Artificial Organs: Regenerative Medicine, Smart Diagnostics and Personalized Medicine; Wiley Online Library, 2017; Vol. 1, pp 1–34.

(2) Mertz, L. Tissue Engineering and Regenerative Medicine: The Promise, the Challenges, the Future. IEEE Pulse 2017, 8 (3), 15–18.

(3) Yong, C.; Kaplan, D. S.; Gray, A.; Ricles, L.; Kwilas, A.; Brubaker, S.; Arcidiacono, J.; Xu, L.; Chang, C.; Robinson, R.; et al. Overview of the US Food and Drug Administration Regulatory Process. In Principles of Regenerative Medicine; Elsevier, 2019; pp 1345–1365.

(4) Berthiaume, F.; Maguire, T. J.; Yarmush, M. L. Tissue Engineering and Regenerative Medicine: History, Progress, and Challenges. Annu. Rev. Chem. Biomol. Eng. 2011, 2, 403–430.

(5) Theocharis, A. D.; Skandalis, S. S.; Gialeli, C.; Karamanos, N. K. Extracellular Matrix Structure. Adv. Drug Deliv. Rev. 2016, 97, 4–27.

(6) Yi, S.; Ding, F.; Gong, L.; Gu, X. Extracellular Matrix Scaffolds for Tissue Engineering and Regenerative Medicine. Curr. Stem Cell Res. Ther. 2017, 12 (3), 233–246.

(7) Ng, I. C.; Pawijit, P.; Tan, J.; Yu, H. Anatomy and Physiology for Biomaterials Research and Development. In Encyclopedia of Biomedical Engineering; Elsevier, 2019; pp 225–236.

(8) Nair, L. S.; Laurencin, C. T. Biodegradable Polymers as Biomaterials. Prog. Polym. Sci. 2007, 32 (8–9), 762–798.

(9) Ma, P. X. Biomimetic Materials for Tissue Engineering. Adv. Drug Deliv. Rev. 2008, 60 (2), 184–198.

(10) Sarkar, K.; Xue, Y.; Sant, S. Host Response to Synthetic versus Natural Biomaterials. In The Immune Response to Implanted Materials and Devices; Springer, 2017; pp 81–105.

(11) Chen, Q.-Z.; Harding, S. E.; Ali, N. N.; Lyon, A. R.; Boccaccini, A. R. Biomaterials in Cardiac Tissue Engineering: Ten Years of Research Survey. Mater. Sci. Eng. R Reports 2008, 59 (1–6), 1–37.

(12) Hinderer, S.; Layland, S. L.; Schenke-Layland, K. ECM and ECM-like Materials - Biomaterials for Applications in Regenerative Medicine and Cancer Therapy. Adv. Drug Deliv. Rev. 2016, 97, 260–269. https://doi.org/10.1016/j.addr.2015.11.019.

(13) He, W.; Feng, Y.; Ma, Z.; Ramakrishna, S. Polymers for Tissue Engineering. In Polymers for Biomedical Applications; ACS Publications, 2008; pp 310–335.

(14) Kaushik, K.; Sharma, R. B.; Agarwal, S. Natural Polymers and Their Applications. Int. J. Pharm. Sci. Rev. Res. 2016, 37 (2), 30–36.

(15) Bejleri, D.; Davis, M. E. Decellularized Extracellular Matrix Materials for Cardiac Repair and Regeneration. Adv. Healthc. Mater. 2019, 8 (5), 1–29. https://doi.org/10.1002/adhm.201801217.

(16) Kabirian, F.; Mozafari, M. Decellularized ECM-Derived Bioinks: Prospects for the Future. Methods 2020, 171, 108–118.

(17) Deus, I. A.; Mano, J. F.; Custódio, C. A. Perinatal Tissues and Cells in Tissue Engineering and Regenerative Medicine. Acta Biomater. 2020, 110, 1–14.

(18) Gupta, A.; Kedige, S. D.; Jain, K. Amnion and Chorion Membranes: Potential Stem Cell Reservoir with Wide Applications in Periodontics. Int. J. Biomater. 2015, 2015, 1–9. https://doi.org/10.1155/2015/274082.

(19) Lockhart, M.; Wirrig, E.; Phelps, A.; Wessels, A. Extracellular Matrix and Heart Development. Birth Defects Res. Part A - Clin. Mol. Teratol. 2011, 91 (6), 535–550. https://doi.org/10.1002/bdra.20810.

(20) Moore, M. C.; Van De Walle, A.; Chang, J.; Juran, C.; McFetridge, P. S. Human Perinatal-Derived Biomaterials. Adv. Healthc. Mater. 2017, 1700345, 1–12. https://doi.org/10.1002/adhm.201700345.

(21) Shakouri-Motlagh, A.; Khanabdali, R.; Heath, D. E.; Kalionis, B. The Application of Decellularized Human Term Fetal Membranes in Tissue Engineering and Regenerative Medicine (TERM). Placenta 2017, 59, 124–130. https://doi.org/10.1016/j.placenta.2017.07.002.

(22) SABKLLA, N. Use of the Fetal Membranes in Skin Grafting. Med. Rec. 1913, 83 (11), 478.

(23) Schneider, K. H.; Enayati, M.; Grasl, C.; Walter, I.; Budinsky, L.; Zebic, G.; Kaun, C.; Wagner, A.; Kratochwill, K.; Redl, H.; et al. Acellular Vascular Matrix Grafts from Human Placenta Chorion: Impact of ECM Preservation on Graft Characteristics, Protein Composition and *in vivo* Performance. Biomaterials 2018, 177, 14–26. https://doi.org/10.1016/j.biomaterials.2018.05.045.

(24) Francis, M. P.; Breathwaite, E.; Bulysheva, A. A.; Varghese, F.; Rodriguez, R. U.; Dutta, S.; Semenov, I.; Ogle, R.; Huber, A.; Tichy, A.; et al. Human Placenta Hydrogel Reduces Scarring in a Rat Model of Cardiac Ischemia and Enhances Cardiomyocyte and Stem Cell Cultures. Acta Biomater. 2017, 52, 92–104. https://doi.org/10.1016/j.actbio.2016.12.027.

(25) Khorramirouz, R.; Kameli, S. M.; Fendereski, K.; Daryabari, S. S.; Kajbafzadeh, A.-M. Evaluating the Efficacy of Tissue-Engineered Human Amniotic Membrane in the Treatment of Myocardial Infarction. Regen. Med. 2019, 14 (2), 113–126.

(26) Suresh, D. K.; Gupta, A. Gingival Biotype Enhancement and Root Coverage Using Human Placental Chorion Membrane. Clin. Adv. Periodontics 2013, 3 (4), 237–242.

(27) Kothiwale, S. V. The Evaluation of Chorionic Membrane in Guided Tissue Regeneration for Periodontal Pocket Therapy: A Clinical and Radiographic Study. Cell Tissue Bank. 2014, 15 (1), 145–152.

(28) Esteves, J.; Bhat, K. M.; Thomas, B.; Varghese, J. M.; Jadhav, T. Efficacy of Human Chorion Membrane Allograft for Recession Coverage: A Case Series. J. Periodontol. 2015, 86 (8), 941–944.

(29) Hills, D. Evaluation of Demineralized Freeze-Dried Bone Allograft in Combination with Chorion Membrane in the Treatment of Grade II Furcation Defects: A Randomized Controlled Trial. Int. J. Periodontics Restor. Dent. 2019, 39, 659–667.

(30) Go, Y. Y.; Kim, S. E.; Cho, G. J.; Chae, S.-W.; Song, J.-J. Differential Effects of Amnion and Chorion Membrane Extracts on Osteoblast-like Cells Due to the Different Growth Factor Composition of the Extracts. PLoS One 2017, 12 (8), e0182716–e0182716.

(31) Mohr, S.; Portmann-Lanz, C. B.; Schoeberlein, A.; Sager, R.; Surbek, D. V. Generation of an Osteogenic Graft from Human Placenta and Placenta-Derived Mesenchymal Stem Cells. Reprod. Sci. 2010, 17 (11), 1006–1015.

(32) D'Lima, C.; Samant, U.; Gajiwala, A. L.; Puri, A. Human Chorionic Membrane: A Novel and Efficient Alternative to Conventional Collagen Membrane. Trends Biomater. Artif. Organs 2020, 34 (1), 33–37.

(33) Smagul, S.; Kim, Y.; Smagulova, A.; Raziyeva, K.; Nurkesh, A.; Saparov, A. Biomaterials Loaded with Growth Factors / Cytokines and Stem Cells for Cardiac Tissue Regeneration. Int. J. Mol. Sci. 2020, 21 (17), 5952–5972.

(34) Achari, A. E.; Jain, S. K. Adiponectin, a Therapeutic Target for Obesity, Diabetes, and Endothelial Dysfunction. J. Tissue Eng. Regen. Med. 2017, 13 (11), 2055–2066. https://doi.org/10.3390/ijms18061321.

(35) Wassmer, C. H.; Berishvili, E. Immunomodulatory Properties of Amniotic Membrane Derivatives and Their Potential in Regenerative Medicine. Curr. Diab. Rep. 2020, 20 (8), 31–41.

(36) Jensen, C.; Teng, Y. Is It Time to Start Transitioning From 2D to 3D Cell Culture? Front. Mol. Biosci. 2020, 7 (33), 1–15.

(37) Loh, Q. L.; Choong, C. Three-Dimensional Scaffolds for Tissue Engineering Applications: Role of Porosity and Pore Size. Tissue Eng. Part B Rev. 2013, 19 (6), 485–502.

(38) Peppas, N. A.; Hoffman, A. S. Hydrogels. In Biomaterials science; Elsevier, 2020; pp 153–166.

(39) Ferreira, P.; Coelho, J. F. J.; Almeida, J. F.; Gil, M. H. Photocrosslinkable Polymers for Biomedical Applications. Biomed. Eng. Challenges 2011, 1, 55–74.

(40) Naahidi, S.; Jafari, M.; Logan, M.; Wang, Y.; Yuan, Y.; Bae, H.; Dixon, B.; Chen, P. Biocompatibility of Hydrogel-Based Scaffolds for Tissue Engineering Applications. Biotechnol. Adv. 2017, 35 (5), 530–544.

Chapter II*

Extracellular matrix scaffolds for Cardiac Tissue Engineering

*This chapter is based on the following publication:

Martins E et al. “Extracellular matrix scaffolds for Cardiac Tissue Engineering” (manuscript under preparation)

Extracellular matrix scaffolds for Cardiac Tissue Engineering

Abstract

Ischemic heart disease is the first leading cause of death worldwide, according to the World Health Organization (WHO). After ischemia, heart experiences a healing process for months, called ischemic cascade in which is deposited a fibrotic tissue with low conductivity and elasticity properties. Consequently, spontaneous contraction is blocked and cell infiltration on that region is ceased. As conventional treatments are often not efficient, the search for other alternatives is a reality. Tissue engineering and Regenerative Medicine (TERM) has emerged as an alternative to produce structures that potentiate cardiac regeneration or structures that allow studying the mechanisms and evolution of diseases and drug screening. Tissue engineering (TE) strategies typically combine biomaterials, cells and bioactive molecules to provide an adequate environment for cell adhesion and growth. Due to the fundamental function of extracellular matrix (ECM) to maintain adequate cardiac integrity and pump function, the poor representativeness of 2D models and the physiological differences of animal models arose a growing interest in producing 3D structures for TE based on decellularized-ECM or ECM compounds. This review focuses on these 3D structures, highlighting electrical and mechanical properties and, when applicable, cell attachment and alignment.

1. Introduction

Ischemic heart disease (IHD) is the leading cause of death worldwide, according to the World Health Organization (WHO) [1]. It is mainly provoked due to atherosclerosis, which is the gradually and progressively narrowing of the coronary arteries, due to the obstruction of the coronary lumen by build-up of fatty material or by blood clot (thrombus) formation resultantly from acute plaque rupture. This obstruction leads to insufficient heart blood flow thus limiting the supplying of nutrients and oxygen to the cardiomyocytes from the ventricular wall. In acute events of total coronary artery obstruction, heart muscle tissue death occurs and ultimately may lead to patient death [2,3]. The pharmacological therapies to prevent and/or treat heart diseases may be divided into antiplatelet and antithrombotic drugs, β-blockers and statins for IHD stabilization. Alternatively, on percutaneous coronary intervention also called coronary angioplasty, the occlusion is mechanically expanded (e.g.,

with a stent) to restore blood flow. Furthermore, in more urgent cases, as for instance after heart stop, a coronary artery bypass graft must be performed. This is a highly invasive surgery which implies to open the heart and to do a vein graft [3–5]. Moreover, after MI, patients may suffer of heart failure which, in the most advanced form, the end-stage heart failure, only have two possible treatments: i) the use of ventricular assist devices and ii) heart transplantation [6]. Despite the success of these strategies in saving and improving the quality of life of some patients, they do not address the underlying cause of the disease and do not replace the tissue function that is lost. Furthermore, the low donor availability, limit the number of transplants. Hence, there is a need for new therapies that stimulate better healing postinjury for a more functional cardiac repair [7].

Even though the human heart has the capacity to regenerate cardiomyocytes, this process is extremely slow. Hence, following a heart attack or other ischemic cardiac event, damaged cardiac tissue usually turns into non-functional connective (or scar) tissue. In the past decade, cardiac TERM has evolved as a promising and actively developing area of research that aims to repair, replace, and regenerate the myocardium [8]. Cell-based strategies have shown potential to decrease scar formation and enhance heart contractility. However, as therapeutic cells are mostly delivered by direct injection, the retention and engraftment of cells is generally low and thus persistent obstacles to successful myocardial regeneration [9].

Currently, therapeutic drug discovery and screening are mainly tested *in vitro* in two-dimensional (2D) models of cellular assays and *in vivo* on animal models [10]. However, 2D tissue culture models fail in recapitulate the complexity of *in vivo* tissues. Furthermore, drug diffusion kinetics and drug doses from 2D models are not representatively once they are unable to precisely recapitulate the complex cell-cell, cell-ECM and tissue-level interactions [10,11]. Animal models are the gold standard for drug and biomaterials testing due to their tissue-level representation. Nevertheless, the relevance of the obtained results due to the physiological differences and other unpredictable characteristics is questionable. In addition, they have associated high costs and ethical concerns [10–13]. Instead, three-dimensional (3D) *in vitro* culture environments offer the possibility to be precisely positioned to recapitulate the native tissue architecture, cellular composition and vasculature to mimic disease mechanisms, screening drugs and investigate the regeneration potential of biomaterials in (TE) [13].

Cardiac tissue is composed of different cells aligned in a specific order, embedded in the ECM and is exposed to biochemical, mechanical, electrical and other stimuli, in order to contract to pump blood in a synchronized rhythm [14]. Moreover, ECM has a role in modulate biological activities including cell proliferation, maturation, migration, and differentiation [15]. In this context, 3D cardiac scaffold-based structures composed by ECM or ECM components have been widely explored in TERM strategies. The efficacy of scaffold-based therapies is related to the capacity of the material to recapitulate healthy or diseased tissue for drug development and study physiological processes [16]. Additionally, scaffold-based strategies offer several advantages in tissue regeneration therapies [17,18].

Recent works have suggested that direct injection of biomaterials, such as alginate, fibrin or chitosan, into the heart, could act as a stabilizer to internally the infarcted area [19]. In this context, phase II clinical trials were already performed constrain to test the feasibility of intracoronary delivery of an injectable alginate scaffold, to prevent ventricular remodeling and congestive heart failure after myocardial infarction (MI) [20]. Despite the promising outcomes, the results suggest that the injection of the alginate hydrogel in patients with large MI did not significantly reduces adverse left ventricular remodeling. This limitation may have explanation in the limited bioactivity of the injected materials.

In this context, bioactive materials, namely decellularized ECM, components from ECM and human proteins, appear as promising materials for repairing tissue and for developing cardiovascular disease models. Once they are found in native tissue, such materials provide ideal cues for regeneration, repair, and tissue remodeling [16]. This review focuses on 3D *in vitro* cardiac structures based on decellularized-ECM, ECM compounds and proteins for cardiovascular TERM and drug screening, highlighting their physiological properties. Moreover, cardiac tissue organization and structure will be discussed.

2. Cardiac tissue

ECM was already seen as an inert scaffold, whose function was just supporting cells embedded in its environment. Nowadays, it is acknowledged that ECM is a signal transducer for cell-cell communication modulating cell motility, differentiation and cell proliferation [21,22]. In cardiac tissue, it has a role in distributing mechanical forces throughout the organ since it is responsible for myocyte alignment. Furthermore, cardiac ECM regulates blood flow during contraction and is responsible for compliance and maintenance of appropriate

tissue tensile modulus. Hence, ECM is fundamental to keep suitable cardiac integrity and pump function [22].

At the cellular level, the main components present are cardiomyocytes, fibroblasts, blood and lymphatic endothelial cells, vascular smooth muscle cells and pericytes (**Figure II.1**). Cardiomyocytes can be divided into pacemaker cells and force-producing cells and are considered the foremost cardiac cells due to their role in pump function to maintain the blood circulation. Vascular endothelial cells beyond having a structural role in the interior surfaces of blood vessels, also are metabolically active, control vasomotor tone, and regulate angiogenesis. Whereas fibroblasts are connective tissue cells that synthesize constituents of the ECM, vascular smooth muscle cells and pericytes control blood flow in the cardiac vasculature [23].

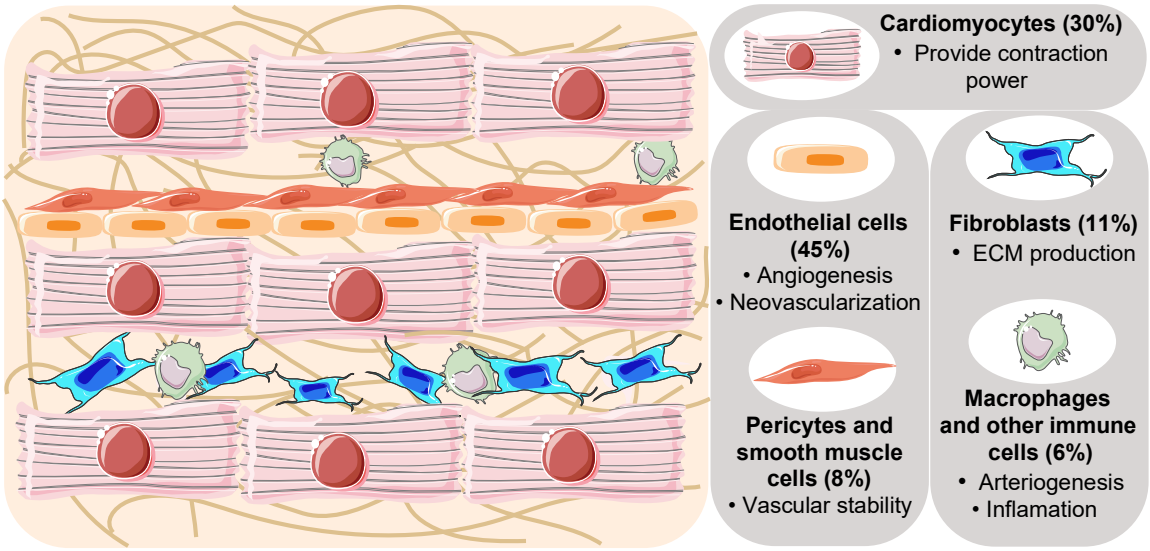

Figure II.1. The main cardiac cell types that provide contraction power, vascular stability, produce ECM and that potentiate inflammation and arteriogenesis.

At the molecular level, ECM is composed of proteoglycans, glycoproteins such as laminin, collagens, fibronectin, fibrillin and nidogen and yet proteases. Proteoglycans are composed by one of the four glycosaminoglycans (GAGs): (i) hyaluronic acid (HA), (ii) chondroitin sulphate/dermatan sulphate, (iii) heparan sulphate/heparin, and (iv) keratin sulphate linked to a protein core as for instance agrecan, versican and perlecan [16,21]. Relatively to the major component of cardiac ECM, the collagen, stands out the collagens I, III, V and VI that are present on ventricular myocardium. Fibrillar collagens I, III and V promote stiffness, elasticity and integrity respectively. Collagen type V maintains integrity

because is responsible for fibrillation of types I and III collagen. Collagen VI is a network-forming, which is thought to be necessary to provide tensile strength to the surrounding tissue. Finally, collagens XV and XVIII are nonfibrillar collagens. While collagen XV is expressed in the basal membranes and capillaries of the myocardium, collagen XI is believed to be involved in regulating the initiation and assembly of collagen fibrils. Fibronectin mediates cellular behavior interacting with multiple integrins, heparan sulphate proteoglycans, collagens, and fibrins. Fibrillin forms microfibrils along with other ECM molecules such as elastin due to its elastic properties [21,24]. ECM proteases have the function of preserve homeostasis with a tight balance between matrix metalloproteinases (MMPs) and tissue inhibitors of metalloproteinases (TIMPs), in order to regulate ECM remodeling, being the overexpression of MMP related to cardiovascular diseases [22,24].

3. Mechanisms of cardiac repair process

Diseased tissue, for example after ischemia, experiences a healing process, called ischemic cascade consisting by diverse phases such as an early inflammatory phase, a proliferative phase and at the end, a maturation phase, involving responses at molecular, cellular, and physiological levels (**Figure II.2**). The inflammatory phase is started due to signals released passively from damaged ECM and necrotic or stressed cells, for instance, damage-associated molecular patterns (DAMPs) and inflammatory cytokines (e.g., interleukin (IL)-1α and IL-33). Tissue-resident macrophages are activated and recruit neutrophils that release pro-inflammatory cytokines (e.g., tumor necrosis factor (TNF)-α, interleukin (IL)-1β and IL-6), proteases and reactive oxygen species (ROS). Both pro-inflammatory cytokines and chemoattractant protein secreted by damaged and dying cardiomyocytes alert the immune system and recruit monocytes that latter will differentiate into M1-like tissue-resident macrophages that in turn will remove the dead cardiomyocytes and their debris and degrade the ECM, which can weaken the myocardial wall and increase the susceptibility of rupture and sudden death. Afterwards, begins the proliferation phase in which, monocytes differentiate into M2-like reparative tissue-resident macrophages. Both M2-like macrophages and endothelial cells release anti-inflammatory markers such as interleukin IL-10, growth factors (e.g., vascular endothelial growth factor A (VEGF), platelet-derived growth factor, and insulin-like growth factor (IGF)), ECM components, wound healing factors like arginase and tumor growth factor (TGF)-β. As a consequence angiogenesis is promoted, that supplies blood to the infarcted area, ECM synthesis, and myofibroblast

proliferation and reorganization [2,5,25,26]. Finally, throughout the maturation phase, is deposited a fibrotic type I collagen-rich scar to avoid heart dilatation and rupture. This fibrotic scar has low conductivity properties, being able to block the electrical signal and spontaneous contraction [2]. Furthermore, elasticity is reduced mainly due to the significantly faster collagen crosslinking, turning myocardium stiffer and consequently, decreases cell infiltration [27,28].

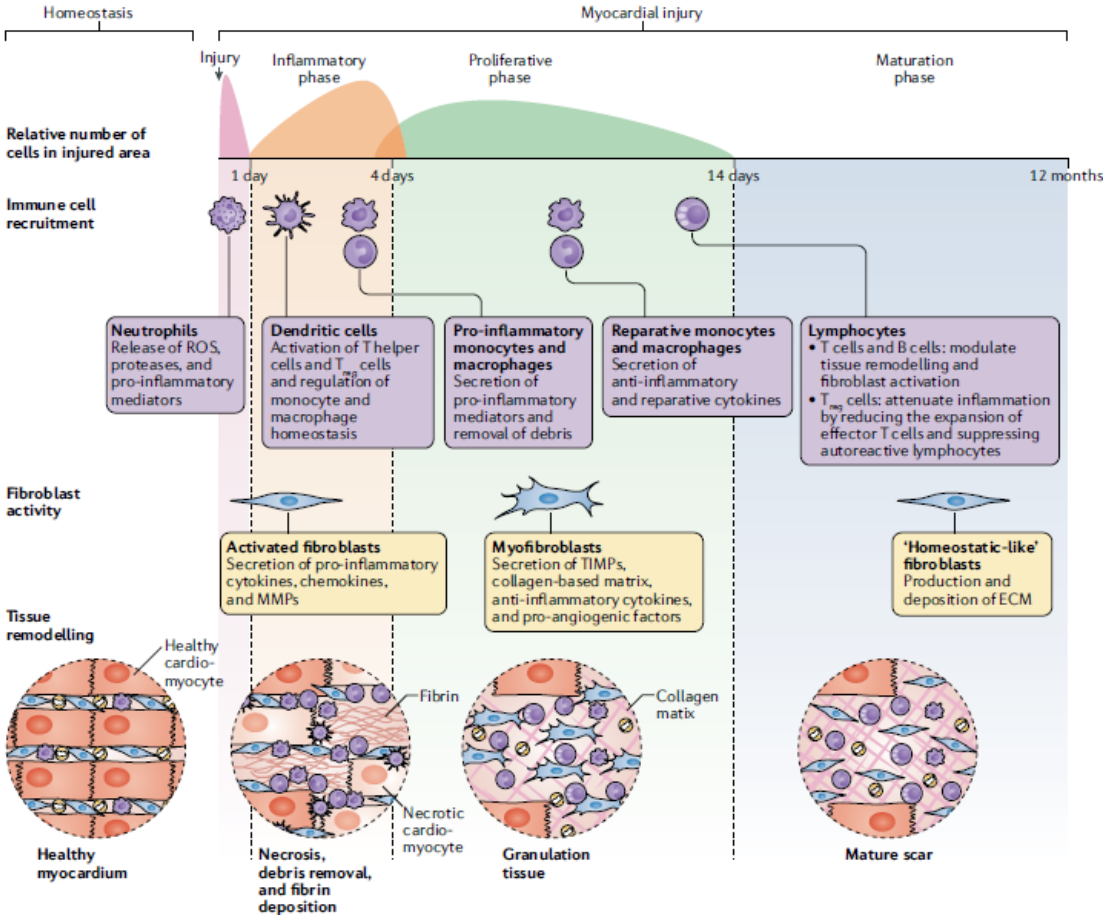

Figure II.2. Ischemic cascade that leads to myocardial scar production. At left is represented the homeostasis state and at the right, all the steps that occur after injury. The myocardium cross three different phases, each with different time consumption and the relative number of injured cells. Are highlighted the immunologic response, the fibroblast activity and it is also represented the myocardium aspect over time. Adapted from Forte et al [29].

4. Scaffolds for Cardiac Tissue Engineering

Simplified 2D models and animal models fail to recapitulate the complexity and physiology of the human tissue microenvironment. Therefore, search alternatives for these conventional options is essential. To this end, the production of 3D engineering structures is a promising option. The ideal 3D structure must combine several structural and functional properties namely high porosity, structures with branched blood arteries and capillaries

microvascular network for suitable oxygenation and cellular exchanges, mechanical and conductive properties should match that of the myocardium, providing a synchronous spontaneous contraction [5,17,30]. As human myocardium has a stiffness of 10-20 kPa in the transverse direction (orthogonal to cardiomyocyte alignment) and 40-50 kPa in the longitudinal direction the produced structure may have a similar stiffness range [31]. Furthermore, biocompatibility must be ensured, supporting cells survival and growth and lastly, must be biodegradable with a biodegradation rate matching the kinetic growth of the native myocardium in order to allow replacement of damaged tissue at the same rate of new tissue formation [5,17,30,32].

Biomaterials may have a natural or synthetic origin or both conjugated to form hybrids. Synthetic polymers have been widely used in TERM applications since they have predictable and reproducible mechanical and physical properties (e.g., tensile strength, elastic modulus). Still, such materials are associated with low biodegradability and limited bioactivity [17,32]. Oppositely, several natural polymers have intrinsic bioactivity, namely peptide sequences recognized by cells promoting cellular attachment, proliferation, and differentiation in their native state. However, the typical inadequate mechanical stiffness requires the addition of other compounds to enhance the structural stability [32,33].

Among natural derived materials, a special attention has been given to proteins and ECM-derived scaffolds. In particular, ECM-derived components are promising biomaterials as scaffolds for cardiovascular TERM since they are inherently present in native cardiac tissue.

In a 3D cell culture approach, the scaffold supplies the necessary provisional support for cell adhesion, proliferation, and phenotypic differentiation. Furthermore, it provides biochemical and biophysical cues to modulate the neo-tissue formation by mimicking both functional and structural characteristics of the native ECM, which perform an essential role in controlling and regulating cell behavior and in maintaining tissue homeostasis [34].

Biophysical signals can be divided in mechanical and electrical. Particularly, mechanical signals activate numerous transduction pathways and regulate reprogramming of numerous genes and synthesis of proteins. Hence, these signals play a role in the cellular organization of the heart and regulation of synthesis and accumulation of ECM components. For instance, the loading applied on cardiomyocytes influence their maturation, therefore mechanical signals should be precisely controlled, since the excessive load can cause pathological

hypertrophy and apoptosis. These loads are developed by wall shear stress caused by blood flow, and the strain caused by blood pressure and cell contractions [18]. Electrical forces influence the expression of cardiac markers and affects cell migration and alignment, as well as the formation of gap junctions and intercellular connections, being fundamental for preserving cardiac chamber morphology [33].

5. 3D ECM-based structures for cardiac tissue engineering and regenerative medicine

3D structures for cardiac TE have been developed using different materials composed by decellularized ECM or ECM components, namely collagen, fibrin, elastin or hyaluronic acid (HA). These 3D structures were engineered from a combination of single components from ECM to form microtissues, or else produced matrices of higher complexity by the decellularization of whole tissues [35]. ECM-derived compounds may have natural origin if they are isolated from human or animal tissues, however, they may also be artificially produced by genetically engineered biological models for the secretion of recombinant proteins [36].

Over the last two decades, regenerative medicine has emerged as alternative from only treating disease symptoms to directly repairing/regenerating injured or diseased tissue. In order to provide the proper capacity for heart to regenerate, it is fundamental to produce structures that recapitulate the organ-specific structure at multiple length scales [18].

The complexity and ethical concerns associated with drug screening with animal and human models, lead to the development necessity of specific *in vitro* models [37]. Since 2D cell cultures and animal models fail to accurately and fully recapitulate human physiology in healthy and pathological conditions, 3D models emerged as an alternative for drug development and testing, and the investigation of disease onset and progression [38]. In fact, cardiotoxicity caused by pharmacological drugs has historically been a major cause of drug removal from the pharmaceutical market, since the drug screening platforms were not the most appropriate [39]. On an ideal 3D *in vitro* cardiac tissue model, anisotropic structure and vasculature of heart should accurately be reproduced both in healthy and pathological state. Moreover, cell-cell and cell-ECM interactions should be correctly guided and cell fate and functions should be defined.

Advanced materials composed of decellularized ECM or specific components from ECM have been shown to improve healing of the cardiac wound and promote angiogenesis. In the next topics, will be discussed particular examples (**Table II-1**) of the use of these materials for cardiac TERM in recent studies and the commonly used bioengineering approaches. The strategies employed in cardiac TE to produce biomaterials may be divided into three categories: the decellularized whole organs, hydrogels and yet the patches.

Table II-1. 3D ECM-based biomaterials explored as capable of enhancing cardiac regeneration.

Model type	ECM based biomaterials	Cell lines	*In vivo* model	Outcomes	Ref.
Decellularized organs	Whole rat heart	Neonatal cardiac cells or rat aortic endothelial cells	_____	By day 8, the constructs demonstrated about 2% of pump function.	40
	Whole murine heart	Human iPSC-derived cardiomyocytes	_____	iPSCs differentiated into CMs, SMCs and ECs. Heterogeneous conduction efficiency. Insufficient pump blood function.	41
	Whole rabbit heart, collagen and fibrin hydrogels	Human fibroblasts and endothelial cells	_____	Hydrogels show Improved cell attachment.	42
	Whole porcine heart	_____	Swine and bovine	Allogenic endothelial cells and cardiomyocytes adhered to the scaffold.	43
	Whole Human heart	Human hCPCs, hMSCs, HUVECs, and H9c1 and HL-1 cardiomyocytes	_____	H9c1 and HL-1 cardiomyocytes and showed electrical activity. HUVECs formed a lining of endocardium and vasculature.	44
Injectable hydrogels	Whole Human heart	Human iPSC-derived cardiomyocytes	_____	The seeded ventricle displayed ≤50% cellular repopulation and maintained 90% cell viability after 14 days in culture. Cardiomyocytes maturate and the myocardial tissue demonstrated adequate contractile function.	45
	Type-I collagen	Murine cardiac progenitor cells (CPCs)	_____	Encapsulated cells were viable after 3 days of culture.	46
	Carbon nanotube-incorporated collagen hydrogels	Neonatal rat ventricular myocytes	_____	Enhanced cell adhesion, elongation and alignment of cardiomyocytes, leading to stronger contraction potential.	47
	Elastin-like proteins modified with RGD motifs	Murine iPSCs	_____	Higher expression levels of a contractile protein, when compared to the most effective described in iPSC differentiation into cardiac cells, a collagen-I hydrogel.	48

	HA hydrogel and PRP based hydrogel.	_____	Swine	Decrease of the injured heart muscle area while attenuating adverse cardiac remodeling.	49
	Rat Cardiac ECM and fibrin	Human Cardiac Progenitor cells	_____	Hydrogels with tunable mechanical and biochemical properties that direct cell fate.	50
	Neonatal Mouse cardiac ECM	_____	Mice	Reduced scar expansion in the left ventricle and revascularization of the injured region.	51
	Zebrafish decellularized heart	_____	Mice	Zebrafish ECM allowed cardiac functional recovery and regeneration of adult mouse heart tissues after acute MI.	52
	Human Amniotic Membrane	Bovine aortic endothelial cells	_____	Decrease in MI size.	53
Patches	Human Chorionic plate and growth factors	hiPSC-derived cardiomyocytes	Rat	Good electrical activity. Reduction of infarct size and normal electrophysiological contraction.	54
	Porcine myocardium slices	_____	Rat	Prevention of left ventricular wall thinning after MI, improved contraction and cardiac functional parameters. Formation of vessel structures.	55
	Rat heart slices	hiPSC-derived cardiomyocytes	Rat	Beating activity and electrophysiology similar to human normal heart. Reduced infarct size and improve the heart function.	56
	Porcine myocardium slices	hiPSC-derived cardiomyocytes	_____	Cell differentiation into elongated and functional cardiomyocytes. Drug sensitivity proved.	57
	Human Amniotic Membrane	hiPSC-derived cardiomyocytes	_____	Improved differentiation and cardiomyogenesis of cells cultured on the AM patch.	58
	Blended Collagen-Fibrin Hydrogels	Human iPSC-derived cardiomyocytes	_____	Cell density and purity affected capacity of produce beating tissues.	59
	Fibrin	Spheroids of human iPSC-derived cardiomyocytes	Rat	Increased engraftment rate of cells when applied *in vivo* and improved recovery from myocardial injury.	60
	Porcine cardiac ECM and GelMA	hCPCs	Rat	Increased angiogenic potential when compared to GelMA hydrogel.	61
	Metacrylated Tropoelastin	Cardiomyocytes	_____	Micropatterns promoted aligned attachment, spreading, function, and intercellular communication of cardiomyocytes.	62

5.1.Decellularized whole organs

Decellularized hearts which aims to be a biocompatible and living organ equivalent, emerged as an alternative to bioengineered artificial hearts or allogenic hearts for transplantation at end-stage cardiac failure[65]. Moreover, decellularized organs may present a strategy to surpass donor shortage, graft rejection and life-long immunosuppression usually need after organ transplantation [66].

In 2008 it was reported for the first time the successfully decellularized whole complex organ: the heart [40]. Since then, many other organs have been successfully decellularized. The process of decellularization may be performed through chemical, physical and/or enzymatic methods with the purpose of cells and nuclear material removal from tissue, whereas retaining the composition, biological activity, and mechanical structure of the ECM as much as possible [67]. Furthermore, the preservation of 3D structural architecture at the macro and micro scale, including the most of native vasculature of the organ as well as identical tensile strength, are some of the advantages of organs and tissues decellularization [35].

The decellularized whole organs have the potential to be used in drug screening, studies of mechanisms and evolution of diseases and moreover, in organ transplantation as ECM template. Ott *et al* [40] were the first to publish successful whole organ decellularization. They decellularized rat hearts (**Figure II.3**) perfusing them with detergents [69]. Since then, the decellularization of whole hearts from different species was reported [40–44,68].

Thereafter, they proved that the underlying ECM, vascular architecture, competent valves and intact chamber geometry were retained. The structure was then recellularized by coronary perfusion in a bioreactor with neonatal cardiac cells or rat aortic endothelial cells and the hearts were able to pump. However, by day 8, they only achieved about 2% of adult or 25% of 16-week fetal heart function. The used decellularization techniques demonstrated to be effective to obtain a heart whose retain native tridimensionality and intact vasculature. The major challenge to improve was the recellularization process and, consequently, improve cell distribution and contractility with physiologically rates. In an attempt to overcome that, Lu *et al* [41] decellularized mouse hearts through the same perfusion mechanism but reseeded them with human induced pluripotent stem cells (iPSC)-derived multipotential cardiovascular progenitors to produce humanized hearts.

They demonstrated that the reseeded iPSC-derived multipotential cardiovascular progenitors were able to grow and differentiate into cardiomyocytes, smooth muscle cells and endothelial cells. In fact, the constructed hearts were responsive to drug administration, a required factor for drug screening platforms, and demonstrated many regions of uniform wave propagation (**Figure II.3**, II)).

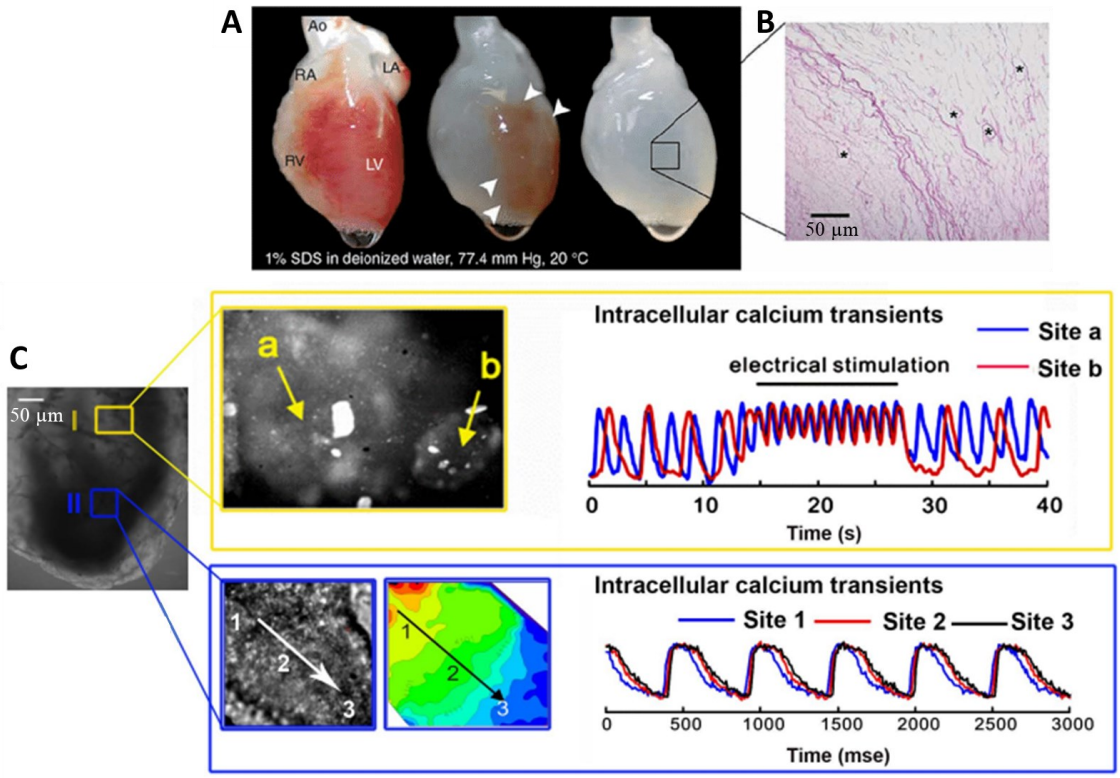

Figure II.3. Rat heart decellularization through 1% SDS perfusion; A) During decellularization, the heart becomes completelly translucent where B) no intact cells or nuclei are visible in H&E staining of a thin section [40]. C) CaiT mapping of a recellularized heart. I) Asynchronized region, that re-synchronizes under electrical stimulation. II) Synchronized region. [41]

However, they had an insufficient mechanical force to pump blood adequately and the evaluation of intracellular Ca^{2+} also revealed anatomical block zones with irregular wave propagation. That may be explained by insufficient gap-junctions or a limited number of cardiomyocytes, since during electrical stimulation the waves re-synchronized (**Figure II.3**, I)). Therefore, to overcome this anatomical block zones the authors suggested the repopulation of the constructs with cardiac fibroblasts and multipotent cardiovascular progenitor cells, since the fibroblasts have an important function in regulating heart functions, namely electrical conduction and respond to myocardial contractions.

As a way to increase the efficiency of decellularization and recellularization methods, alternatives were investigated. As for instance, Nguyen *et al* [69] decellularized and recellularized rat hearts through detergents perfusion not only into the coronary arteries but also into the cardiac veins decreasing the amount of time required and increasing the efficiency of the methods.

Alternatively, Compton *et al* [42] developed a system for rabbit hearts decellularization, perfusing them through the ascending aorta and the pulmonary trunk. Aiming to increase the recellularization efficiency, the authors, followed a different approach. Instead of simply reseeding the scaffolds through the same rotating perfusing system used for decellularization, they used a layer-by-layer approach with cells and collagen and fibrin hydrogels, in order to stimulate cellular attachment and provide a framework for reconstitution of the endocardium. They reported that the cells not only attached the ventricular wall, but also the interventricular septum. Nevertheless, they were not able to seed and distribute the hydrogels uniformly on the endocardium. Thereby, that approach still requires further improvements.

In order to test a new recellularization method, Taylor *et al* [43] proposed a heterotopic method. This method is based on the implantation of a decellularized and acellular heart, in a patient who still has his own heart, so that the patient's own cells adhere and proliferate in the decellularized scaffold. Therefore, the authors decellularized porcine hearts and implanted them in porcine and bovine. They found that at short-term endothelial cells implanted within the vessels and after 60 days of implantation, cardiomyocytes also attached to the heart. Besides this technique have been proved efficient, was considered invasiveness to the patient, hence it is not considered as an alternative to be used in humans. Consequently, the investigation of better bioreactors that may control mechanical and electrical functions after cells seeding, as a way of stimulating the proliferation of the various cardiac cells, seems to be the correct path to follow.

Sánchez *et al* [44] were the first to report human heart decellularization and recellularization. They chose to decellularize a human heart due to the “dynamic reciprocity” that is established between the ECM and the resident cell populations that affect their metabolic activity, the mechanical requirements of the tissue and the predominant conditions of the microenvironmental niche. The decellularized human hearts were reseeded with diverse human cells, such as human cardiac progenitor cells (hCPCs), human bone-marrow

mesenchymal cells (hBM-MSCs), human umbilical vein endothelial cells (HUVECs), and H9c1 and HL-1 cardiomyocytes to study the cytocompatibility of the scaffold. The authors found that only cardiomyocytes H9c2 and HL1 cells organized on longitudinal sections appearing to be muscle islands surrounded by ECM, exhibiting Ca^{2+} dynamics and impulse propagation, which suggested that they formed functional intercellular connections. Moreover, HUVECs attached within large-diameter cardiac vessels in the matrix milieu and on endocardial surface of the ECM. Oppositely, hCPCs and hBM-MSCs, which failed to organize on the matrix, did not generated intracellular Ca^{2+} transients or propagated electrical signal. The authors concluded that it was possible to obtain a study model or a transplantable heart with a coating of HUVECs in the endocardium with vasculature and electrical properties [68].

After that, many other works have reported the decellularization and recellularization of human hearts. Until now, the most successful engineered whole human heart was obtained by Guyette *et al* [45]. In this study, the decellularized human hearts were recellularized by injection of iPSC-derived cardiomyocytes in different regions of the left ventricle. Then, the authors placed the recellularized hearts in bioreactors, exposing them to mechanical stimulation through coronary artery perfusion with media. The seeded ventricle displayed ≤50% cellular repopulation and maintained 90% cell viability after 14 days in culture. Some of the reseeded cardiomyocytes acquired elongated and striated phenotypes, whereas the others showed rounded immature sarcomere formation. Moreover, when electrically stimulated, the repopulated myocardial tissue demonstrated contractile function. These preliminary results were promising, however, the repopulation of all heart should be done, and the culture time should be increase to verify if cells achieve full maturity and all heart develop the adequate contractile function.

Despite all the promising achievements, it is not yet possible to obtain functional hearts for implantation in acute patients with end-stage cardiac failure. Accomplish that would be of great importance, since non-transplantable human hearts or porcine hearts could be used, leading to the availability of unlimited number of transplantable organs [70].

5.2.Injectable Hydrogels

Initial stages of heart failure or right after ischemic heart disease do not require the entire removal of the heart but approaches that help the regeneration of the damage zone. For that, strategies such as direct injection of cells in the affected region have been applied with

limited success, since the cells have low retention and engraftment. This may be improved by adding a structure where the cells adhere before being implanted [9]. Thus, hydrogels prepared from solubilized decellularized ECM or ECM components have also been explored for cardiac TERM. Hydrogels are 3D crosslinked hydrophilic polymer networks with the capacity to uptake a high percentage of water and tunable biochemical and mechanical properties in order to produce structures that better mimic the extracellular environment [71–73,74]. Their characteristics depend on the biomaterials used and the manufacturing process [73]. The crosslinking of the hydrogels may be physical and/or chemically induced. The physical stimuli, that produce transient junctions, include temperature, electric or magnetic field, light, pressure, and sound while the chemical stimuli, that produce permanent junctions, include pH, solvent composition, ionic strength, and molecular species (e.g., photoinitiator) [75].

Injectable hydrogels are flowable aqueous solutions that polymerize or have a sol-gel transition *in situ* after administration, forming a gel. They have attracted significant attention due to their ease administration, production of minimal surgical wounds reducing patient's discomfort, risk of infection and the ease of cells and bioactive compounds incorporation simply mixing before injection. After injection and consequent gelation, the hydrogels become cell-growing and/or drug delivery reservoirs [76,77]. They must fulfil certain requirements, namely being liquid before gelation and jellifying under mild conditions with proper gelation rates in order to simplify their homogenization with cells and bioactive compounds, handling, and consequent injection, whereas avoiding toxicity, overheating caused by harsh reactions and also extravasation to the surrounding tissues [78,79].

Numerous hydrogels produced from ECM components have already been reported to be used in cardiac TERM. Since the major component of ECM is collagen, it is the source of several studies in the field of cardiac TE. The reservoirs of collagen type I in myocardial ECM decrease from 80% to 40% after MI, while collagen type III increase from 10% to 35%, creating pathological fibrosis, thus the majority of studies that use collagen as a biomaterial for cardiac repair use type I collagen [80,81]. Nevertheless, knowing that stiffness influences the phenotype of the cells, the studies that have been done in recent years that involve collagen I include other components to increase mechanical function [82].

For example, Ravichandran *et al* [46] functionalized type-I collagen, through the reaction with methacrylic anhydride or using thiol-Michael addition click chemistry tuning the

elasticity modulus from Pa to kPa. Moreover, the authors encapsulated murine cardiac progenitor cells within the hydrogel and observed that cells were highly viable after 3 days of culture. The incorporation of carbon nanotubes in hydrogels, have been reported to increase both stiffness [83] and electrical properties [84]. Hence, Sun *et al* [47] proposed a carbon nanotube-collagen nanocomposite hydrogel to encapsulate neonatal rat ventricular myocytes. They compared their hydrogel with a collagen I hydrogel and found that the incorporation of carbon nanotubes within collagen hydrogels enhanced cell adhesion, elongation and alignment of cardiomyocytes, leading to the formation of engineered cardiac tissues with stronger contraction potential.

Other ECM components have been used in cardiac TE, as for instance, elastin. This protein have been reported as responsible to enhance angiogenesis, which is fundamental for cardiac TE applications due to its highly vascularized nature [85]. Furthermore, is required from a mechanical point of view and directly interact with cells being involved in many cell-signaling processes [85]. Kambe *et al* [48] produced recombinant elastin-like proteins to construct an elastin-like protein-based hydrogel to study the influence in cardiac differentiation of iPSCs and compared to the most effective described in literature, the collagen-I hydrogel. This hydrogel was modified with the peptide sequence, Arginine-Glycine-Aspartate (RGD) cell adhesion motif and crosslinked with tetrakis(hydroxymethyl)phosphonium chloride. The authors mimic the elasticity of embryonic cardiac tissue (0.3 kPa) and seeded the hydrogels with murine iPSCs. They verified that cells cultured on the hydrogel of elastin-like protein-RGD had four times higher expression of encoding for a contractile protein than those cultured on collagen I.

The crescent interest for personalized medicine, and autologous materials obtained with minimally invasiveness made Vu *et al* [49] to study the formulation of a hydrogel based on autologous platelet-rich plasma (PRP). PRP is a rich source of autologous growth factors and cytokines involved in wound healing and angiogenesis and had already been direct intramyocardial injected proving that promote angiogenesis and attenuated cardiac remodeling in a rodent model. Nevertheless, due to a low retention rate, the forbidding microenvironment of a high blood flow rate in the heart and a high degree of ventricular remodeling after MI become this technique low efficient when without biomaterials as delivery vehicles. Therefore, the authors tested the evolution of myocardial scar in pigs using: i) an hyaluronan-based hydrogel commercially available (Extracel-HP™), ii) an

autologous PRP hydrogel, iii) an antioxidant and anti-inflammatory PRP hydrogel with ascorbic acid combined with intravenous ibuprofen and allopurinol and finally iv) a PRP-cocktail hydrogel. They verified that scar area and scar thickness decreased in all cases, but decreased most in the PRP-cocktail group, due to their higher density of blood vessels in the peri-infarct area. However, the hyaluronan-based hydrogel alone was the one that most preserved left ventricular ejection fraction.

Decellularized tissues in the form of an injectable hydrogel, have also been studied for cardiac TE [86]. Many studies have been performed in order to produce injectable hydrogels for cardiac TE from decellularized cardiac tissue, since are the closest to the tissue to replicate. To that, some works reported the development of hydrogels from animals decellularized cardiac tissue, as for instance rat [50,87], mouse [51], zebrafish [52] and porcine [88].

The most used strategy combines the decellularization followed by enzymatic digestion, usually using pepsin in order to solubilize the obtained decellularized material, making it possible to be injectable [87].

ECM derived hydrogels have typically very soft mechanical properties that often do not match those of the native tissue. Thus, the use of crosslinking agents to increase the elasticity modulus has been explored. For example, Williams *et al* [50] combined solubilized decellularized cardiac rat ECM with fibrin, which have angiogenic properties, and transglutaminase crosslinker to produce stiffer hydrogels.

Having neonatal animals increased capacity of regeneration, Wang *et al* [51], compared the injection of hydrogels derived from neonatal mouse heart ECM and adult heart-derived ECM in an *in vivo* adult mice model of MI, to explore the neonatal mammal's capacity of cardiomyocyte proliferation and regeneration within a week of birth. With this study, the authors verified that the treatment with neonatal ECM drastically reduced the fractional area occupied by a collagen-rich scar and improved the ejection fraction, demonstrating its potential for cardiac applications.

Chen *et al* [52] studied the potential of zebrafish ECM hydrogel administration to induce mammalian heart regeneration. To that, the authors decellularized normal and healing adult zebrafish ventricles as well as healthy adult mouse ventricles to be used as control. After intramyocardial administration of decellularized cardiac ECM zebrafish, murine heart tissue was capable to have an endogenous regeneration and multiple resident cardiac precursor cell

populations demonstrated increased proliferation. Besides, zebrafish ECM induced 61% recovery of cardiac ejection fraction, while mouse ECM provided only 17%.

So far there are no hydrogels produced from human cardiac decellularized tissue. Alternatively, decellularized human tissue from other sources have been explored for cardiac TE. An appealing source of ECM is the human placenta. These are commonly discarded as medical waste after birth, having no ethical issues associated. Furthermore, due to their rich ECM composition, they have gained increased attention as alternative sources to obtain 3D decellularized scaffolds composed by important ECM molecules from human origin. The use of human amniotic membrane (AM) was first reported in 1910 in skin transplantation. Posteriorly, it was reported its use in various skin, corneal, ocular and periodontics disturbances to suppress inflammation, stimulate growth of epithelial cells and reduce scarring in mesenchymal tissue [89]. AM has special interest in TERM applications due to its low immunogenicity, immunosuppressive properties and healing capacity [89]. Henry *et al* [53] produced a thermoresponsive injectable hydrogel from decellularized human AM and consequent enzymatic digestion (**Figure II.4** A-D).

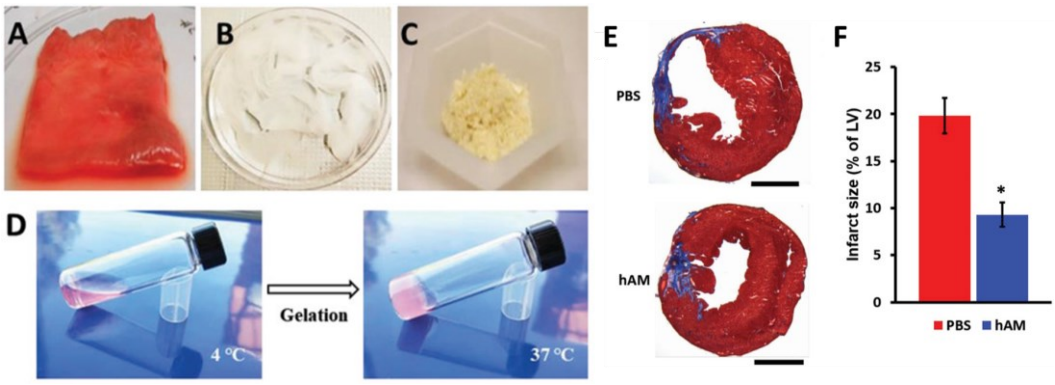

Figure II.4. Physical aspect of human AM during the processing. A) Fresh AM, before decellularization. B) Decellularized AM. C) Solubilized and lyophilized AM. D) Gelation of decellularized AM matrix at 37 °C. E) Representative images of Masson trichrome-stained rat heart sections of adult myocardial regeneration after MI at 5 weeks after AM matrix or PBS injection. Scale bars = 4 mm. F) Measurement of infarcted size at 5 weeks after AM matrix or PBS injection analyzed by Masson trichrome staining. n = 5 for each group, *p < 0.05. Adapted from Henry et al [53].

The jellification occurred when the hydrogel was placed at 37ºC. Beyond the resultant hydrogel was very soft, its injection in adult rat heart tissue after MI, showed a significantly decrease in the infarct size (**Figure II.4** E and F) and improvement of left ventricular ejection fraction, proving its efficacy in attenuating degenerative changes in cardiac function [53].

Besides the AM, chorion plate from human placenta, also has important properties for TERM [89]. As it is a vascularized tissue, has been studied, for example, as a source to isolate small diameter vascular structures [90]. Francis *et al* [54] used decellularized human chorionic plate as source of ECM components for cardiac regeneration. The decellularized tissue was also solubilized and jellified at 37ºC. The peptides resulting from enzymatic digestion were determined and a huge diversity of proteins was identified namely collagens, laminins, fibronectin, fibrinogen, elastin, glycoproteins, among others and growth factors, as for instance, pro-regenerative, pro-angiogenic, and stem cell-recruiting factors. The authors compared their hydrogel with Matrigel®, a commercially available soluble extract of basement membrane proteins derived from mouse Engelbreth-Holm-Swarm (EHS) sarcoma that forms a hydrogel at 37 °C and supports cell morphogenesis, differentiation, and tumor growth, widely used in TE [91,92]. The authors seeded iPSCs-derived cardiomyocytes in both hydrogels and verified that after 24-30 hours, only chorionic plate-derived hydrogel demonstrated early contractility, coupling and cell synchronization. Furthermore, was proved that chorionic plate-derived hydrogel injections in ischemic myocardium reduced significantly infarcted area size and allowed normal electrophysiological contraction [54]. The reported studies proved the potential of these temporary organs that are usually discarded to prepare 3D bioactive matrices for cell culture and TE.

5.3.Patches

Epicardium is the outer layer of the heart, being essential for heart regeneration after injury by providing paracrine factors and progenitor/stem cells that contribute to regeneration of cardiomyocytes, vascular smooth muscle cells, and endothelial cells [93]. Hence, the application of patches on the pericardium, thick enough for powerful contractions and to synchronize its rhythm with the heart's own, may be a promising strategy for heart regeneration [94].

The patch functionality will not only depend on the material composition, but also on its architecture, that may be precisely controlled through the biofabrication approach to achieve anisotropic tissue structures, similar to the native myocardium [95]. Therefore, different strategies have been studied, namely the use of decellularized tissues maintaining their original structure, or specific components from ECM, in the form of a polymerized hydrogel. These second type of patches may be produced through 3D casting, producing smooth surface patches or by other techniques, in order to produce topographical cues [96].

Topographical patterns, have already demonstrated that even solely, in the absence of electrical or mechanical stimulation, may have a role in cell migration, alignment and elongation [97,98]. In the next sections, the most relevant examples of patches to be applied in myocardium repair will be discussed.

5.3.1. Decellularized tissue patches

Similarly to the whole decellularized organs, also slices of decellularized organs may have a role in heart regeneration when applied as a patch and may be supportive to be used as drug test platform. For instance, Shah *et al* [55] decellularized porcine myocardium slices and implanted them as acellular patch in a rat acute MI model. The authors verified that the patch prevented thinning of the left ventricular wall after MI, helped in the formation of new vessels and finally, contraction of the left ventricular wall and cardiac functional parameters were significantly improved, 4 weeks after surgery. Also, Blazeski *et al* [57] decellularized porcine myocardium slices, repopulating them with hiPSCs-derived cardiomyocytes to study their application in drug studies. Their results evidenced that cardiomyocytes differentiated, exhibiting elongated, multicellular and aligned bundles with organized sarcomeres, presented anisotropic conduction of action potentials and electrophysiological functionality. Finally, the developed model demonstrated a higher clear drug sensitivity when compared to 2D cell cultures, thus having the potential to be used in electrophysiology and drug screening studies. On the other hand, Wang *et al* [56] prepared decellularized rat heart slices and repopulated in the endocardial side with hiPSCs-derived cardiomyocytes and fibroblasts. Whereas *in vitro,* the developed patches presented beating similar activity and electrophysiology to human normal heart and a good response to pharmaceutical agents, when implanted *in vivo* in rat MI models, they reduced the infarct size and improved the heart function.

In addition, decellularized AM slices, dehydrated human amnion/chorion membrane acellular patches or trypsinized and cryopreserved AM from human placenta have been studied as a patch for cardiac TERM. In particular, Roy *et al* [99] demonstrated that acellular patches from human decellularized AM, besides do not decreased the infarct size, helped to prevent pathologic postinfarct remodeling processes, improving systolic and diastolic function. In another study, Lim *et al* [100] also have very interesting results when applied dehydrated human amnion/chorion membrane acellular patches (EpiFix® and AmnioFix®) in mice after acute MI, resulting in a reduction of fibrotic scarring size, a higher recruitment

of hematopoietic and cardiac stem cells, increased cell proliferation markers and cell surface marker for vascular endothelial cells, while inhibited apoptosis cell markers. Taking these great results into account, Parveen *et al* [58] studied the potential of trypsinized and cryopreserved human AM as platform for human heart research, comparing the behavior of hiPSC-derived cardiomyocytes when cultured on the human AM or Matrigel™ in order to generate cardiomyocytes with maturity close to adult cardiac cells. The authors verified that, actually, cardiomyocytes cultured on human AM achieved a higher development than Matrigel due to their faster intracellular calcium transients and higher mitochondrial density with regular arrangement. Moreover, they verified elongated and aligned cells, contrary to the chaotic distribution and round large morphology of cells in Matrigel™. However, despite the complete maturation, the major drawback of this study was the incapacity of cardiomyocytes to generate spontaneous contraction. The obtained results corroborate that fetal membranes have a positive effect in cardiac regeneration when applied as a patch influencing both cardiomyocyte proliferation and alignment, and also hematopoietic cells recruitment and proliferation.

5.3.2. Smooth hydrogel patches

The simplest method to polymerize crosslinkable hydrogels is through gel casting. The gel solution is transferred to a mold where polymerization occurs forming the hydrogel with controlled shape. Kaiser *et al* [59] used solvent casting to produce hydrogels patches for cardiac TE. In this study the authors blended relevant ECM components, such as collagen I, the predominant protein in healthy heart, and fibrin, a critical component of the wound healing cascade, to encapsulate human iPSC-derived cardiomyocytes. The authors compared different concentrations of collagen and fibrin, and also different purities of iPSC - derived cardiomyocytes for cardiac applications. Beyond the expected results, beating tissues only appeared in the gels of pure collagen with higher cardiac cells purity (≥ 60%).

Mattapally *et al* [60]. reported the production of fibrin cardiac patches with encapsulated cell spheroids. After 24 h of spheroid formation, synchronized contractions were observed and was confirmed the presence of both Ca^{2+} transients and propagating action potentials. The fibrin patches with iPSC-derived cardiomyocyte spheroids were implanted in rats after myocardial injury, resulting in higher engraftment rate than direct intramyocardial injection (more than ~ 25% vs. less than ~ 10%, respectively).

Another approach to produce patches with smooth surface, but controlled porosity is 3D bioprinting. For example, Bejleri *et al* [61] blended solubilized decellularized porcine heart, gelatin methacrylate (GelMA) to behave as support material and human CPCs. That mixture was bioprinted and consequently polimerized. Patches were polymerized via white light to induce radical polymerization of GelMA, followed by incubation at 37 °C to induce cardiac ECM polymerization. hCPCs remained viable and showed increased cardiogenic gene expression, compared to hCPCs grown in pure GelMA patches. Moreover, comparing this hydrogel with GelMA hydrogel, decellularized porcine heart-based hydrogel has an increased angiogenic potential. After 14 days of *in vivo* implantation the patches integrated with the native myocardium and allowed for nutrient delivery to the implanted cells.

5.3.3 Topographical hydrogel patches

Topographical cues have been introduced in biomaterials as patches since cells are strongly influenced by surface features. For example, stem cells differentiation towards myocardial lineage is modulated by aligned orientation [104]. Moreover, topographical cues influence cells phenotype, morphology and maturity [105].

5.3.3.1. Microcontact printing

In this technique are usually used molds of PDMS with micropatterns that are applied above prepolymer solutions so that the patterns are engraved on the hydrogels after polymerization. An example of micropatterned hydrogels for cardiac TE are the methacrylated tropoelastin patches reported from Annabi *et al* [62]. In this study two versions of methacrylated tropoelastin were prepared: one containing aligned microchannels mimicking those of the native myocardium, and the other unpatterned as a control. Micropatterns promoted aligned attachment, spreading, function, and intercellular communication of cardiomyocytes, oppositely to the unpatterned in which cardiomyocytes randomly attached, the actin filaments elongated less and the cardiac function early decreased.

Graphene oxide is responsible to increase strength, the contractility and promote a faster spontaneous beating rate in cardiomyocytes [107]. Hence, the production of micropatterned gelatin-graphene oxide hydrogel allowed to obtain a hydrogel with improved mechanical properties and which affected cellular behavior including adhesion, proliferation, and differentiation [63]. The authors compared an unpatterned gelatin hydrogel, with a patterned

gelatin hydrogel and gelatin-graphene oxide micropatterned hydrogel. They verified that the micropattern effectively induced cardiomyocytes to develop elongated constructs and promote synchronous contraction and the addition of graphene oxide enhanced cell alignment and beating of cultured cardiomyocytes.

5.3.3.2. 3D Bioprinting

Wang *et al* [64] prepared a fibrin-based bioink with suspended rat primary cardiomyocytes aiming to produce a model to study physiologic reactions during tissue development or to pharmacologic application. To that, they produced cardiac tissue constructs using an integrated tissue-organ printing system, where a fibrin-based hydrogel, combined with gelatin, aprotinin, glycerol and HA with suspended primary cardiomyocytes was used as a cell-laden hydrogel, a gelatin, glycerol and HA hydrogels was used as a sacrificial hydrogel and Poly(ε-caprolactone) (PCL), was used as the supporting frame to maintain the printed pattern (**Figure II.5** A).

This strategy allowed cell alignment (**Figure II.5** E) and showed strong and synchronous contraction (**Figure II.5** D) after 4 weeks in culture. The intrinsic force generated by PCL frame after bioprinting was essential for cardiac tissue development and maturation. Posteriorly the tissue construct was evaluated as a feasible source for drug screening and was verified that these 3D tissue models responded as expected to drug that increase or decrease the beating frequency. Finally, when the exposure to drugs was ceased, the previous synchronous contraction was restored.

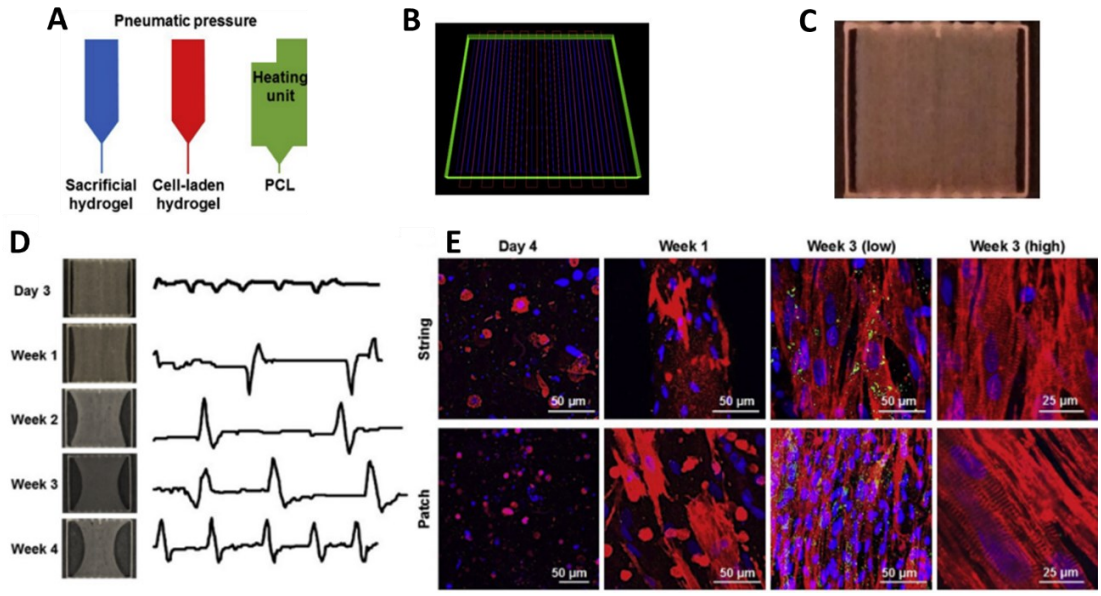

Figure II.5. A) Three dispensing modules used for cardiac tissue constructs printing; B) Basic motion program; C) String form; D) Progress of tissue over 4 weeks (left) and plotting of spontaneous beating based on bright-field video over the same time (right); E) Rapid increase in α-actinin positive cell area, cardiomyocyte perimeter and alignment of muscle fibers. Adapted from Wang *et al* [64].

6. ECM derived hydrogels in clinical trials

VentriGel™, an ECM hydrogel derived from decellularized porcine myocardium has also been used for tissue remodeling after MI. A first clinical trial was performed to evaluate cardiac repair in 15 patients with moderate left ventricular dysfunction [109]. The objective of the study was to evaluate the safety and feasibility of VentriGel™ transendocardial injections. No deaths occurred and no patients were discontinued from the study. However, a patient whose history included trifascicular block suffered cardiogenic shock and complete heart block was reported as possibly related to study treatment, nevertheless improved measures of left ventricular remodeling were reported.

PeriCord cardiac bioimplant, a decellularized human pericardial matrix patch, was colonized with human viable Wharton's jelly-derived mesenchymal stromal cells (WJ-MSCs) and implanted in human heart [110]. This first-in-human study was performed in a 63-year-old male patient. The three-month clinical follow-up showed ~9% reduction in scar mass in the treated area. This preliminary report suggests the possibility of proceeding to next steps of the study, including more patients.

7. Typical cell sources for cardiac TERM

The selection of the most appropriate cell type for cardiac TERM is still a challenge. Relatively to cell sources, they may be divided into three groups: primary cells, cell lines and stem cells. Primary cells are directly isolated from human or animal tissues and have health age accordingly to the donor. Despite they have huge potential to recapitulate the specific tissue functions and the advantage of possible isolation from the own patient towards personalized medicine, the availability of human primary cells is usually low or even rare. Cell lines have diverse advantages in starting stages of cells testing since their virtual unlimited division capacity, reduced cost, easily handle, rapid growth and optimal for cancer models. However, they may differ from the targeted cells being not representatively. Moreover, they are not adequate for tissue regeneration applications. When the primary cell source is unavailable and cell lines are inadequate, stem cells are the best option. The category of stem cells includes embryonic stem cells (ESCs), mesenchymal stem cells (MSCs), and induced pluripotent stem cells (iPSCs) [111,112]. ESCs are cells resulting from fecundation and are pluripotent, having the capacity to differentiate into any type of cell and to be maintained for long (theoretically indefinite) culture periods. However, due to their origin, there are many ethical issues that limit their use in TE [113,114]. MSCs are cells that retain postnatal capacity for self-renewal and multilineage differentiation such as osteocytes, chondrocytes, adipocytes, and myocytes. They can be found in the bone marrow, adipose tissue, umbilical cord blood, and many other tissues. A main disadvantage of MSCs for cardiac TERM is the very low survival rate after transplantation in heart [115,116]. Lastly, human iPSCs promise to revolutionize human health through precision and personalized medicine towards an individual level. They are pluripotent stem cells with capabilities of indefinite self-renewal and that can be differentiated into almost all cell types of the body. The ability of iPSCs to differentiate into specific cells such as cardiomyocytes allows the possibility of obtaining theoretically unlimited patient-specific human cells for use in disease modelling, personalized drug screening, and regenerative approaches (**Figure II.6**). Therefore, human iPSC-derived cardiomyocytes offer several advantages over current *in vitro* models such as immortalized cell lines, human cadaveric tissue, and primary cultures of human or animal origin cells [117].

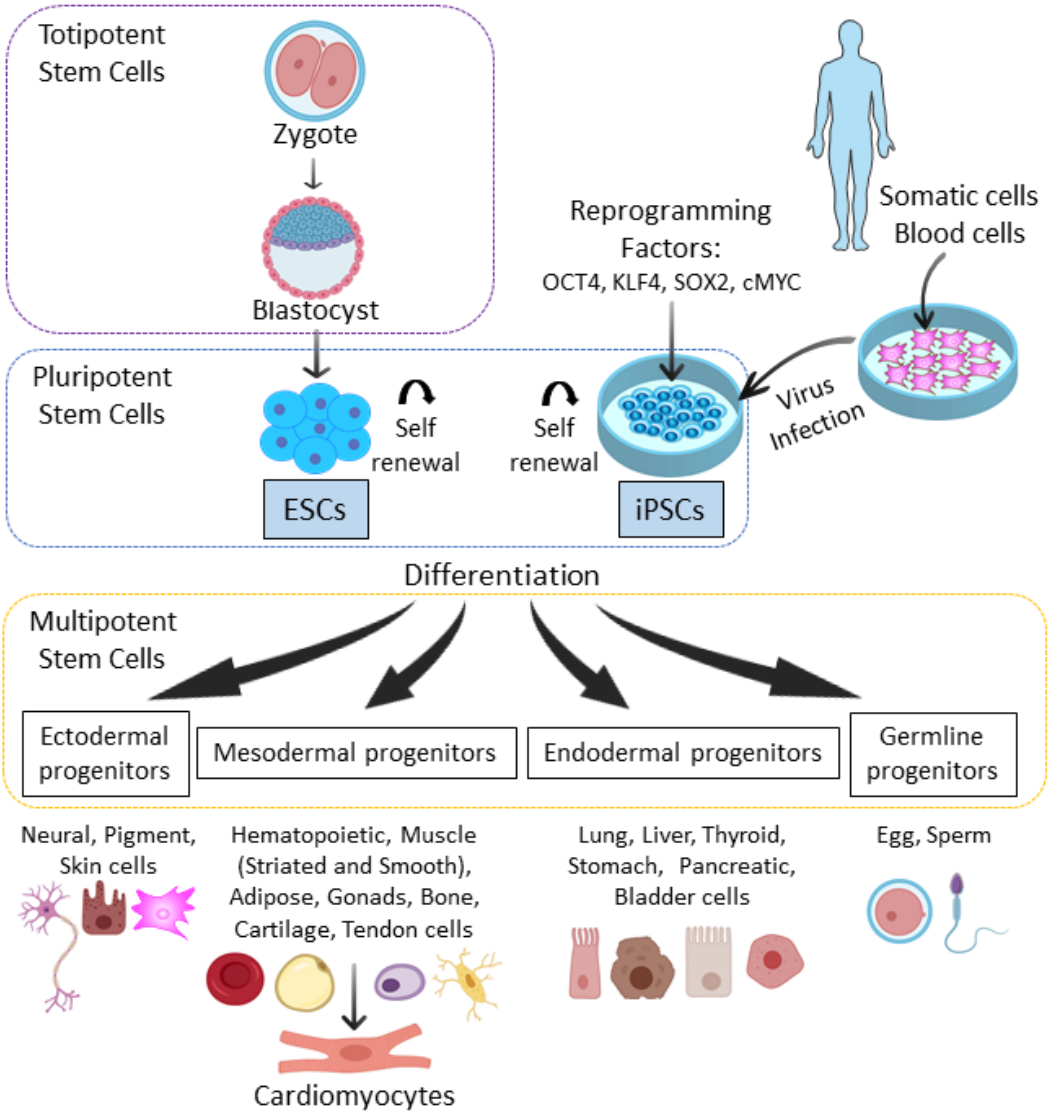

Figure II.6. Diagram of pluripotent stem cells sources, namely Embryonic Stem Cells (ESCs) and human induced Pluripotent Stem cells (iPSCs) that have self-renewal capacity and are able to differentiate in almost all cell types of the body.

8. Conclusion and future perspectives

The increase in average life expectancy and population ageing make IHD a major concern worldwide. Hence, the need for solutions to treat infarcted hearts is a demand. Understanding the remodelling process that occurs after MI and the native and damaged cardiac ECM compositions, may help to produce a tissue that more closely mimic native or damaged cardiac ECM.

Besides 2D structures do not precisely recapitulate the complex cell–cell, cell–ECM and tissue-level interactions, animal models also are not the ideal solution due to the physiological differences that may cause unpredictable results and ethical concerns. A

promising solution is the conjugation of ECM-based biomaterials with cells in a 3D platform. Different 3D structures that can be used alone or in combination with cells have been produced with components from native cardiac ECM, decellularized cardiac ECM from different organs, including placental membranes. The emerging of placenta as a possible ECM source arouses growing interest since, as well as many other human tissues, own many proteins, growth factors and proteases present in heart ECM, also is a biological waste after birth, being cost-effective and have low immunogenicity. Besides some studies have achieved great cell function allowing synchronous contraction, decreased scar formation and increased angiogenesis, this area still have many issues to be studied, namely material stability, rate of degradation or the rate of cell differentiation must be tightly regulated in order to avoid uncontrolled cell growth.

The use of both human-derived raw materials and hiPSCs promise to revolutionize human health through precision and personalized medicine towards an individual level.

9. References

(1) World Health Organization. Projections of Mortality and Causes of Death, 2015 and 2030.

(2) Lavin Plaza, B.; Theodoulou, I.; Rashid, I.; Hajhosseiny, R.; Phinikaridou, A.; Botnar, R. M. Molecular Imaging in Ischemic Heart Disease. Curr. Cardiovasc. Imaging Rep. 2019, 12 (7). https://doi.org/10.1007/s12410-019-9500-x.

(3) Johnson, T.; Zhao, L.; Manuel, G.; Taylor, H.; Liu, D. Approaches to Therapeutic Angiogenesis for Ischemic Heart Disease. J. Mol. Med. 2019, 97 (2), 141–151. https://doi.org/10.1007/s00109-018-1729-3.

(4) Peña, B.; Laughter, M.; Jett, S.; Rowland, T. J.; Taylor, M. R. G.; Mestroni, L.; Park, D. Injectable Hydrogel for Cardiac Tissue Engineering. Macromol. Biosci. 2018, 18 (3), 1–22. https://doi.org/10.1002/mabi.201800079.

(5) Qasim, M.; Haq, F.; Kang, M. H.; Kim, J. H. 3D Printing Approaches for Cardiac Tissue Engineering and Role of Immune Modulation in Tissue Regeneration. Int. J. Nanomedicine 2019, 14, 1311–1333. https://doi.org/10.2147/IJN.S189587.

(6) Miller, L.; Birks, E.; Guglin, M.; Lamba, H.; Frazier, O. H. Use of Ventricular Assist Devices and Heart Transplantation for Advanced Heart Failure. Circ. Res. 2019, 124 (11), 1658–1678. https://doi.org/10.1161/CIRCRESAHA.119.313574.

(7) Stoppel, W. L.; Gao, A. E.; Greaney, A. M.; Partlow, B. P.; Bretherton, R. C.; Kaplan, D. L.; Black, L. D. Elastic, Silk-Cardiac Extracellular Matrix Hydrogels Exhibit Time-Dependent Stiffening That Modulates Cardiac Fibroblast Response. J. Biomed. Mater. Res. - Part A 2016, 104 (12), 3058–3072. https://doi.org/10.1002/jbm.a.35850.

(8) Weinberger, F.; Mannhardt, I.; Eschenhagen, T. Engineering Cardiac Muscle Tissue: A Maturating Field of Research. Circ. Res. 2017, 120 (9), 1487–1500. https://doi.org/10.1161/CIRCRESAHA.117.310738.

(9) Terrovitis, J. V.; Smith, R. R.; Marbán, E. Assessment and Optimization of Cell Engraftment after Transplantation into the Heart. Circ. Res. 2010, 106 (3), 479–494. https://doi.org/10.1161/CIRCRESAHA.109.208991.

(10) Veldhuizen, J.; Migrino, R. Q.; Nikkhah, M. Three-Dimensional Microengineered Models of Human Cardiac Diseases. J. Biol. Eng. 2019, 13 (1), 1–12. https://doi.org/10.1186/s13036-019-0155-6.

(11) Skardal, A.; Shupe, T.; Atala, A. Organoid-on-a-Chip and Body-on-a-Chip Systems for Drug Screening and Disease Modeling. Drug Discov. Today 2016, 21 (9), 1399–1411. https://doi.org/10.1016/j.drudis.2016.07.003.

(12) Savoji, H.; Mohammadi, M. H.; Rafatian, N.; Toroghi, M. K.; Wang, E. Y.; Zhao, Y.; Korolj, A.; Ahadian, S.; Radisic, M. Cardiovascular Disease Models: A Game Changing Paradigm in Drug Discovery and Screening. Biomaterials 2019, 198, 3–26. https://doi.org/10.1016/j.biomaterials.2018.09.036.

(13) Kim, J. Bin. Three-Dimensional Tissue Culture Models in Cancer Biology. Semin. Cancer Biol. 2005, 15 (5), 365–377. https://doi.org/10.1016/j.semcancer.2005.05.002.

(14) Zuppinger, C. 3D Cardiac Cell Culture: A Critical Review of Current Technologies and Applications. Front. Cardiovasc. Med. 2019, 6 (87), 1–9. https://doi.org/10.3389/fcvm.2019.00087.

(15) Ma, X.; Liu, J.; Zhu, W.; Tang, M.; Lawrence, N.; Yu, C.; Gou, M.; Chen, S. 3D Bioprinting of Functional Tissue Models for Personalized Drug Screening and *in vitro* Disease Modeling. Adv. Drug Deliv. Rev. 2018, 132, 235–251. https://doi.org/10.1016/j.addr.2018.06.011.

(16) Bejleri, D.; Davis, M. E. Decellularized Extracellular Matrix Materials for Cardiac Repair and Regeneration. Adv. Healthc. Mater. 2019, 8 (5), 1–29. https://doi.org/10.1002/adhm.201801217.

(17) Domenech, M.; Polo-Corrales, L.; Ramirez-Vick, J. E.; Freytes, D. O. Tissue Engineering Strategies for Myocardial Regeneration: Acellular versus Cellular Scaffolds? Tissue Eng. - Part B Rev. 2016, 22 (6), 438–458. https://doi.org/10.1089/ten.teb.2015.0523.

(18) Parsa, H.; Ronaldson, K.; Vunjak-Novakovic, G. Bioengineering Methods for Myocardial Regeneration. Adv. Drug Deliv. Rev. 2016, 96, 195–202. https://doi.org/10.1016/j.addr.2015.06.012.

(19) Curley, C. J.; Dolan, E. B.; Otten, M.; Hinderer, S.; Duffy, G. P.; Murphy, B. P. An Injectable Alginate/Extra Cellular Matrix (ECM) Hydrogel towards Acellular Treatment of Heart Failure. Drug Deliv. Transl. Res. 2019, 9 (1), 1–13. https://doi.org/10.1007/s13346-018-00601-2.

(20) Frey, N.; Linke, A.; Süselbeck, T.; Müller-Ehmsen, J.; Vermeersch, P.; Schoors, D.; Rosenberg, M.; Bea, F.; Tuvia, S.; Leor, J. Intracoronary Delivery of Injectable Bioabsorbable Scaffold (IK-5001) to Treat Left Ventricular Remodeling after ST-Elevation Myocardial Infarction: A First-in-Man Study. Circ. Cardiovasc. Interv. 2014, 7 (6), 806–812. https://doi.org/10.1161/CIRCINTERVENTIONS.114.001478.

(21) Lockhart, M.; Wirrig, E.; Phelps, A.; Wessels, A. Extracellular Matrix and Heart Development. Birth Defects Res. Part A - Clin. Mol. Teratol. 2011, 91 (6), 535–550. https://doi.org/10.1002/bdra.20810.

(22) Valiente-Alandi, I.; Schafer, A. E.; Blaxall, B. C. Extracellular Matrix-Mediated Cellular Communication in the Heart. J. Mol. Cell. Cardiol. 2016, 91, 228–237. https://doi.org/10.1016/j.yjmcc.2016.01.011.

(23) Talman, V.; Kivelä, R. Cardiomyocyte - Endothelial Cell Interactions in Cardiac Remodeling and Regeneration. Front. Cardiovasc. Med. 2018, 5 (July), 1–8. https://doi.org/10.3389/fcvm.2018.00101.

(24) Gallagher, G. L.; Jackson, C. J.; Hunyor, S. N. Myocardial Extracellular Matrix Remodeling in Ischemic Heart Failure. Front. Biosci. 2007, 12, 1410–1419. https://doi.org/10.2741/2157.

(25) Alvarez, M. M.; Liu, J. C.; Trujillo-de Santiago, G.; Cha, B. H.; Vishwakarma, A.; Ghaemmaghami, A. M.; Khademhosseini, A. Delivery Strategies to Control Inflammatory Response: Modulating M1–M2 Polarization in Tissue Engineering Applications. J. Control. Release 2016, 240, 349–363. https://doi.org/10.1016/j.jconrel.2016.01.026.

(26) Julier, Z.; Park, A. J.; Briquez, P. S.; Martino, M. M. Promoting Tissue Regeneration by Modulating the Immune System. Acta Biomater. 2017, 53, 13–28. https://doi.org/10.1016/j.actbio.2017.01.056.

(27) Kuraitis, D.; Hosoyama, K.; Blackburn, N. J. R.; Deng, C.; Zhong, Z.; Suuronen, E. J. Functionalization of Soft Materials for Cardiac Repair and Regeneration. Crit. Rev. Biotechnol. 2019, 39 (4), 451–468. https://doi.org/10.1080/07388551.2019.1572587.

(28) O'Rourke, S. A.; Dunne, A.; Monaghan, M. G. The Role of Macrophages in the Infarcted Myocardium: Orchestrators of ECM Remodeling. Front. Cardiovasc. Med. 2019, 6 (101), 1–12. https://doi.org/10.3389/fcvm.2019.00101.

(29) Forte, E.; Furtado, M. B.; Rosenthal, N. The Interstitium in Cardiac Repair: Role of the Immune–Stromal Cell Interplay. Nat. Rev. Cardiol. 2018, 15 (10), 601–616. https://doi.org/10.1038/s41569-018-0077-x.

(30) Radisic, M.; Christman, K. L. Materials Science and Tissue Engineering: Repairing the Heart Milica. Mayo Clin. Proced. 2013, 88 (8), 884–898. https://doi.org/10.1016/j.mayocp.2013.05.003.

(31) Morrissette-mcalmon, J.; Ginn, B.; Somers, S.; Fukunishi, T.; Thanitcul, C.; Rindone, A.; Hibino, N.; Tung, L. Biomimetic Model of Contractile Cardiac Tissue with Endothelial Networks Stabilized by Adipose- Derived Stromal / Stem Cells. Sci. Rep. 2020, 10 (1), 1–12. https://doi.org/10.1038/s41598-020-65064-3.

(32) Chen, Q. Z.; Harding, S. E.; Ali, N. N.; Lyon, A. R.; Boccaccini, A. R. Biomaterials in Cardiac Tissue Engineering: Ten Years of Research Survey. Mater. Sci. Eng. R Reports 2008, 59, 1–37. https://doi.org/10.1016/j.mser.2007.08.001.

(33) Portillo-Lara, R.; Spencer, A. R.; Walker, B. W.; Shirzaei Sani, E.; Annabi, N. Biomimetic Cardiovascular Platforms for *in vitro* Disease Modeling and Therapeutic Validation. Biomaterials 2019, 198 (March 2018), 78–94. https://doi.org/10.1016/j.biomaterials.2018.08.010.

(34) Lu, H.; Hoshiba, T.; Kawazoe, N.; Chen, G. Autologous Extracellular Matrix Scaffolds for Tissue Engineering. Biomaterials 2011, 32 (10), 2489–2499. https://doi.org/10.1016/j.biomaterials.2010.12.016.

(35) Taylor, D. A.; Sampaio, L. C.; Ferdous, Z.; Gobin, A. S.; Taite, L. J. Decellularized Matrices in Regenerative Medicine. Acta Biomater. 2018, 74, 74–89. https://doi.org/10.1016/j.actbio.2018.04.044.

(36) Hinderer, S.; Layland, S. L.; Schenke-Layland, K. ECM and ECM-like Materials - Biomaterials for Applications in Regenerative Medicine and Cancer Therapy. Adv. Drug Deliv. Rev. 2016, 97, 260–269. https://doi.org/10.1016/j.addr.2015.11.019.

(37) Matai, I.; Kaur, G.; Seyedsalehi, A.; McClinton, A.; Laurencin, C. T. Progress in 3D Bioprinting Technology for Tissue/Organ Regenerative Engineering. Biomaterials 2020, 226, 1–32. https://doi.org/10.1016/j.biomaterials.2019.119536.

(38) Caddeo, S.; Boffito, M.; Sartori, S. Tissue Engineering Approaches in the Design of Healthy and Pathological *in vitro* Tissue Models. Front. Bioeng. Biotechnol. 2017, 5, 1–22. https://doi.org/10.3389/fbioe.2017.00040.

(39) Sharma, A.; McKeithan, W. L.; Serrano, R.; Kitani, T.; Burridge, P. W.; del Álamo, J. C.; Mercola, M.; Wu, J. C. Use of Human Induced Pluripotent Stem Cell–Derived Cardiomyocytes to Assess Drug Cardiotoxicity. Nat. Protoc. 2018, 13 (12), 3018–3041. https://doi.org/10.1038/s41596-018-0076-8.

(40) Ott, H. C.; Matthiesen, T. S.; Goh, S. K.; Black, L. D.; Kren, S. M.; Netoff, T. I.; Taylor, D. A. Perfusion-Decellularized Matrix: Using Nature's Platform to Engineer a Bioartificial Heart. Nat. Med. 2008, 14 (2), 213–221. https://doi.org/10.1038/nm1684.

(41) Lu, T. Y.; Lin, B.; Kim, J.; Sullivan, M.; Tobita, K.; Salama, G.; Yang, L. Repopulation of Decellularized Mouse Heart with Human Induced Pluripotent Stem Cell-Derived Cardiovascular Progenitor Cells. Nat. Commun. 2013, 4 (2307), 1–11. https://doi.org/10.1038/ncomms3307.

(42) Compton, C.; Canavan, J.; Mcleod, J.; Prevost, C.; Simionescu, D. Reconstitution of the Ventricular Endocardium Within Acellular Hearts. Regen. Eng. Transl. Med. 2020, 6, 90–100. https://doi.org/10.1007/s40883-019-00099-1.

(43) Taylor, D. A.; Frazier, O. H.; Elgalad, A.; Hochman-Mendez, C.; Sampaio, L. C. Building a Total Bioartificial Heart: Harnessing Nature to Overcome the Current Hurdles. Artif. Organs 2018, 42 (10), 970–982. https://doi.org/10.1111/aor.13336.

(44) Sánchez, P. L.; Fernández-Santos, M. E.; Costanza, S.; Climent, A. M.; Moscoso, I.; Gonzalez-Nicolas, M. A.; Sanz-Ruiz, R.; Rodríguez, H.; Kren, S. M.; Garrido, G.; et al. Acellular Human Heart Matrix: A Critical Step toward Whole Heart Grafts. Biomaterials 2015, 61, 279–289. https://doi.org/10.1016/j.biomaterials.2015.04.056.

(45) Guyette, J. P.; Charest, J. M.; Mills, R. W.; Jank, B. J.; Moser, P. T.; Gilpin, S. E.; Gershlak, J. R.; Okamoto, T.; Gonzalez, G.; Milan, D. J.; et al. Bioengineering Human Myocardium on Native Extracellular Matrix. Circ. Res. 2016, 118 (1), 56–72. https://doi.org/10.1161/CIRCRESAHA.115.306874.

(46) Ravichandran, R.; Islam, M. M.; Alarcon, E. I.; Samanta, A.; Wang, S.; Lundström, P.; Hilborn, J.; Griffith, M.; Phopase, J. Functionalised Type-I Collagen as a Hydrogel Building Block for Bio-Orthogonal Tissue Engineering Applications. J. Mater. Chem. B 2015, 4 (2), 318–326. https://doi.org/10.1039/c5tb02035b.

(47) Sun, H.; Zhou, J.; Huang, Z.; Qu, L.; Lin, N.; Liang, C.; Dai, R.; Tang, L.; Tian, F. Carbon Nanotube-Incorporated Collagen Hydrogels Improve Cell Alignment and the Performance of Cardiac Constructs. Int. J. Nanomedicine 2017, 12, 3109–3120. https://doi.org/10.2147/IJN.S128030.

(48) Kambe, Y.; Tokushige, T.; Mahara, A.; Iwasaki, Y.; Yamaoka, T. Cardiac Differentiation of Induced Pluripotent Stem Cells on Elastin-like Protein-Based Hydrogels Presenting a Single-Cell Adhesion Sequence. Polym. J. 2019, 51 (1), 97–105. https://doi.org/10.1038/s41428-018-0110-2.

(49) Vu, T. D.; Pal, S. N.; Ti, L. K.; Martinez, E. C.; Rufaihah, A. J.; Ling, L. H.; Lee, C. N.; Richards, A. M.; Kofidis, T. An Autologous Platelet-Rich Plasma Hydrogel Compound Restores Left Ventricular Structure, Function and Ameliorates Adverse Remodeling in a Minimally Invasive Large Animal Myocardial Restoration Model: A Translational Approach. Vu and Pal "Myocardial Repai. Biomaterials 2015, 45, 27–35. https://doi.org/10.1016/j.biomaterials.2014.12.013.

(50) Williams, C.; Budina, E.; Stoppel, W. L.; Sullivan, K. E.; Emani, S.; Emani, S. M.; Black III, L. D. Cardiac Extracellular Matrix-Fibrin Hybrid Scaffolds with Tunable Properties for Cardiovascular Tissue Engineering. Acta Biomater. 2015, 14, 84–95. https://doi.org/10.1016/j.actbio.2014.11.035.

(51) Wang, Z.; Long, D. W.; Huang, Y.; Chen, W. C. W.; Kim, K.; Wang, Y. Decellularized Neonatal Cardiac Extracellular Matrix Prevents Widespread Ventricular Remodeling in Adult Mammals after Myocardial Infarction. Acta Biomater. 2019, 87, 140–151. https://doi.org/10.1016/j.actbio.2019.01.062.

(52) Chen, W. C. W.; Wang, Z.; Missinato, M. A.; Park, D. W.; Long, D. W.; Liu, H. J.; Zeng, X.; Yates, N. A.; Kim, K.; Wang, Y. Decellularized Zebrafish Cardiac Extracellular Matrix Induces Mammalian Heart Regeneration. Sci. Adv. 2016, 2 (11), 1600844–1600859. https://doi.org/10.1126/sciadv.1600844.

(53) Henry, J. J. D.; Delrosario, L.; Fang, J.; Wong, S. Y.; Fang, Q.; Sievers, R.; Kotha, S.; Wang, A.; Farmer, D.; Janaswamy, P.; et al. Development of Injectable Amniotic Membrane Matrix for Postmyocardial Infarction Tissue Repair. Adv. Healthc. Mater. 2020, 9 (2), 1–8. https://doi.org/10.1002/adhm.201900544.

(54) Francis, M. P.; Breathwaite, E.; Bulysheva, A. A.; Varghese, F.; Rodriguez, R. U.; Dutta, S.; Semenov, I.; Ogle, R.; Huber, A.; Tichy, A. M.; et al. Human Placenta Hydrogel Reduces Scarring

in a Rat Model of Cardiac Ischemia and Enhances Cardiomyocyte and Stem Cell Cultures. Acta Biomater. 2017, 52, 92–104. https://doi.org/10.1016/j.actbio.2016.12.027.

(55) Shah, M.; Kc, P.; Zhang, G. *In vivo* Assessment of Decellularized Porcine Myocardial Slice as an Acellular Cardiac Patch. ACS Appl. Mater. Interfaces 2019, 11 (27), 23893–23900. https://doi.org/10.1021/acsami.9b06453.

(56) Wang, Q.; Yang, H.; Bai, A.; Jiang, W.; Li, X.; Wang, X.; Mao, Y.; Lu, C.; Qian, R.; Guo, F.; et al. Functional Engineered Human Cardiac Patches Prepared from Nature's Platform Improve Heart Function after Acute Myocardial Infarction. Biomaterials 2016, 105, 52–65. https://doi.org/10.1016/j.biomaterials.2016.07.035.

(57) Blazeski, A.; Lowenthal, J.; Zhu, R.; Ewoldt, J.; Boheler, K. R.; Tung, L. Functional Properties of Engineered Heart Slices Incorporating Human Induced Pluripotent Stem Cell-Derived Cardiomyocytes. Stem Cell Reports 2019, 12, 982–995. https://doi.org/10.1016/j.stemcr.2019.04.002.

(58) Parveen, S.; Singh, S. P.; Panicker, M. M.; Gupta, P. K. Amniotic Membrane as Novel Scaffold for Human IPSC-Derived Cardiomyogenesis. Vitr. Cell. Dev. Biol. - Anim. 2019, 55 (4), 272–284. https://doi.org/10.1007/s11626-019-00321-y.

(59) Kaiser, N. J.; Kant, R. J.; Minor, A. J.; Coulombe, K. L. K. Optimizing Blended Collagen-Fibrin Hydrogels for Cardiac Tissue Engineering with Human IPSC-Derived Cardiomyocytes. ACS Biomater. Sci. Eng. 2019, 5 (2), 887–899. https://doi.org/10.1021/acsbiomaterials.8b01112.

(60) Mattapally, S.; Zhu, W.; Fast, V. G.; Gao, L.; Worley, C.; Kannappan, R.; Borovjagin, A. V.; Zhang, J. Spheroids of Cardiomyocytes Derived from Human-Induced Pluripotent Stem Cells Improve Recovery from Myocardial Injury in Mice. Am. J. Physiol. - Hear. Circ. Physiol. 2018, 315 (2), H327–H339. https://doi.org/10.1152/ajpheart.00688.2017.

(61) Bejleri, D.; Streeter, B. W.; Nachlas, A. L. Y.; Brown, M. E.; Gaetani, R.; Christman, K. L.; Davis, M. E. A Bioprinted Cardiac Patch Composed of Cardiac-Specific Extracellular Matrix and Progenitor Cells for Heart Repair. Adv. Healthc. Mater. 2018, 7 (23), 1–13. https://doi.org/10.1002/adhm.201800672.

(62) Annabi, N.; Tsang, K.; Mithieux, S. M.; Nikkhah, M.; Ameri, A.; Khademhosseini, A.; Weiss, A. S. Highly Elastic Micropatterned Hydrogel for Engineering Functional Cardiac Tissue. Adv. Funct. Mater. 2013, 23 (39), 4950–4959. https://doi.org/10.1002/adfm.201300570.

(63) Zhang, F.; Zhang, N.; Meng, H. X.; Liu, H. X.; Lu, Y. Q.; Liu, C. M.; Zhang, Z. M.; Qu, K. Y.; Huang, N. P. Easy Applied Gelatin-Based Hydrogel System for Long-Term Functional Cardiomyocyte Culture and Myocardium Formation. ACS Biomater. Sci. Eng. 2019, No. May. https://doi.org/10.1021/acsbiomaterials.9b00515.

(64) Wang, Z.; Lee, S. J.; Cheng, H. J.; Yoo, J. J.; Atala, A. 3D Bioprinted Functional and Contractile Cardiac Tissue Constructs. Acta Biomater. 2018, 70, 48–56. https://doi.org/10.1016/j.actbio.2018.02.007.

(65) Iop, L.; Dal Sasso, E.; Menabo, R.; Di Lisa, F.; Gerosa, G. The Rapidly Evolving Concept of Whole Heart Engineering. Stem Cells Int. Int. 2017, 1–18.

(66) Tapias, L. F.; Ott, H. C. Decellularized Scaffolds as a Platform for Bioengineered Organs. Curr. Opin. Organ Transplant. 2015, 19 (2), 145–152. https://doi.org/10.1097/MOT.0000000000000051.Decellularized.

(67) Gilbert, T. W.; Sellaro, T. L.; Badylak, S. F. Decellularization of Tissues and Organs. Biomaterials 2006, 27 (19), 3675–3683. https://doi.org/10.1016/j.biomaterials.2006.02.014.

(68) Barreto, R. S. N.; Romagnolli, P.; Fratini, P.; Mess, A. M.; Miglino, M. A. Mouse Placental Scaffolds: A Three-Dimensional Environment Model for Recellularization. J. Tissue Eng. 2019, 10, 1–11. https://doi.org/10.1177/2041731419867962.

(69) Nguyen, D. T.; O'Hara, M.; Graneli, C.; Hicks, R.; Miliotis, T.; Nyström, A. C.; Hansson, S.; Davidsson, P.; Gan, L. M.; Magnone, M. C.; et al. Humanizing Miniature Hearts through 4-Flow Cannulation Perfusion Decellularization and Recellularization. Sci. Rep. 2018, 8 (7458), 1–10. https://doi.org/10.1038/s41598-018-25883-x.

(70) Taylor, D. A.; Elgalad, A.; Sampaio, L. C. What Will It Take before a Bioengineered Heart Will Be Implanted in Patients? Curr. Opin. Organ Transplant. 2018, 23 (6), 664–672. https://doi.org/10.1097/MOT.0000000000000583.

(71) Hoffman, A. S. Hydrogels for Biomedical Applications. Adv. Drug Deliv. Rev. 2012, 64, 18–23. https://doi.org/10.1016/j.addr.2012.09.010.

(72) Tanaka, Y.; Gong, J. P.; Osada, Y. Novel Hydrogels with Excellent Mechanical Performance. Prog. Polym. Sci. 2005, 30 (1), 1–9. https://doi.org/10.1016/j.progpolymsci.2004.11.003.

(73) Saludas, L.; Pascual-Gil, S.; Prósper, F.; Garbayo, E.; Blanco-Prieto, M. Hydrogel Based Approaches for Cardiac Tissue Engineering. Int. J. Pharm. 2017, 523 (2), 454–475. https://doi.org/10.1016/j.ijpharm.2016.10.061.

(74) Mallick, S. P.; Suman, D. K.; Singh, B. N.; Srivastava, P.; Siddiqui, N.; Yella, V. R.; Madhual, A.; Vemuri, P. K. Strategies toward Development of Biodegradable Hydrogels for Biomedical Applications. Polym. Technol. Mater. 2020, 59 (9), 911–927. https://doi.org/10.1080/25740881.2020.1719135.

(75) Ahmed, E. M. Hydrogel: Preparation, Characterization, and Applications: A Review. J. Adv. Res. 2015, 6 (2), 105–121. https://doi.org/10.1016/j.jare.2013.07.006.

(76) Yu, L.; Ding, J. Injectable Hydrogels as Unique Biomedical Materials. Chem. Soc. Rev. 2008, 37 (8), 1473–1481. https://doi.org/10.1039/b713009k.

(77) Yang, J. A.; Yeom, J.; Hwang, B. W.; Hoffman, A. S.; Hahn, S. K. In Situ-Forming Injectable Hydrogels for Regenerative Medicine. Prog. Polym. Sci. 2014, 39 (12), 1973–1986. https://doi.org/10.1016/j.progpolymsci.2014.07.006.

(78) Custódio, C. A.; Reis, R. L.; Mano, J. F. Photo-Cross-Linked Laminarin-Based Hydrogels for Biomedical Applications. Biomacromolecules 2016, 17 (5), 1602–1609.

(79) Li, Y.; Rodrigues, J.; Tomás, H. Injectable and Biodegradable Hydrogels: Gelation, Biodegradation and Biomedical Applications. Chem. Soc. Rev. 2012, 41 (6), 2193–2221. https://doi.org/10.1039/c1cs15203c.

(80) Wu, W.; Peng, S.; Song, Z.; Lin, S. Collagen Biomaterial for the Treatment of Myocardial Infarction : An Update on Cardiac Tissue Engineering and Myocardial Regeneration. Drug Deliv. Transl. Res. 2019, 9, 920–934.

(81) Ahmadi, A.; McNeill, B.; Vulesevic, B.; Kordos, M.; Mesana, L.; Thorn, S.; Renaud, J. M.; Manthorp, E.; Kuraitis, D.; Toeg, H.; et al. The Role of Integrin A2 in Cell and Matrix Therapy That Improves Perfusion, Viability and Function of Infarcted Myocardium. Biomaterials 2014, 35 (17), 4749–4758.

(82) Bhana, B.; Iyer, R. K.; Chen, W. L. K.; Zhao, R.; Sider, K. L.; Likhitpanichkul, M.; Simmons, C. A.; Radisic, M. Influence of Substrate Stiffness on the Phenotype of Heart Cells. Biotechnol. Bioeng. 2010, 105 (6), 1148–1160. https://doi.org/10.1002/bit.22647.

(83) Wang, Q.; Liew, K. M. Mechanical Properties of Carbon Nanotubes. Appl. Phys. A Mater. Sci. Process. 1999, 69, 255–260. https://doi.org/10.1007/s003399900114.

(84) Ramón-Azcón, J.; Ahadian, S.; Obregón, R.; Shiku, H.; Ramalingam, M.; Matsue, T. Applications of Carbon Nanotubes in Stem Cell Research. J. Biomed. Nanotechnol. 2014, 10 (10), 2539–2561. https://doi.org/10.1166/jbn.2014.1899.

(85) Robinet, A.; Fahem, A.; Cauchard, J.; Huet, E.; Vincent, L.; Lorimier, S.; Antonicelli, F.; Soria, C.; Crepin, M.; Hornebeck, W.; et al. Elastin-Derived Peptides Enhance Angiogenesis by Promoting Endothelial Cell Migration and Tubulogenesis through Upregulation of MT1-MMP. J. Cell Sci. 2005, 118 (2), 343–356. https://doi.org/10.1242/jcs.01613.

(86) Hoshiba, T.; Lu, H.; Kawazoe, N.; Chen, G. Decellularized Matrices for Tissue Engineering. Expert Opin. Biol. Ther. 2010, 10 (12), 1717–1728.

(87) Seo, Y.; Jung, Y.; Kim, S. H. Decellularized Heart ECM Hydrogel Using Supercritical Carbon Dioxide for Improved Angiogenesis. Acta Biomater. 2018, 67, 270–281. https://doi.org/10.1016/j.actbio.2017.11.046.

(88) Seif-Naraghi, S. B.; Singelyn, J. M.; Salvatore, M. A.; Osborn, K. G.; Wang, J. J.; Sampat, U.; Kwan, O. L.; Strachan, G. M.; Wong, J.; Schup-Magoffin, P. J.; et al. Safety and Efficacy of an Injectable Extracellular Matrix Hydrogel for Treating Myocardial Infarction. Sci. Transl. Med. 2013, 5 (173), 173ra25.

(89) Gupta, A.; Kedige, S. D.; Jain, K. Amnion and Chorion Membranes: Potential Stem Cell Reservoir with Wide Applications in Periodontics. Int. J. Biomater. 2015, 2015, 1–9. https://doi.org/10.1155/2015/274082.

(90) Schneider, K. H.; Aigner, P.; Holnthoner, W.; Monforte, X.; Nürnberger, S.; Rünzler, D.; Redl, H.; Teuschl, A. H. Decellularized Human Placenta Chorion Matrix as a Favorable Source of Small-Diameter Vascular Grafts. Acta Biomater. 2016, 29, 125–134. https://doi.org/10.1016/j.actbio.2015.09.038.

(91) Kleinman, H. K.; Martin, G. R. Matrigel: Basement Membrane Matrix with Biological Activity. Semin. Cancer Biol. 2005, 15 (5 SPEC. ISS.), 378–386. https://doi.org/10.1016/j.semcancer.2005.05.004.

(92) Salo, T.; Sutinen, M.; Hoque Apu, E.; Sundquist, E.; Cervigne, N. K.; de Oliveira, C. E.; Akram, S. U.; Ohlmeier, S.; Suomi, F.; Eklund, L.; et al. A Novel Human Leiomyoma Tissue Derived Matrix for Cell Culture Studies. BMC Cancer 2015, 15 (981), 2–16. https://doi.org/10.1186/s12885-015-1944-z.

(93) Cao, J.; Poss, K. D. The Epicardium as a Hub for Heart Regeneration. Nat. Rev. Cardiol. 2018, 15 (10), 631–647. https://doi.org/10.1038/s41569-018-0046-4.

(94) Beans, C. The Race to Patch the Human Heart. Proc. Natl. Acad. Sci. U. S. A. 2018, 115 (26), 6518–6520. https://doi.org/10.1073/pnas.1808317115.

(95) Zhang, J.; Zhu, W.; Radisic, M.; Vunjak-Novakovic, G. Can We Engineer a Human Cardiac Patch for Therapy? Circ. Res. 2018, 123 (2), 244–265. https://doi.org/10.1161/CIRCRESAHA.118.311213.

(96) Tomov, M. L.; Gil, C. J.; Cetnar, A.; Theus, A. S.; Lima, B. J.; Nish, J. E.; Bauser-Heaton, H. D.; Serpooshan, V. Engineering Functional Cardiac Tissues for Regenerative Medicine Applications. Curr. Cardiol. Rep. 2019, 21 (9). https://doi.org/10.1007/s11886-019-1178-9.

(97) Gaharwar, A. K.; Singh, I.; Khademhosseini, A. Engineered Biomaterials for in Situ Tissue Regeneration. Nat. Rev. Mater. 2020. https://doi.org/10.1038/s41578-020-0209-x.

(98) Aubin, H.; Nichol, J. W.; Hutson, C. B.; Bae, H.; Sieminski, A. L.; Cropek, D. M.; Akhyari, P.; Khademhosseini, A. Directed 3D Cell Alignment and Elongation in Microengineered Hydrogels. Biomaterials 2010, 31 (27), 6941–6951. https://doi.org/10.1038/jid.2014.371.

(99) Roy, R.; Haase, T.; Ma, N.; Bader, A.; Becker, M.; Seifert, M.; Choi, Y. H.; Falk, V.; Stamm, C. Decellularized Amniotic Membrane Attenuates Postinfarct Left Ventricular Remodeling. J. Surg. Res. 2016, 200 (2), 409–419. https://doi.org/10.1016/j.jss.2015.08.022.

(100) Lim, J. J.; Fonger, J.; Koob, T. J. Dehydrated Human Amnion/Chorion Membrane Allograft Promotes Cardiac Repair Following Myocardial Infarction. J. Cardiol. Cardiovasc. Ther. 2017, 2 (5), 2–7. https://doi.org/10.19080/jocct.2017.02.555599.

(101) Dubbin, K.; Robertson, C.; Hinckley, A.; Alvarado, J. A.; Gilmore, S. F.; Hynes, W. F.; Wheeler, E. K.; Moya, M. L. Macromolecular Gelatin Properties Affect Fibrin Microarchitecture and Tumor Spheroid Behavior in Fibrin-Gelatin Gels. Biomaterials 2020, 250, 120035–100047. https://doi.org/10.1016/j.biomaterials.2020.120035.

(102) Gaetani, R.; Feyen, D. A. M.; Verhage, V.; Slaats, R.; Messina, E.; Christman, K. L.; Giacomello, A.; Doevendans, P. A. F. M.; Sluijter, J. P. G. Epicardial Application of Cardiac Progenitor Cells in a 3D-Printed Gelatin/Hyaluronic Acid Patch Preserves Cardiac Function after Myocardial Infarction. Biomaterials 2015, 61, 339–348. https://doi.org/https://doi.org/10.1016/j.biomaterials.2015.05.005.

(103) Buj-Corral, I.; Bagheri, A.; Petit-Rojo, O. 3D Printing of Porous Scaffolds with Controlled Porosity and Pore Size Values. Materials (Basel). 2018, 11 (9), 1–18. https://doi.org/10.3390/ma11091532.

(104) Tay, C. Y.; Yu, H.; Pal, M.; Leong, W. S.; Tan, N. S.; Ng, K. W.; Leong, D. T.; Tan, L. P. Micropatterned Matrix Directs Differentiation of Human Mesenchymal Stem Cells towards Myocardial Lineage. Exp. Cell Res. 2010, 316 (7), 1159–1168. https://doi.org/https://doi.org/10.1016/j.yexcr.2010.02.010.

(105) Tijore, A.; Irvine, S. A.; Sarig, U.; Mhaisalkar, P.; Baisane, V.; Venkatraman, S. Contact Guidance for Cardiac Tissue Engineering Using 3D Bioprinted Gelatin Patterned Hydrogel. Biofabrication 2018, 10 (2), 25003.

(106) Kim, S.-H.; Lee, G. H.; Park, J. Y. Microwell Fabrication Methods and Applications for Cellular Studies. Biomed. Eng. Lett. 2013, 3 (3), 131–137.

(107) Luong-van, E. K.; Madanagopal, T. T.; Rosa, V. Mechanisms of Graphene in Fl Uence on Cell Differentiation. Mater. Today Chem. 2020, 16, 100250–100265. https://doi.org/10.1016/j.mtchem.2020.100250.

(108) Wu, T.; Cui, C.; Huang, Y.; Liu, Y.; Fan, C.; Han, X.; Yang, Y.; Xu, Z.; Liu, B.; Fan, G.; et al. Coadministration of an Adhesive Conductive Hydrogel Patch and an Injectable Hydrogel to Treat Myocardial Infarction. Am. Chem. Soc. 2020, 12, 2039–2048. https://doi.org/10.1021/acsami.9b17907.

(109) Traverse, J. H.; Henry, T. D.; Dib, N.; Patel, A. N.; Pepine, C.; Schaer, G. L.; DeQuach, J. A.; Kinsey, A. M.; Chamberlin, P.; Christman, K. L. First-in-Man Study of a Cardiac Extracellular Matrix Hydrogel in Early and Late Myocardial Infarction Patients. JACC Basic to Transl. Sci. 2019, 4 (6), 1–11. https://doi.org/10.1016/j.jacbts.2019.07.012.

(110) Prat-Vidal, C.; Rodriguez-Gómez, L.; Aylagas, M.; Nieto-Nicolau, N.; Gastelurrutia, P.; Agusti, E.; Gálvez-Montón, C.; Jorba, I.; Teis, A.; Monguió-Tortajada, M.; et al. First-in-Human PeriCord Cardiac Bioimplant: Scalability and GMP Manufacturing of an Allogeneic Engineered Tissue Graft. EBioMedicine 2020, 54, 102729.

(111) Xuanyi, M.; Zhu, W.; Tang, M.; Lawrence, N.; Yu, C.; Gou, M.; Chen, S. 3D Bioprinting of Functional Tissue Models for Personalized Drug Screening and *in vitro* Disease Modeling. Adv. Drug Deliv. Rev. 2018, 132, 235–251. https://doi.org/10.1016/j.physbeh.2017.03.040.

(112) Caddeo, S.; Boffito, M.; Sartori, S. Tissue Engineering Approaches in the Design of Healthy and Pathological *in vitro* Tissue Models. Front. Bioeng. Biotechnol. 2017, 5 (AUG), 1–22. https://doi.org/10.3389/fbioe.2017.00040.

(113) Howard, D.; Buttery, L. D.; Shakesheff, K. M.; Roberts, S. J. Tissue Engineering: Strategies, Stem Cells and Scaffolds. J. Anat. 2008, 213 (1), 66–72. https://doi.org/10.1111/j.1469-7580.2008.00878.x.

(114) de Miguel-Beriain, I. The Ethics of Stem Cells Revisited. Adv. Drug Deliv. Rev. 2015, 82, 176–180. https://doi.org/10.1016/j.addr.2014.11.011.

(115) Ji, S. T.; Kim, H.; Yun, J.; Chung, J. S.; Kwon, S. M. Promising Therapeutic Strategies for Mesenchymal Stem Cell-Based Cardiovascular Regeneration: From Cell Priming to Tissue Engineering. Stem Cells Int. 2017, 2017, 1–13. https://doi.org/10.1155/2017/3945403.

(116) Golpanian, S.; Wolf, A.; Hatzistergos, K. E.; Hare, J. M. Rebuilding the Damaged Heart: Mesenchymal Stem Cells, Cell-Based Therapy, and Engineered Heart Tissue. Physiol. Rev. 2016, 96 (3), 1127–1168. https://doi.org/10.1152/physrev.00019.2015.

(117) Karakikes, I.; Ameen, M.; Termglinchan, V.; Wu, J. C. Human Induced Pluripotent Stem Cell-Derived Cardiomyocytes: Insights into Molecular, Cellular, and Functional Phenotypes. Circ. Res. 2015, 117, 80–88. https://doi.org/10.1161/CIRCRESAHA.117.305365.

Chapter III

Materials and Methods

Materials and Methods

1. Placenta collection

In order to obtain chorion membranes for this study, placentas were collected at the Hospital Infante D. Pedro from Aveiro, through a collaboration with the COMPASS Research Group. The use of human placenta was approved by the institutional ethics and deontology committee from both institutions. Informed consent from the donors were obtained for all placentas used in this study.

Prior to the placenta collection, a plastic container with 2.5 L of capacity was sterilized under UV light for 30 minutes. After sterilization, was added 1% of antibiotic/antimycotic containing 10,000 units.mL^{-1} of penicillin, 10,000 µg.mL^{-1} of streptomycin, and 25 µg.mL^{-1} of Gibco Amphotericin B (Thermo Fisher Scientific, USA) and 200 mL Dulbecco's Phosphate Buffered Saline without calcium or magnesium (DPBS, Corning, USA) under sterile conditions, in order to avoid bacterial and fungicidal contamination, whereas keep the placentas immersed during the interval between collection and processing. The container to collect the samples was closed inside the flow chamber to maintain the sterile conditions inside and a labeled. Finally, the container was delivered together with the informed consents in the hospital.

2. Chorionic membrane (CM) isolation and decellularization

For the chorionic membrane (CM) isolation, the bottom of the flow chamber was covered with aluminum foil pulverized with 70% ethanol, and all the following materials were also placed inside the flow chamber and pulverized with 70% ethanol: a tray, two Petri dishes, an empty hospital samples container to store the waste to be incinerated. The laminar flow chamber was sterilized under UV light for 30 minutes. Thereafter the 30 minutes of UV light, the following autoclaved instruments were placed inside the flow chamber: tweezers, a scissor, and a scalpel. Also, the container with the placenta was placed inside the flow chamber, and the placenta was transferred to the tray. The umbilical cord face was placed upward with tweezers, the amniotic membrane was detached, the umbilical cord was cut and then chorion membrane (CM) was cut around the chorionic plate. The CM was transferred to the Petri dish and cut into smaller pieces.

Decellularization of CM aims to remove cells whereas preserving the native composition of extracellular matrix (ECM) [1]. The steps usually associated with decellularization are

preformed firstly by lysis of the cell membrane, secondly by separation of cellular components from the ECM, then solubilization of cytoplasmic and nuclear cellular components and lastly removal of cellular debris from the tissue [2].

Many strategies have been used to decellularized organs and tissues as chemical, physical, or enzymatic approaches. However, there is no ideal method, as they all have advantages and disadvantages, hence a combination of strategies is often applied [1,3,4]. Here was also used a mixed protocol including the three approaches: chemical using detergents or enzymatic using nucleases associated with physical using mechanical agitation in order to increase the effectiveness of all process in cellular disruption [5]. The detergents chosen were the Sodium Dodecyl Sulfate (SDS) and Triton X-100. SDS is the ionic detergent most commonly used in tissues decellularization due to its high capacity to disrupt native tissue structure solubilizing both cytoplasmic and nuclear cellular membranes [1,2,5]. However, as SDS is cytotoxic, if any remnants remain in the decellularized tissue, it may have adverse effects when in contact with cells. To avoid that and to remove residual SDS was then used an anionic detergent, the Triton X-100 [6,7]. In fact, the anionic detergents are often more easily removed from the experimental system since they have polar headgroups that carry no charge [8,9]. Moreover, Triton X-100 is milder to the tissues, since it only disrupts lipid-lipid and lipid-protein interactions, yet preserving protein-protein interactions intact [2]. Due to the "sticky" nature of DNA and RNA and its tendency to adhere to ECM proteins, this was followed by a step to removal of DNA and RNA remnants. This was done by incubation with endonucleases DNase and RNase in Trizma® hydrochloride (Tris-HCl) buffer and magnesium chloride hexahydrate ($MgCl_2.6H_2O$). The Tris-HCl beyond having an effect in cell lysis by osmotic shock also has the capacity to promote protein-DNA disruptions. As it has no role in the removal of cellular debris, the use of the referred endonucleases is crucial to break down nucleic acid fragments reducing its length in order to promote more efficient removal of residual cellular debris and consequently preventing significant immunogenic responses [2,5,7,9]. As the reaction conditions for RNase A are rather flexible, they could be chosen taking into account conditions most suitable for DNase I. As for instance, DNase I requires a co-factor for its activation, being used, in this case, $MgCl_2.6H_2O$ to provide Mg^{2+}. Furthermore, as the DNase I, in the presence of Mg^{2+} has its optimal temperature at 37ºC and RNase A also has high activity at that temperature, the reaction should be performed in an incubator at 37ºC [10–12]. For the decellularization, CM was placed into 50 mL falcon tubes

and incubated with 30 mL of 1% SDS solution. Then the falcons were placed in rotation at 25 rpm for 16 hours at RT in the Multi-Purpose Tube Rotator (Fisherbrand™, Thermo Fisher Scientific). After that, the CM was incubated with 35 mL of 1% Triton™ X-100 BioXtra (Sigma-Aldrich, USA) and placed again on the tube rotator for 30 minutes at 25 rpm, at RT in order to finalize cell content extraction and to remove the residual SDS. The CM was washed three times to remove the detergent, being transferred to new Falcon tubes with 35mL DPBS and placed on tube rotator for 15 minutes between washes. Subsequently were produced 30 mL of a nuclease solution (50 mM Trizma® hydrochloride (Tris HCl, Sigma), 10 mM magnesium chloride hexahydrate ($MgCl_2.6H_2O$, Panreac, Spain), adding 70 µL recombinant DNase I (STEMCELL™ Technologies, Canada), and 30 µL of bovine pancreatic PureLink™ RNase A ((20 $mg.mL^{-1}$), Sigma). Were added 10 mL to each falcon and incubated at 37 °C for 3 h, under continuous stirring in the Compact Digital Microplate Shaker (Thermo Fisher Scientific). The decellularized CM (dCM) was washed again as previously described, frozen with liquid nitrogen, lyophilized and stored at -20°C until further use.

To confirm the decellularization efficiency, a piece of fresh non-decellularized CM and a piece of decellularized were fixed in fixed in 4% formaldehyde (Sigma-Aldrich) overnight at room temperature (RT). After that, samples were stained with a 4',6'-diamino-2-fenil-indol (DAPI, 5 $\mu g.mL^{-1}$, Thermo Fisher Scientific) solution diluted 1:1000 in PBS incubating for 5 minutes at RT, protected from light. After PBS washes, the CM pieces were observed under a fluorescence microscope (Fluorescence Microscope Zeiss, Axio Imager 2, Carl Zeiss, Germany).

DNA quantification was also performed to evaluate the efficiency of the decellularization process. To quantify double-stranded DNA (dsDNA) per mg of dry ECM from non-decellularized CM and dCM, was used the Quant-iT™ PicoGreen® dsDNA kit (Invitrogen, Thermo Fisher Scientific). PicoGreen reagent is an ultra-sensitive fluorescent nucleic acid stain that binds to AT- or GC- regions with low selectivity. To do that, 5 g of CM (n = 3) and dCM (n = 2) were digested in 1 mL of papain at 65 ºC for 16 h. Afterwards, was performed a centrifugation (10000 g, 10 minutes) and the pellet was diluted (1 : 1) in 1 X TRIS-EDTA buffer. To achieve a standard curve, were prepared dsDNA standards with concentrations ranging between 0 and 1 $ug.mL^{-1}$. Both samples and standards were incubated with Picogreen reagent for 5 minutes at RT, protected from light. Fluorescence was

measured using an excitation wavelength of 480 nm and an emission wavelength of 528 nm in a 96-well flat-bottom opaque black plate using Synergy HTX microplate reader (BioTek Instruments, Winooski, USA).

3. dCM solubilization

In order to solubilize ECM components, was used pepsin. Pepsin is a gastric enzyme with its highest enzymatic activity at a pH of 2 and a temperature between 37 - 40 ºC, capable of hydrolyzing specific peptide bonds in proteins [13]. This enzyme preferentially cleaves C terminal bonds from peptides containing linkages with aromatic residues (phenylalanine, tyrosine and tryptophan) or leucine. Nevertheless, all other natural amino acids (with exception of proline and isoleucine) may be cleaved by pepsin. Furthermore, pepsin has the capacity to cleave the telopeptide bonds of collagen triple helix structure to unravel collagen fibril aggregates [14,15]. In order to achieve a low pH, usually pepsin is incubated with a diluted acid solution, being the most used hydrochloric acid (HCl) and acetic acid. Skierka *et al* [16] compared different acids with pepsin and concluded that the yield of collagen using pepsin and acetic acid was ≈ 90%, while with HCl yielding was ≈ 18%. Moreover, Delgado *et al* [17], compared both acids in collagen extraction and observed high yield, high purity and low macrophage response, using pepsin with acetic acid. Hence the chosen acid was the acetic acid. For the digestion, dCM was incubated with a solution of pepsin (Promega, USA) (1 $mg.mL^{-1}$) in 0.5 M acetic acid (Glacial, 99-100%, CHEM-LAB, Belgium) at a ratio of 10 mg sample per mL of pepsin solution. The solution was stirred in the Multi-Purpose Tube Rotator for 3 days with 50 rpm at RT. After that, the undigested pieces were separated from the solution using a 380 µm sieve. A separation phase step was performed to purify and concentrate solubilized dCM proteins. This step allows to separate the membrane proteins from the solution containing soluble proteins and other hydrophilic impurities. The addition of the salt NaCl provides ions with high charge density and causes a process called salting-out. The salting-out effect occurs since there is not enough free water available to keep the protein fully hydrated and thus, soluble. Hence, the combination of electronic repulsions and enhancement of the hydrophobic effect in pure water are the responsible forces for protein precipitation through salting out. Likewise, the detergent micelles aggregate [18,19]. NaCl was added to a final concentration of 5% (w/v) and stirred in the Multi-Purpose Tube Rotator overnight at RT with 50 rpm. This was followed by a centrifugation step at 10.000 rpm at 4ºC for 15 minutes. The precipitate was collected and the precipitation step was repeated 4

times in the supernatant. Finally, the precipitated proteins were dissolved in 1.0 M acetic acid and the solution purified by dialysis using a membrane with a cutoff of 3.5 kDa (SnakeSkin™, Thermo Fisher Scientific) for at least 24h against distilled water at 4°C, in order to remove NaCl, remaining detergent and acetic acid. Pepsin cannot be removed by dialysis, as its molecular weight is 34.5 kDa, however, as dialysis is against water, increases the pH of the solution and consequently, irreversibly denatures the pepsin. After that, the solution was frozen with liquid nitrogen, lyophilized (LyoQuest Plus Eco, Telstar, Spain) and stored at -20°C until further use. A schematic image of the employed methods in this study is represented in **Figure III.1**.

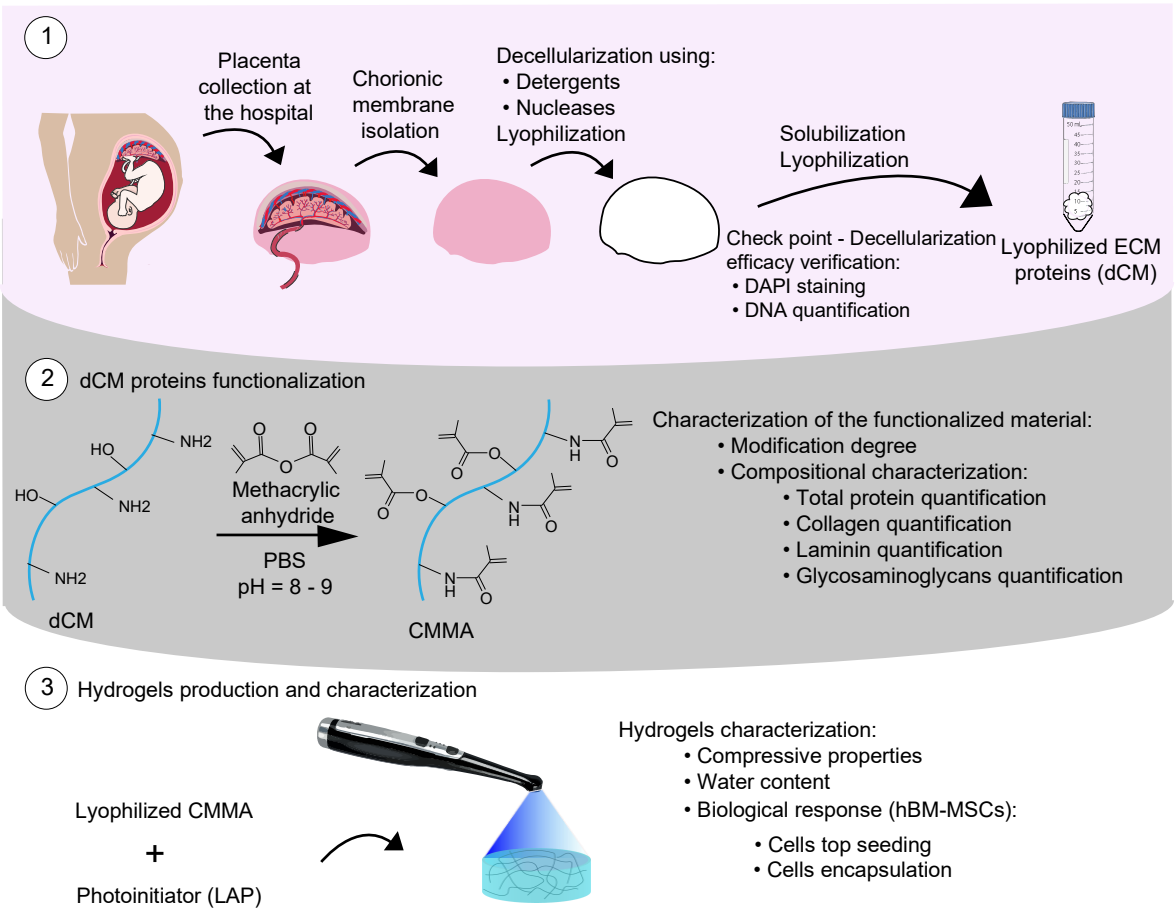

Figure III.1. Schematic image of methods employed in this work.

4. dCM proteins functionalization

Conventionally, ECM derived hydrogels have poor mechanical properties, making them prone to functional failure. As a way to overcome this, alternatives have emerged, as for instance polymer functionalization, to generate mechanically strong and stable hydrogels [20,21]. Here we propose the modification of dCM derived proteins with acrylate groups to yield photocrosslinkable dCM – methacrylate (CMMA) (**Figure III.2**).

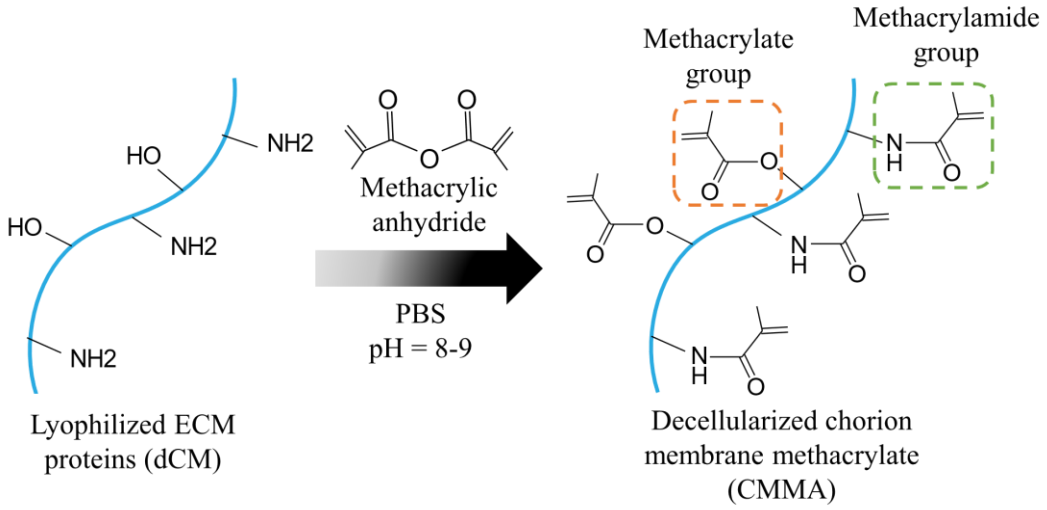

Figure III.2 Schematic representation of the methacrylation reaction of dCM derived proteins. dCM proteins are dissolved in PBS and reacted with methacrylic anhydride at pH controlled to 8-9 producing methacrylate and methacrylamide groups.

In brief, CMMA was synthesized by reacting dCM with methacrylic anhydride (MA) 94% (Sigma, Germany). To do that, dCM was solubilized in PBS (Sigma-Aldrich Germany) at a concentration of 1% (w/v), and subsequently, either 100 µL or 250 µL of MA per 10 mL of solution were added, to synthesize CMMA100 (low-degree of modification) or CMMA250 (high-degree of modification) respectively. The mixtures were stirred for 4 hours at RT, protected from light with the pH adjusted to 8-9 during all reaction. In order to remove all the unreacted MA, the CMMA was purified by dialysis using a membrane with molecular weight cutoff of 6-8 kDa (Spectra/Por^{TM}, Thermo Fisher Scientific) for 3 days against distilled water at 4°C, protected from light. Thereafter, the solution was frozen with liquid nitrogen, lyophilized (LyoQuest Plus Eco, Telstar, Spain) and stored at -20°C until further use.

5. Characterization of CMMA degree of modification

5.1.Proton nuclear magnetic resonance (^{1}H NMR)

The chemical modification of CMMA was assessed by proton (^{1}H NMR) nuclear magnetic resonance spectroscopy, by comparation with non-modified dCM. ^{1}H NMR spectra is used for determining the amount of methacrylate and methacrylamide groups in modified material, as well as for identifying the presence of the byproduct (methacrylic acid). Double bonds of acrylic protons (C = CH_2) from methacrylamide have characteristic peaks between δ = 5.3 and 5.5 ppm, while peaks between δ = 5.4 and 6.1 correspond to acrylic protons (C = CH_2) from methacrylate. The peak at δ = 1.8 ppm corresponds to the methyl group (CH_3) of methacrylate. Furthermore, δ = 2.89 ppm is a characteristic peak from non-modified material assigning the methylene hydrogen of lysine amines, which can be used as a reference signal to quantify the degree of modification [22–24]. For ^{1}H NMR analyses dCM and CMMA with both modification degrees were dissolved in Deuterium Oxide (D_2O, 99.8 atom% D, TCI Chemicals, USA) at a final concentration of 10 mg.mL^{-1}. The ^{1}H NMR spectra was recorded on an Avance III NMR spectrometer at 300.13 MHz.

5.2.TNBSA (2,4,6-Trinitrobenzene Sulfonic Acid)

TNBSA (2,4,6-Trinitrobenzene Sulfonic Acid) is a simple, sensitive and direct spectrophotometric method used for the quantification of primary amino groups present in proteins, using free amino acids as reference standards. As the reaction of TNBSA with primary amines produces a chromogenic (orange) product it is possible to measure the absorbance from standards to perform a calibration curve and yet determine amount of primary amino acids of the samples since the absorbance from sample amino acids and standards is directly proportional [25]. Hence, reacting free amino acids with TNBS reagent, allows to determine the degree of substitution by comparation of unmodified sample and the modified sample. Thereby, lyophilized dCM and CMMA were dissolved in reaction buffer of 0.1 M sodium bicarbonate (Fisher Scientific) at pH = 8.5. Glycine (Sigma-Aldrich, USA) standards were prepared at 0, 2.5, 5, 10 and 20 μg.mL^{-1} of concentration. Afterwards TNBSA reagent was added (Fisher Scientific, USA) at a concentration of 0.01% (w/v) to each samples and standards, the final mixture was incubated at 37 ºC for two hours. To stop the reaction, 10% (w/v) SDS (Sigma-Aldrich) and 1 M hydrochloric acid (HCI, Sigma-Aldrich) were added. The absorbance of all the solutions was measured at 335 nm using a microplate

reader (Synergy™ HTX). The degree of amine functionalization was determined using the formula (1).

$$\text{Degree of amine functionalization (\%)} = 1 - \left(\frac{{OD_{CMMA}}/{[CMMA]}}{{OD_{dCM}}/{[dCM]}} \right) \times 100 \quad (1)$$

6. Biochemical characterization of CMMA100 and CMMA250

As the ECM is mainly composed of proteins, proteoglycans, glycosaminoglycans and soluble factors, and each ECM component provides different functionalities to this complex network, the quantification of the major proteins and glycosaminoglycans in CMMA was performed [26,27].

6.1.Total protein quantification

Some proteins and proteoglycans have a structural function, while others have an adhesive function, fundamental for cell migration, adhesion, spreading, and proliferation. However, as a first approach, in view to have a broad knowledge about retained proteins, total quantification of proteins was assessed using the Thermo Scientific™ Micro BCA™ Protein Assay Kit (Thermo Scientific). This method is based on the reduction of Cu^{2+} to Cu^{+} by proteins in an alkaline environment, in the presence of bicinchoninic acid. Thus, is produced a purple-colored product formed by the chelation of two molecules of BCA with one Cu^{+} ion, which exhibits a strong absorbance at 562nm, linear with the increasing protein concentrations. Hence, CMMA100 (n = 2) and CMMA250 (n = 2) were dissolved in PBS to a final concentration of 20 $\mu g.mL^{-1}$. The standard curve was assessed using diluted albumin standards with concentrations from 0 until 200 $\mu g.mL^{-1}$. The absorbance of all the solutions was measured at 562 nm using a microplate reader (Synergy™ HTX).

6.2.Collagen quantification

Collagen is the most abundant protein in the ECM network. In the case of the CM, it has in its composition collagens type I, III, IV, V and VI. The collagen fibers provide principally tensile strength and elasticity, which, in turn, has a role in regulating cell adhesion, growth, proliferation, and differentiation [28,29]. In order to quantify collagens from CMMA, the Total Collagen Assay Kit (Perchlorate-Free) (Abcam, UK) was used. To perform this assay, the samples of CMMA100 (n = 1) and CMMA250 (n = 1) with a concentration of 25 $mg.mL^{-1}$ and collagen I standard with 1 $mg.mL^{-1}$ of concentration were alkaline hydrolyzed to yield

free hydroxyproline. Collagen standards with a range concentration between 0 and 1000 $\mu g.mL^{-1}$ were prepared. Then, 10 µL of each hydrolyzed standard and sample were pipetted to a 96-well plate. The released hydroxyproline was oxidized to form a reaction intermediate, which further formed a brightly colored chromophore that was measured at 560 nm using a microplate reader (Synergy™ HTX).

6.3.Laminin quantification

Laminin is a basement membrane glycoprotein also present on the CM and, in particular, is the major non-collagenous component and has a structural function. It is essential for morphogenesis and interacts with cell surface receptors initiating intracellular signaling events that regulate cellular organization and differentiation [28]. The quantification of human laminin was assessed with the Human Laminin ELISA Kit (Abcam), an immunochemical method with specific antibodies to detect specifically human laminin. Here, to the antigen (Anti-Human Laminin Antibody) immobilized on the bottom of the well-plate were added the standards and samples. Therefore, biotin antibody was complexed with the standards, with a range concentration of 0 and 1000 $pg.mL^{-1}$, and samples of CMMA100 (n = 1) and CMMA250 (n = 1) with 5 $mg.mL^{-1}$ of concentration and a reporter enzyme (Avidin-Biotin-Peroxidase Complex) was conjugated with the linked antibody. Afterwards, a color developing agent (TMB) was added, that was catalyzed by the reporter enzyme, producing a blue color product that after adding acidic stop solution changed to yellow. As the density of yellow coloration is directly proportional to the Human Laminin amount of sample captured in plate, the absorbance was measured at 450 nm using a microplate reader (Synergy™ HTX).

6.4.Sulfated proteoglycans and glycosaminoglycans (GAGs) quantification

Sulfated glycosaminoglycans (GAGs) are very important in ECM since they are responsible for high water uptake, allowing the hydration of the ECM. Consequently, they are a supply of resistance to compressive forces, being partially a source of mechanical stability. Moreover, GAGs specifically interact with other biological molecules, such as growth factors, having the role of protecting them from proteolysis or inhibiting factors [30]. Hence, was performed the quantification of GAGs retained in CMMA100 (n = 1) and CMMA250 (n = 1). To that was used the Blyscan™ sGAG Assay (Biocolor Life Science Assays, UK), which is a quantitative dye-binding method for the analysis of GAGs. All the

samples were first incubated with papain in order to extract sulfated GAGs for 16 hours. The standards were prepared with a range concentration between 0 and 50 $\mu g.mL^{-1}$. After extraction of the sulfated GAGs, the dye label 1,9-dimethylmethylene blue was added and a sulphated glycosaminoglycan-dye complex was formed precipitating out from the soluble unbound dye. The supernatant was discarded and the dissociation reagent was added to the precipitate. Since Blyscan Dye in the Dissociation Reagent has a peak maximum of 656 nm the absorbance was measured at that wavelength using a microplate reader (Synergy™ HTX).

7. Preparation of CMMA hydrogels

The photocrosslinkable CMMA is composed of a polymeric backbone and photoreactive moieties. The polymerization is triggered when the photoinitiator, added to the CMMA pre-polymer, is exposed to a light source. The absorbed photons cleave the photoinitiator producing free radical molecules. The free radicals react with the unreacted double bonds from the pre-polymer leading to the formation of covalent crosslinks between the polymer chains and, therefore producing the hydrogel [31]. Irgacure 2959 (1-[4-(2-hydroxyethoxy)-phenyl]-2-hydroxy-2-methyl-1-propane-1-one) has been widely explored for the preparation of hydrogels for TE applications. This photoinitiator has moderate water solubility, low cytotoxicity and minimal immunogenicity. However, the need of a source light from ultra-violet (UV) (365 nm) wavelength may have harmful effects both in irradiated cells and host tissues. Contrarily, the use of a photoinitiator that absorbs in the visible light region is prone to cause less cell damage. Furthermore, visible light may deeply penetrate tissues with relatively low energy, making it suitable for the development of *in situ* injectable hydrogels for *in vivo* applications in a minimally invasive manner. Hence, the visible light photoinitiator lithium phenyl-2,4,6-trimethylbenzoylphosphinate (LAP) is considered advantageous [31,32].

To prepare the CMMA hydrogels (**Figure III.3**), a solution of 0.5% (w/v) LAP (Sigma, Germany) in 1 X PBS was added to the lyophilized pre-polymer CMMA in order to achieve 0.25, 0.5, 1 and 2% (w/v) concentrations of CMMA. These precursor hydrogel solutions were injected into PDMS molds and were crosslinked under visible light (385-515 nm) with a power of 1000 $mW.cm^{-2} \pm 10\%$ using the LED, VALO^{TM} Cordless curing light (Ultradent products, Inc, USA).

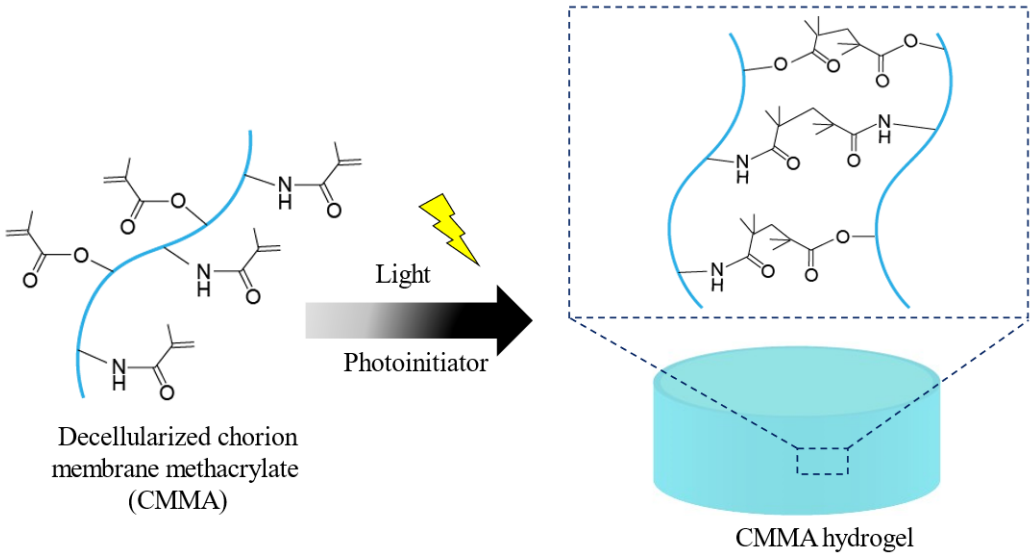

Figure III.3 Scheme of CMMA hydrogel production when dCM derived proteins methacrylated (CMMA) are irradiated in the presence of a photoinitiator.

8. Characterization of CMMA hydrogels

8.1. Mechanical properties

The mechanical properties of hydrogels are very important in TE, since cells sense mechanical stimuli. This process is called mechanotransduction and may be explained by the capacity of cells percept mechanical stimuli such as elasticity, viscosity, and nanotopography of ECM and translate them into biochemical signals, which will affect cell behavior, including migration, proliferation, and differentiation in a time-dependent manner [33]. In order to determine the compressive properties of CMMA100 (n = 3) 1% and 2% (w/v) hydrogels and CMMA250 hydrogels (n = 3) of 0.25%, 0.5%, 1% and 2% (w/v), with 6 mm diameter and 3 mm height were analyzed using the Instron 3340 Series Universal Testing System (Instron, USA) equipped with a 50 N load cell, at RT. The Young's modulus was determined as the slope in the linear region of the stress-strain curve between 0 and 5% of strain. The ultimate stress and strain values were considered as the point in which a failure was originated in the hydrogel.

8.2. Water content

Hydrogels are hydrophilic polymer chains highly hydrated polymer networks which may have a water content of ≥ 90% by weight [34]. As the total amount of water absorbed by a hydrogel can determine the overall permeation of nutrients into and cellular products out of

the gel, is an important factor to be characterized [35]. In this study, hydrogel of CMMA100 at 1% and 2% (w/v), and CMMA250 at 0.25%, 0.5%, 1% and 2% (w/v), were made in triplicate and immersed in PBS. Samples were incubated at RT overnight. After that time, the wet weight (w_w) was measured, and samples were frozen and lyophilized. After lyophilization, dry weight (w_d) was measured and compared with the initial wet weight. The water content was calculated according to the Equation (2).

$$\text{Water content (\%)} = \frac{W_w - W_d}{W_w} \times 100 \quad (2)$$

9. Cell culture and hydrogels biological response

The biological performance of CMMA hydrogels was assessed using human bone marrow-derived mesenchymal stem cells (hBM-MSCs) (ATCC, USA). Were cultured in minimum essential medium alpha (α-MEM) (Thermo Fisher Scientific) supplemented with sodium bicarbonate (2.2 $g.L^{-1}$, Sigma-Aldrich), 10% heat-inactivated fetal bovine serum (FBS) (Thermo Fisher Scientific), and 1% antibiotic/antimycotic (Thermo Fisher Scientific). All cells were cultured in T-flasks, maintained under 5% CO_2 atmosphere at 37 °C (standard culture conditions) and used until passage 8. The medium was replaced every 2 to 3 days. To obtain cell suspensions, cells from T-flaks were detached with 0.25% trypsin/EDTA (Gibco, Thermo Fisher Scientific).

For the cellular assays, the CMMA100 and CMMA250 lyophilized powder was sterilized for 30 minutes under UV light and the LAP solution, was sterilized using a 0.2 µm sterile syringe filter of cellulose acetate (Whatman™ 10462205, UK). Hydrogel precursor solutions were prepared as aforementioned.

9.1. Top seeding

In top seeding assays, 10 µL of 0.25%, 0.5% and 1% (w/v) CMMA100 and CMMA250 in 0.5% LAP precursor hydrogel solutions were pipetted into each µ-Slide Angiogenesis (ibidi, Germany) well. The hydrogels well polymerized for 20 seconds with a power of 1000 $mW.cm^{-2}$ ± 10% using the VALO™ Cordless curing light (Ultradent products, Inc). Afterwards, the hydrogels were washed with DPBS and a 50 µL cell suspension containing 20.000 cells was placed above the polymerized hydrogel and cultured at standard culture conditions for 7 days with medium change each 2-3 days.

9.2.Encapsulation

For the cell encapsulation assays, a cell suspension was incorporated in 0.25% and 0.5% (w/v) CMMA100 precursor hydrogel solutions to achieve a final concentration of 5×10^6 cells.mL^{-1}. Then, 10 µL of this cell suspension was pipetted to each µ-Slide Angiogenesis (ibidi, Germany) well and polymerized for 20 seconds with a power of 1000 mW.cm^{-2} ± 10% using the VALO^{TM} Cordless curing light (Ultradent products, Inc). Finally, were added 50 µL of culture medium to each well and cells were cultured at standard culture conditions for 7 days with medium change each 2-3 days.

9.2.1. Cell viability analysis

In order to determine if cells were live or dead, after 1, 3 and 7 days of culture, Live/Dead cell assay was performed. Calcein acetoxymethyl ester (Calcein AM) is a nonfluorescent cell-permeant dye that is metabolized by viable cells, in which their intracellular esterases hydrolyze acetoxymethyl ester and convert it in a fluorescent green calcein. Hence, the hydrogels were incubated in a solution of 1:500 of Calcein AM solution in DMSO (4×10^{-3} M, Life Technologies, Thermo Fisher Scientific) and 1:1000 of propidium iodide (PI) (1 mg.mL^{-1}, Thermo Fisher Scientific) in PBS at standard culture conditions (5% CO_2 at 37 °C) both for 30 minutes. After washing with DPBS, the cultured cells were observed in a fluorescence microscope (Axio Imager 2, Carl Zeiss).

9.2.2. Cell morphology analysis

Cell morphology was evaluated after 7 days of culture, using DAPI/phalloidin staining. As aforementioned DAPI is a fluorochrome that binds to the AT-rich regions of double-stranded DNA forming highly fluorescent complexes, staining nuclei with blue color. On the other hand, phalloidin is a peptide that tightly binds to F-actin filaments. After the pre-determined time point, hydrogels were washed with PBS and fixed with 4% formaldehyde (Sigma-Aldrich) for 1 hour at RT. After this time, the hydrogels were washed with PBS. Thereafter, hydrogels were incubated in a phalloidin solution (Flash Phalloidin Red 594, Biolegend, USA) diluted 1:40 in PBS at RT for 45 minutes. After washing with PBS, a DAPI (5 µg.mL^{-1}, Thermo Fisher Scientific, USA) solution diluted 1:1000 in PBS was prepared and used to incubate the hydrogels for 5 minutes at RT. After several PBS washes, the hydrogels were observed in a fluorescence microscope (Axio Imager 2, Carl Zeiss).

10. Statistical analysis

The statistical analysis was performed using GraphPad Prism 8 Software and data are expressed as mean ± standard deviation (SD). For mechanical characterization and water content evaluation, statistical significance between the different groups was identified using one-way ANOVA analysis of variance combined with Tukey's multiple comparisons test, and the differences were considered significant when $p < 0.05$.

11. References

(1) Kim, B. S.; Kim, H.; Gao, G.; Jang, J.; Cho, D. W. Decellularized Extracellular Matrix: A Step towards the next Generation Source for Bioink Manufacturing. Biofabrication 2017, 9 (3). https://doi.org/10.1088/1758-5090/aa7e98.

(2) Gilbert, T. W.; Sellaro, T. L.; Badylak, S. F. Decellularization of Tissues and Organs. Biomaterials 2006, 27 (19), 3675–3683. https://doi.org/10.1016/j.biomaterials.2006.02.014.

(3) Heath, D. E. A Review of Decellularized Extracellular Matrix Biomaterials for Regenerative Engineering Applications. Regen. Eng. Transl. Med. 2019, 5 (2), 155–166. https://doi.org/10.1007/s40883-018-0080-0.

(4) Kawecki, M.; Łabuś, W.; Klama-Baryla, A.; Kitala, D.; Kraut, M.; Glik, J.; Misiuga, M.; Nowak, M.; Bielecki, T.; Kasperczyk, A. A Review of Decellurization Methods Caused by an Urgent Need for Quality Control of Cell-Free Extracellular Matrix' Scaffolds and Their Role in Regenerative Medicine. J. Biomed. Mater. Res. - Part B Appl. Biomater. 2018, 106B (2), 909–923. https://doi.org/10.1002/jbm.b.33865.

(5) Dzobo, K.; Shirley, K.; Motaung, C. M.; Adesida, A. Recent Trends in Decellularized Extracellular Matrix Bioinks for 3D Printing : An Updated Review. Int. J. Mol. Sci. 2019, 20 (18), 1–28.

(6) Barreto, R. S. N.; Romagnolli, P.; Fratini, P.; Mess, A. M.; Miglino, M. A. Mouse Placental Scaffolds: A Three-Dimensional Environment Model for Recellularization. J. Tissue Eng. 2019, 10, 1–11. https://doi.org/10.1177/2041731419867962.

(7) Shakouri-motlagh, A.; Khanabdali, R.; Heath, D. E.; Kalionis, B. The Application of Decellularized Human Term Fetal Membranes in Tissue Engineering and Regenerative Medicine (TERM). Placenta 2017, 59, 124–130. https://doi.org/10.1016/j.placenta.2017.07.002.

(8) Yeagle, P. L. Detergents. In The Membranes of Cells; 2016; pp 73–84. https://doi.org/10.1016/B978-0-12-800047-2.00004-8.

(9) Gilpin, A.; Yang, Y. Decellularization Strategies for Regenerative Medicine: From Processing Techniques to Applications. Biomed Res. Int. 2017, 1–13. https://doi.org/10.1155/2017/9831534.

(10) Takahashi, T.; Irie, M.; Ukita, T. Effect of Divalent Cations on Bovine Pancreatic Ribonucrease*. J. Biochem. 1967, 61 (6), 669–678.

(11) Campbell, V. W.; Jackson, D. A. The Effect Divalent Cations on the Mode of Action of DNase I. THE INITIAL REACTION PRODUCTS PRODUCED FROM COVALENTLY CLOSED CIRCULAR DNA. J. Biol. Chem. 1980, 255 (8), 3726–3735.

(12) Eun, H.-M. Nucleases. In Enzymology Primer for Recombinant DNA Technology; Academic Press Limited: France, 1996; pp 145–232. https://doi.org/10.1016/b978-0-12-243740-3.x5000-5.

(13) Harvey, R. F.; Grossman, M. I. Gastrointestinal Hormones. In Hormones; Academic Press, 2015; pp 141–169. https://doi.org/10.1016/B978-0-08-091906-5.00007-0.

(14) Ali, M.; Anil Kumar, P. R.; Yoo, J. J.; Zahran, F.; Atala, A.; Lee, S. J. A Photo-Crosslinkable Kidney ECM-Derived Bioink Accelerates Renal Tissue Formation. Adv. Healthc. Mater. 2019, 8 (7), 1–10. https://doi.org/10.1002/adhm.201800992.

(15) Keil, B. Specificity of Proteolysis; 1992. https://doi.org/10.1007/978-3-642-48380-6.

(16) Skierka, E.; Sadowska, M. The Influence of Different Acids and Pepsin on the Extractability of Collagen from the Skin of Baltic Cod (Gadus Morhua). Food Chem. 2007, 105 (3), 1302–1306. https://doi.org/10.1016/j.foodchem.2007.04.030.

(17) M., D. L.; Sholugu, N.; Fuller, K.; Zeugolis, D. I. Acetic Acid and Pepsin Result in High Yield, High Purity and Low Macrophage Response Collagen for Biomedical Applications This. Biomed. Mater. 2017, 12 (6), 065009. https://doi.org/https://doi.org/10.1088/1748-605X/aa838d This.

(18) Hyde, A. M.; Zultanski, S. L.; Waldman, J. H.; Zhong, Y.; Shevlin, M.; Peng, F. General Principles and Strategies for Salting-Out Informed by the Hofmeister Series. Org. Process Res. Dev. 2017, 21, 1355–1370. https://doi.org/10.1021/acs.oprd.7b00197.

(19) Arnold, T.; Linke, D. Phase Separation in the Isolation and Purification of Membrane Proteins. Biotechniques 2007, 43 (4), 427–440. https://doi.org/10.2144/000112566.

(20) Yao, H.; Wang, J.; Mi, S. Photo Processing for Biomedical Hydrogels Design and Functionality: A Review. Polymers (Basel). 2018, 10 (1), 11.

(21) Pepelanova, I.; Kruppa, K.; Scheper, T.; Lavrentieva, A. Gelatin-Methacryloyl (GelMA) Hydrogels with Defined Degree of Functionalization as a Versatile Toolkit for 3D Cell Culture and Extrusion Bioprinting. Bioengineering 2018, 5 (3), 55.

(22) Ravichandran, R.; Islam, M. M.; Alarcon, E. I.; Samanta, A.; Wang, S.; Lundström, P.; Hilborn, J.; Griffith, M.; Phopase, J. Functionalised Type-I Collagen as a Hydrogel Building Block for Bio-Orthogonal Tissue Engineering Applications. J. Mater. Chem. B 2015, 4 (2), 318–326. https://doi.org/10.1039/c5tb02035b.

(23) Hoch, E.; Schuh, C.; Hirth, T.; Tovar, G. E. M.; Borchers, K. Stiff Gelatin Hydrogels Can Be Photo-Chemically Synthesized from Low Viscous Gelatin Solutions Using Molecularly Functionalized Gelatin with a High Degree of Methacrylation. J. Mater. Sci. Mater. Med. 2012, 23 (11), 2607–2617.

(24) Spicer, C. D. Hydrogel Scaffolds for Tissue Engineering: The Importance of Polymer Choice. Polym. Chem. 2020, 11 (2), 184–219.

(25) Sashidhar, R. B.; Capoor, A. K.; Ramana, D. Quantitation of ϵ-Amino Group Using Amino Acids as Reference Standards by Trinitrobenzene Sulfonic Acid: A Simple Spectrophotometric Method for the Estimation of Hapten to Carrier Protein Ratio. J. Immunol. Methods 1994, 167 (1–2), 121–127.

(26) Hinderer, S.; Layland, S. L.; Schenke-Layland, K. ECM and ECM-like Materials - Biomaterials for Applications in Regenerative Medicine and Cancer Therapy. Adv. Drug Deliv. Rev. 2016, 97, 260–269. https://doi.org/10.1016/j.addr.2015.11.019.

(27) Hoshiba, T. Decellularized Extracellular Matrix for Cancer Research. Materials (Basel). 2019, 12 (8), 1311–1327.

(28) D'Lima, C.; Samant, U.; Gajiwala, A. L.; Puri, A. Human Chorionic Membrane: A Novel and Efficient Alternative to Conventional Collagen Membrane. Trends Biomater. Artif. Organs 2020, 34 (1), 33–37.

(29) Klimek, K.; Ginalska, G. Proteins and Peptides as Important Modifiers of the Polymer Scaffolds for Tissue Engineering Applications—A Review. Polymers (Basel). 2020, 12 (4), 844–882.

(30) Neves, M. I.; Araújo, M.; Moroni, L.; da Silva, R. M. P.; Barrias, C. C. Glycosaminoglycan-Inspired Biomaterials for the Development of Bioactive Hydrogel Networks. Molecules 2020, 25 (4), 978–1017.

(31) Choi, J. R.; Yong, K. W.; Choi, J. Y.; Cowie, A. C. Recent Advances in Photo-Crosslinkable Hydrogels for Biomedical Applications. Biotechniques 2019, 66 (1), 40–53.

(32) Monteiro, N.; Thrivikraman, G.; Athirasala, A.; Tahayeri, A.; França, C. M.; Ferracane, J. L.; Bertassoni, L. E. Photopolymerization of Cell-Laden Gelatin Methacryloyl Hydrogels Using a Dental Curing Light for Regenerative Dentistry. Dent. Mater. 2018, 34 (3), 389–399.

(33) Angelo, M. d'; Benedetti, E.; Tupone, M. G.; Catanesi, M.; Castelli, V.; Antonosante, A.; Cimini, A. The Role of Stiffness in Cell Reprogramming: A Potential Role for Biomaterials in Inducing Tissue Regeneration. Cells 2019, 8 (9), 1036–1061.

(34) Naahidi, S.; Jafari, M.; Logan, M.; Wang, Y.; Yuan, Y.; Bae, H.; Dixon, B.; Chen, P. Biocompatibility of Hydrogel-Based Scaffolds for Tissue Engineering Applications. Biotechnol. Adv. 2017, 35 (5), 530–544. https://doi.org/10.1016/j.biotechadv.2017.05.006.

(35) Hoffman, A. S. Hydrogels for Biomedical Applications. Adv. Drug Deliv. Rev. 2012, 64, 18–23.

Chapter IV*

Chorionic membrane derived hydrogels as an innovative human based platform for 3D cell culture

*This chapter is based on the following publication:

Martins E. et al. “Chorionic membrane derived hydrogels as an innovative human based platform for 3D cell culture” (manuscript under preparation)

Chorionic membrane derived hydrogels as an innovative human based platform for 3D cell culture

Abstract

Tissue engineering and regenerative medicine (TERM) have emerged as an alternative to the therapies currently used in the treatment or replacement of damaged tissues or organs. The extracellular matrix (ECM) of decellularized tissues has been widely used as biological biomaterials for TERM purposes. Of particular interest, placentas are easily available sources of ECM, without associated ethical issues, immunoprivileged and biocompatible. Thus, the preparation of scaffold materials made of the total placenta or its layer fractions, as the chorionic membrane (CM) have attracted particular interest in tissue engineering. However, most of the current hydrogels produced from decellularized and solubilized ECM, display low mechanical properties and very limited stability *in vitro*.

The objective of this work is to produce, for the first time, photocrosslinkable CM-derived hydrogels with tunable mechanical properties as 3D cell culture platform. In this study, CM prepolymers were produced by the reaction of solubilized CM ECM with methacrylic anhydride. Two degrees of modification: lower (CMMA100) and higher degree of modification (CMMA250) were obtained. The modified ECM derived proteins are then able to form a hydrogel when irradiated with light in the presence of a photoinitiator. Quantifications of some of the most important ECM proteins confirmed their presence in the modified material. The evaluation of the mechanical properties shown that it was possible to produce robust hydrogels and whose properties vary with polymer concentration and degree of modification, covering a range of human tissue elastic modulus. In addition, the degree of modification also influences the physical properties such as the water absorption capacity. Moreover, it was possible to verify that the produced CMMA hydrogels support the culture of human derived stem cells. Further quantification of specific proteins and quantitative analysis of cell growth is still needed, but the results obtained so far suggest that these CMMA-based hydrogels are promising for 3D cell culture.

1. Introduction

Tissue engineering (TE) combines living cells, biocompatible materials, and suitable biochemical (e.g., growth factors) and physical (e.g., cyclic mechanical loading) factors. This area appeared due to the limited capacity of the human body to regenerate and incapacity to heal large defects [1]. When an organ begins to fail, the solutions that exist at present are mostly pharmacological therapies and, in more severe cases, organ transplantation. However, there is a shortage of viable donor organs, and these are often associated with rejection problems [2]. As an alternative, biomaterials capable of mimicking the 3D microenvironment in which cells reside: the extracellular matrix (ECM) and promoting regeneration have been investigated. ECM consists of numerous proteins, glycosaminoglycans and soluble factors that have the ability to influence cell migration, proliferation and differentiation [3]. Decellularized ECM has high potential as a biomaterial, since cells are removed and consequently, potential antigens that may cause an inflammatory response or immune-mediated implant rejection are removed [4]. An interesting source of human ECM are the perinatal tissues. These are temporary organs, virtually unlimited and cost-effective, since they are discarded after birth. Moreover, perinatal tissues have demonstrated to retain important therapeutic properties, which mostly result from anti-microbial, anti-inflammatory and immunomodulatory activities of resident cells [5]. Fetal membranes have been used for more than a century, in TE applications [6]. Nevertheless, their reported use is a bit restrict to amniotic membrane (AM) isolated or the conjugation of both AM and chorionic membrane (CM). Specifically, isolated CM, is quite unexplored as biomaterial. However, its potentiality as a biomaterial has already been proven in the area of periodontal regeneration and osteogenic induction [7–12].

Hydrogels are a unique class of 3D materials composed by a hydrophilic polymeric network with structural similarity to the ECM. They are able to uptake large amounts of water, diffuse nutrients, metabolites and wastes. Hydrogels have been used in cell culture, since they allow proliferation and differentiation mimicking more precisely the ECM, than conventional 2D cell culture platforms [13–15]. Contrary to hydrogels composed of individual ECM components, decellularized derived ECM hydrogels retain the biochemical complexity of the native tissue, and unlike Matrigel, are not composed of a protein source that is a product of a tumorigenic cell line [16]. However, the mechanical properties of hydrogels from decellularized ECM polymerized through temperature or pH are usually very soft with

elastic modulus in the range of Pascal, what limits their application in TE [17]. Hence, the aim of this work is to produce robust and tunable photocrosslinkable CM - derived hydrogels as 3D cell culture platforms. The chemical modification of decellularized CM (dCM) through the reaction with methacrylic anhydride, produce photocrosslinkable ECM derived proteins that form hydrogels with tunable properties that support cell culture. Moreover, the biochemical characterization proved the retention of ECM fundamental proteins and glycosaminoglycans in the obtained hydrogels.

2. Materials and methods

2.1.Placenta collection

In order to obtain chorion membranes for this study, placentas were collected at the Hospital Infante D. Pedro from Aveiro, through a collaboration with the COMPASS Research Group. The use of human placenta was approved by the institutional ethics and deontology committee from both institutions. Informed consent from the donors were obtained for all placentas used in this study.

2.2.Chorionic membrane (CM) isolation and decellularization

For the chorionic membrane (CM) isolation, the umbilical cord face was placed upward, the amniotic membrane was detached, the umbilical cord was cut and then the CM was cut around the chorionic plate and cut into smaller pieces.

For the decellularization, CM was placed into 50 mL falcon tubes and incubated with 30 mL of 1% SDS solution. Then the falcons were placed in rotation at 25 rpm for 16 hours at RT in the Multi-Purpose Tube Rotator (Fisherbrand™, Thermo Fisher Scientific). After that, the CM was incubated with 35 mL of 1% Triton™ X-100 BioXtra (Sigma-Aldrich, USA) and placed again on the tube rotator for 30 minutes at 25 rpm, at RT in order to finalize cell content extraction and to remove the residual SDS. The CM was washed to remove the detergent, being transferred to new Falcon tubes with 35mL DPBS and placed on tube rotator for 15 minutes between washes. Subsequently were produced 30 mL of a nuclease solution (50 mM Trizma® hydrochloride (Tris HCl, Sigma), 10 mM magnesium chloride hexahydrate ($MgCl_2.6H_2O$, Panreac, Spain), adding 70 µL recombinant DNase I (STEMCELL™ Technologies, Canada), and 30 µL of bovine pancreatic PureLink™ RNase A ((20 $mg.mL^{-1}$), Sigma). Were added 10 mL to each falcon and incubated at 37 °C for 3 h, under continuous stirring in the Compact Digital Microplate Shaker (Thermo Fisher Scientific).

The decellularized CM (dCM) was washed again as previously described, frozen with liquid nitrogen, lyophilized and stored at -20°C until further use.

To confirm the decellularization efficiency, a piece of fresh non-decellularized CM and a piece of dCM were fixed in 4% formaldehyde (Sigma-Aldrich) overnight at RT. After that, samples were stained with a DAPI (5 $\mu g.mL^{-1}$, Thermo Fisher Scientific) solution diluted 1:1000 in PBS incubating for 5 minutes at RT, protected from light. After PBS washes, the CM pieces were observed under a fluorescence microscope (Fluorescence Microscope Zeiss, Axio Imager 2, Carl Zeiss, Germany).

DNA quantification was also performed to evaluate the efficiency of the decellularization process. To do that, 5 g of CM (n = 3) and dCM (n = 2) were digested in 1 mL of papain at 65 ºC for 16 hours. Afterwards, was performed a centrifugation (10000 g, 10 minutes) and the pellet was diluted (1 : 1) in 1 X TRIS – EDTA (TE) buffer. To achieve a standard curve, dsDNA standards were prepared with concentrations ranging between 0 and 1 $ug.mL^{-1}$. Both samples and standards were incubated with Picogreen reagent for 5 minutes at RT, protected from light. Fluorescence was measured using an excitation wavelength of 480 nm and an emission wavelength of 528 nm in a 96-well flat-bottom opaque black plate using Synergy HTX microplate reader (BioTek Instruments, Winooski, USA).

2.3.dCM solubilization

In order to solubilize ECM components, dCM was incubated with a solution of pepsin (Promega, USA) (1 $mg.mL^{-1}$) in 0.5 M acetic acid (Glacial, 99-100%, CHEM-LAB, Belgium) at a ratio of 10 mg sample per mL of pepsin solution. The solution was stirred in the Multi-Purpose Tube Rotator for 3 days with 50 rpm at RT. After that, the undigested pieces were separated from the solution using a 380 µm sieve. In order to purify and concentrate solubilized dCM proteins, was added NaCl to a final concentration of 5% (w/v) and stirred in the Multi-Purpose Tube Rotator overnight at RT with 50 rpm. This was followed by a centrifugation step at 10.000 rpm at 4ºC for 15 minutes. The precipitate was collected and the precipitation step was repeated 4 times in the supernatant. Finally, the precipitated proteins were dissolved in 1.0 M acetic acid and the solution purified by dialysis using a membrane with a cutoff of 3.5 kDa (SnakeSkin™, Thermo Fisher Scientific) for at least 24h against distilled water at 4°C, in order to remove NaCl, remaining detergent and

acetic acid. After that, the solution was frozen with liquid nitrogen, lyophilized (LyoQuest Plus Eco, Telstar, Spain) and stored at -20°C until further use.

2.4.dCM proteins functionalization

In brief, CMMA was synthesized by reacting dCM with methacrylic anhydride (MA) 94% (Sigma, Germany). For that, lyophilized dCM was solubilized in PBS (Sigma-Aldrich Germany) at a concentration of 1% w/v, and subsequently, either 100 µL or 250 µL of MA per 10 mL of solution were added, to synthesize CMMA100 (low-degree of modification) or CMMA250 (high-degree of modification) respectively. The mixtures were stirred for 4 hours at RT, protected from light with the pH adjusted to 8-9 during all reaction. In order to remove all the unreacted MA, the CMMA was purified by dialysis using a membrane with molecular weight cutoff of 6-8 kDa (Spectra/Por^{TM}, Thermo Fisher Scientific) for 3 days against distilled water at 4°C, protected from light. Thereafter, the solution was frozen with liquid nitrogen, lyophilized (LyoQuest Plus Eco, Telstar, Spain) and stored at -20°C until further use.

2.5.Characterization of CMMA degree of modification

2.5.1. Proton nuclear magnetic resonance (^{1}H NMR)

The chemical modification of CMMA was assessed by proton (^{1}H NMR) nuclear magnetic resonance spectroscopy, by comparation with non-modified dCM. ^{1}H NMR spectra is used for determining the presence of methacrylate and methacrylamide groups in modified material. For ^{1}H NMR analyses dCM and CMMA with both modification degrees were dissolved in Deuterium Oxide (D_2O, 99.8 atom% D, TCI Chemicals, USA) at a final concentration of 10 mg.mL^{-1}. The ^{1}H NMR spectra was recorded on an Avance III NMR spectrometer at 300.13 MHz.

2.5.2. TNBSA (2,4,6-Trinitrobenzene Sulfonic Acid)

TNBSA (2,4,6-Trinitrobenzene Sulfonic Acid) is a simple, sensitive and direct spectrophotometric method used for the quantification of primary amino groups present in proteins, using free amino acids as reference standards. Thereby, lyophilized dCM (n = 2) and CMMA (n = 2) were dissolved in a reaction buffer of 0.1 M sodium bicarbonate (Fisher Scientific) at pH = 8.5. Glycine (Sigma-Aldrich, USA) standards were prepared at 0, 2.5, 5, 10 and 20 µg.mL^{-1} of concentration. Afterwards TNBSA reagent was added (Fisher

Scientific, USA) at a concentration of 0.01% (w/v) to each samples and standards, the final mixture was incubated at 37ºC for two hours. To stop the reaction, 10% (w/v) SDS (Sigma-Aldrich) and 1 M hydrochloric acid (HCI, Sigma-Aldrich) were added. The absorbance of all the solutions was measured at 335 nm using a microplate reader (Synergy™ HTX). The degree of amine functionalization was determined using the formula (2).

$$\text{Degree of amine functionalization (\%)} = 1 - \left(\frac{OD_{CMMA}/_{[CMMA]}}{OD_{dCM}/_{[dCM]}} \right) \times 100 \qquad (2)$$

2.6.Biochemical characterization of CMMA100 and CMMA250

2.6.1. Total protein quantification

The total protein concentration was assessed using the Thermo Scientific™ Micro BCA™ Protein Assay Kit (Thermo Scientific). For this, CMMA100 (n = 2) and CMMA250 (n = 2) were dissolved in PBS to a final concentration of 20 $\mu g.mL^{-1}$ and the standard curve was assessed using diluted albumin standards with concentrations from 0 until 200 $\mu g.mL^{-1}$. The absorbance of all the solutions was measured at 562 nm using a microplate reader (Synergy™ HTX).

2.6.2. Collagen quantification

In order to quantify collagens from CMMA, the Total Collagen Assay Kit (Perchlorate-Free) (Abcam, UK) was used. To perform this assay, the samples of CMMA100 (n = 1) and CMMA250 (n = 1) with a concentration of 25 $mg.mL^{-1}$ and collagen I standard with 1 $mg.mL^{-1}$ of concentration were alkaline hydrolyzed to yield free hydroxyproline. Then standards with a range concentration between 0 and 1000 µg/mL were prepared. 10 µL of each hydrolyzed standard and sample were then pipetted to each well of a 96-well plate. The released hydroxyproline was oxidized to form a reaction intermediate, which further formed a brightly colored chromophore that was measured at 560 nm using a microplate reader (Synergy™ HTX).

2.6.3. Laminin quantification

The quantification of human laminin was assessed with the Human Laminin ELISA Kit (Abcam). To the antigen (Anti-Human Laminin Antibody) immobilized on the bottom of the well-plate the standards and samples were added. Therefore, a biotin antibody was

complexed with the standards, with a range concentration of 0 and 1000 pg.mL^{-1}, and samples of CMMA100 (n = 1) and CMMA250 (n = 1) with 5 mg.mL^{-1} of concentration and a reporter enzyme (Avidin-Biotin-Peroxidase Complex) was conjugated with the linked antibody. Afterwards, a color developing agent (TMB) was added, that was catalyzed by the reporter enzyme, producing a blue color product that after adding acidic stop solution changed to yellow and the absorbance measured at 450 nm using a microplate reader (Synergy™ HTX).

2.6.4. Sulfated proteoglycans and glycosaminoglycans (GAGs) quantification

The retained sulphated Glycosaminoglycans (GAGs) in CMMA100 (n = 1) and CMMA250 (n = 1) were quantified using the Blyscan™ sGAG Assay (Biocolor Life Science Assays, UK), which is a quantitative dye-binding method for the analysis of GAGs. All samples were first incubated with papain in order to extract sulfated GAG for 16 hours. The standards were prepared with a range concentration between 0 and 50 µg.mL^{-1}. After extraction of the sulfated GAGs, the dye label 1,9-dimethylmethylene blue was added and a sulphated glycosaminoglycan-dye complex was formed precipitating out from the soluble unbound dye. The supernatant was discarded and the dissociation reagent was added to the precipitate. Since Blyscan Dye in the Dissociation Reagent has a peak maximum of 656 nm the absorbance was measured at that wavelength using a microplate reader (Synergy™ HTX).

2.7.Preparation of CMMA hydrogels

To prepare the CMMA hydrogels, a solution of 0.5% (w/v) Lithium phenyl-2,4,6-trimethylbenzoylphosphinate (LAP) (Sigma, Germany) in 1 X PBS was added to the lyophilized CMMA in order to achieve 0.25, 0.5, 1 and 2% (w/v) concentrations of CMMA. These precursor hydrogel solutions were injected into PDMS molds and crosslinked under visible light (385-515 nm) with a power of 1000 mW.cm^{-2} ± 10% using the LED, VALO^{TM} Cordless curing light (Ultradent products, Inc, USA).

2.8.Characterization of CMMA hydrogels

2.8.1. Mechanical properties

The mechanical properties, more specifically the compressive properties of CMMA100 (n = 3) 1% and 2% (w/v) hydrogels and CMMA250 hydrogels (n = 3) of 0.25%, 0.5%, 1%

and 2% (w/v), with 6 mm diameter and 3 mm height were analyzed using the Instron 3340 Series Universal Testing System (Instron, USA) equipped with a 50 N load cell, at RT. The Young's modulus was determined as the slope in the linear region of the stress-strain curve between 0 and 5% of strain. The ultimate stress and strain values were considered as the point in which a failure was originated in the hydrogel.

2.8.2. Water content

In this study, hydrogels of CMMA100 at 1% and 2% (w/v), and CMMA250 at 0.25%, 0.5%, 1% and 2% (w/v), were made and immersed in PBS. Samples were incubated at 4 ºC overnight. After that time, the wet weight (w_w) was measured, and samples were frozen and lyophilized. After lyophilization, dry weight (w_d) was measured and compared with the initial wet weight. The water content was calculated according to the Equation (3).

$$\text{Water content (\%)} = \frac{W_w - W_d}{W_w} \times 100 \quad (3)$$

2.9.Cell culture and hydrogels biological response

The biological performance of CMMA hydrogels was assessed using human bone marrow-derived mesenchymal stem cells (hBM-MSCs) (ATCC, USA). Both were cultured in minimum essential medium alpha (α-MEM) (Thermo Fisher Scientific) supplemented with sodium bicarbonate (2.2 $g.L^{-1}$, Sigma-Aldrich), 10% heat-inactivated fetal bovine serum (FBS) (Thermo Fisher Scientific), and 1% antibiotic/antimycotic (Thermo Fisher Scientific). All cells were cultured in T-flasks, maintained under 5% CO_2 atmosphere at 37 °C (standard culture conditions) and used until passage 8. The medium was replaced every 2 to 3 days. To obtain cell suspensions, cells from T-flaks were detached with 0.25% trypsin/EDTA (Gibco, Thermo Fisher Scientific).

For the cellular assays, the CMMA100 and CMMA250 lyophilized powder was sterilized for 30 minutes under UV light and the LAP solution, was sterilized using a 0.2 µm sterile syringe filter of cellulose acetate (Whatman™, UK). Hydrogel precursor solutions were prepared as aforementioned.

2.9.1. Top seeding

In top seeding assays, 10 µL of 0.25%, 0.5%, 1% and 2% (w/v) CMMA100 and CMMA250 in 0.5% LAP precursor hydrogel solutions were pipetted into each µ-Slide Angiogenesis (ibidi, Germany) well. The hydrogels well polymerized for 20 seconds with a power of 1000 $mW.cm^{-2}$ ± 10% using the VALO^{TM} Cordless curing light (Ultradent products, Inc). Afterwards, the hydrogels were washed with DPBS and a cell suspension was placed above the polymerized hydrogel and cultured at standard culture conditions for 7 days with medium change each 2-3 days.

2.9.2. Encapsulation

For the cell encapsulation assays, a cell suspension was incorporated in 0.25% and 0.5% (w/v) CMMA100 precursor hydrogel solutions to achieve a final density of 5×10^6 $cells.mL^{-1}$. Then, 10 µL of this cell suspension was pipetted to each µ-Slide Angiogenesis (ibidi, Germany) well and polymerized for 20 seconds with a power of 1000 $mW.cm^{-2}$ ± 10% using the VALO^{TM} Cordless curing light (Ultradent products, Inc). Finally, were added 50 µL of culture medium to each well and cells were cultured at standard culture conditions for 7 days with medium change each 2-3 days.

2.9.3. Cell viability analysis

In order to identify live and dead cells after 1, 3 and 7 days of culture, a Live/Dead cell assay was performed. In this sense, the hydrogels were incubated in a solution of 1:500 of Calcein AM solution in DMSO (4×10^{-3} M, Life Technologies, Thermo Fisher Scientific) and 1:1000 of propidium iodide (PI) (1 $mg.mL^{-1}$,Thermo Fisher Scientific) in PBS at standard culture conditions (5% CO_2 at 37 °C) both for 30 minutes. After washing with DPBS, the cultured cells were observed in a fluorescence microscope (Axio Imager 2, Carl Zeiss).

2.9.4. Cell morphology analysis

Cell morphology was evaluated after 7 days of culture, using DAPI/phalloidin staining. At the pre-determined time point, hydrogels were washed with PBS and fixed with 4% formaldehyde (Sigma-Aldrich) for 1 hour at RT. After this time, the hydrogels were washed with PBS. Thereafter, hydrogels were incubated in a phalloidin solution (Flash Phalloidin Red 594, Biolegend, USA) diluted 1:40 in PBS at RT for 45 minutes. After washing with

PBS, a DAPI (5 μg.mL^{-1}, Thermo Fisher Scientific, USA) solution diluted 1:1000 in PBS was prepared and used to incubate the hydrogels for 5 minutes at RT. After several PBS washes, the hydrogels were observed in a fluorescence microscope (Axio Imager 2, Carl Zeiss).

2.10. Statistical analysis

The statistical analysis was performed using GraphPad Prism 8 Software and data are expressed as mean ± standard deviation (SD). For mechanical characterization and water content evaluation, statistical significance between the different groups was identified using one-way ANOVA analysis of variance combined with Tukey's multiple comparisons test, and the differences were considered significant when $p < 0.05$.

3. Results and discussion

Fetal membranes have been used as a biomaterial for applications in TE with great success [6]. However, the use of CM is quite unexplored, having only been used as fresh allograft in regeneration due to periodontitis, and in the extract form in a study comparing the potential for osteogenic differentiation with an amniotic membrane extract [7–12]. Hence this study aims to produce, to the best of our knowledge, for the first time, photocrosslinkable CM-derived hydrogels.

3.1.CM isolation, decellularization and solubilization

The whole placenta (**Figure IV.1** A) collect at the hospital was processed as aforementioned, starting with umbilical cord faced upward, separating by blunt dissection the amniotic membrane, the translucent membrane at the (**Figure IV.1** A) and the umbilical cord was cut. Then, turning the placenta upside down, the structure of **Figure IV.1** B was obtained, being the chorionic membrane cut around the chorionic plate. After blood vessels and clots removal and CM cut into small pieces was obtained fresh pink CM non decellularized (**Figure IV.1** C). Posteriorly to decellularization, the pink color (**Figure IV.1** C), changed to whitish yellow (**Figure IV.1** D). Finally, after digestion to solubilize CM, was obtained a white viscous suspension (**Figure IV.1** E).

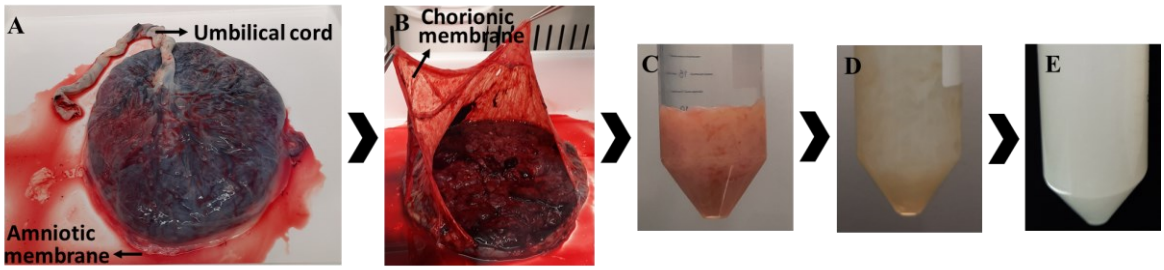

Figure IV.1.Steps from isolation until solubilization of CM. A) Whole placenta with fetal side faced upward. B) Chorionic membrane. The maternal side of the CM on the side of the arrow. C) CM cut into small pieces after removing clots and blood vessels. D) Decellularized CM (dCM). E) Solubilized dCM.

It is accepted that, to determine if the decellularization was efficient, the obtained tissue should obey the following conditions: (i) have less than 50 ng double-stranded DNA per mg dry ECM, (ii) have DNA fragment length with less than 200 base pair, and (iii) lack of visible nuclear material in tissue sections stained with 4',6-diamidine-2-phenyl indole (DAPI) or Hematoxylin and Eosin (H&E) [19].

Hence, the efficiency of the decellularization process was assessed through DAPI staining and DNA quantification in both not decellularized CM and dCM. DAPI staining demonstrated a decrease in cell nuclei stained blue after decellularization, and consequently a decrease in cell number (**Figure IV.2** A and **Figure IV.2** B). Furthermore, through a quantitative analysis of DNA was verified that the decellularization was successful since a decrease in DNA down to 41.9 ± 5.6 ng double-stranded DNA was obtained after the decellularization process (**Figure IV.2** C). The total quantification effectuated in not decellularized CM and dCM show an increase from 592 ± 48 µg of proteins / mg of product, to 724 ± 47 µg of proteins / mg of product, respectively (**Figure IV.2** D). This increase in protein content could be explained by the removal of other components, as for instance nuclei. Moreover, the quantification of proteins from dCM shows that was obtained a product of a high protein content (≈ 72%).

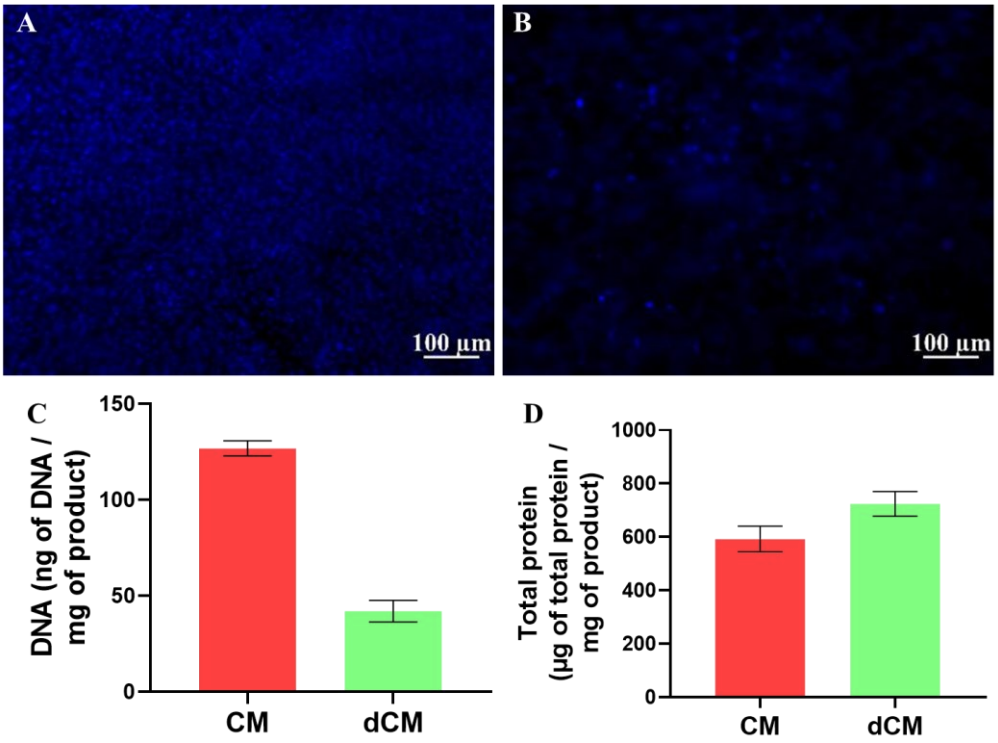

Figure IV.2: CM decellularization: A) Representative CM section stained with DAPI and B) Representative dCM section stained with DAPI. C) Quantification of double-stranded DNA per mg of dry CM or dCM. D) Quantification of total protein in CM or dCM.

3.2.Characterization of CMMA degree of modification

Decellularized ECM have been used to produce hydrogels for TE and other biomedical applications. However, the most frequently used polymerization strategies employed in digested decellularized ECM are triggered by pH or temperature and, consequently, the produced hydrogels are often very soft, with poor mechanical properties and easily degradable [20] . To overcome that problem and to produce stiffer hydrogels with tunable mechanical properties, recent studies proved the possibility to obtain tunable photocrosslinkable hydrogels derived from human plasma proteins [21,22] or porcine ECM-proteins by the reaction with methacrylic anhydride [23,24]. This is possible due to amino and hydroxyl groups present in the proteins making them likely for modification by reaction with methacrylic anhydride producing methacrylate and methacrylamide groups. As the added amount of methacrylic anhydride has influence in the polymerization degree, two modification degrees were tested in this study: the low modification degree, CMMA100, and the high modification degree, CMMA250, based in the previously reported protocol for platelet lysates [6]. The successul modification was confirmed by comparing the ^{1}NMR spectra of both CMMA and dCM proteins (**Figure IV.3** B). Analysing the obtained spectra, is

possible to verify that methacrilation occur comparing the non modified dCM with CMMA spectra. The modified proteins, have peaks between δ = 5.7 and 5.8 ppm corresponding to double bonds of acrylic protons (C = CH_2) from methacrylamide, while peaks between δ = 5.8 and 6.3 correspond to acrylic protons (C = CH_2) from methacrylate. The peak at δ ≈ 1.9 ppm corresponds to the methyl group (-CH_3) of methacrylate and methacrylamide.

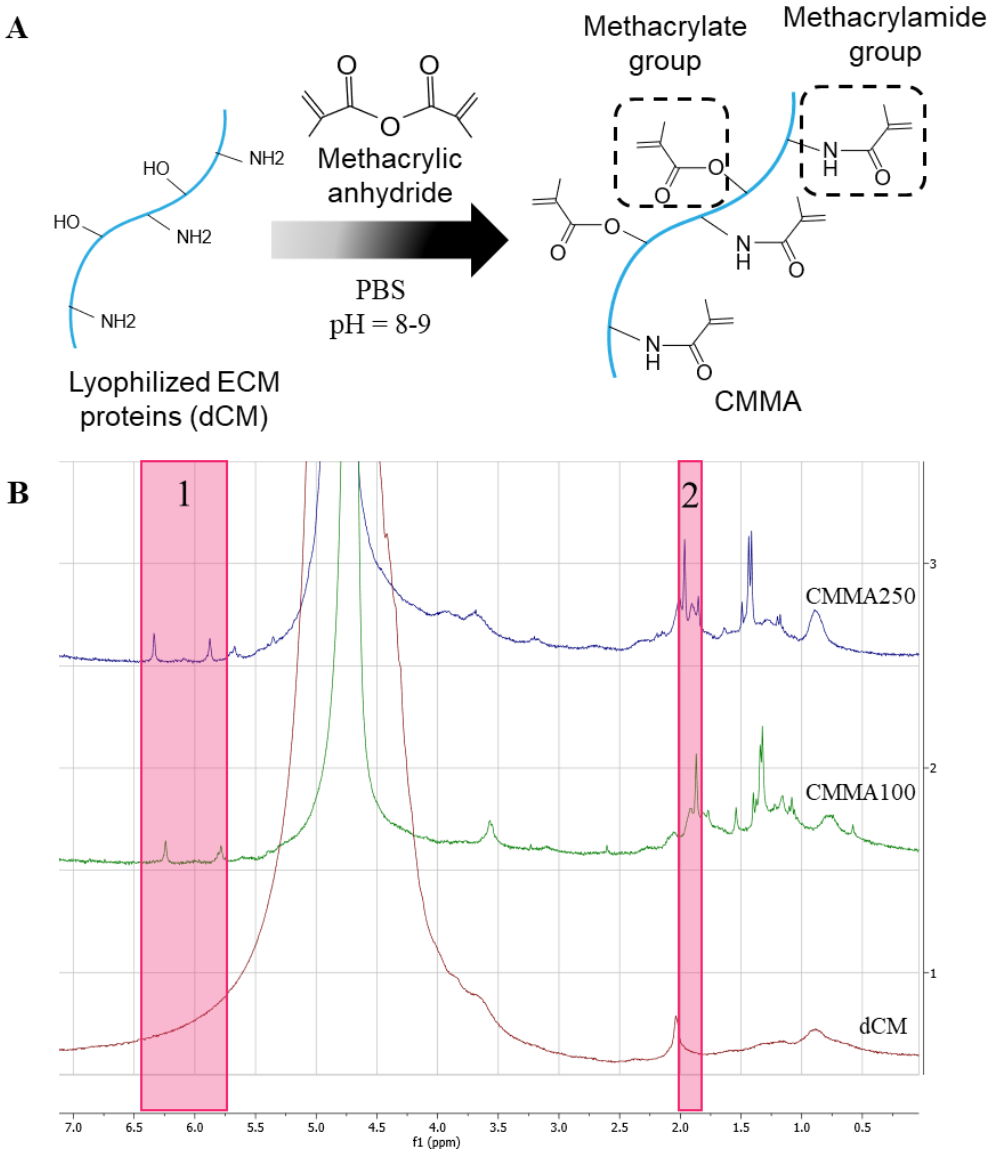

Figure IV.3. A) dCM modification and CMMA synthesis. B) ^{1}H NMR spectra of dCM, CMMA100, and CMMA250: 1) double-bound methacrylate and methacrylamide; and 2) CH_3 of methacrylate and methacrylamide groups.

TNBSA assay was also performed to estimate the degree of functionalization of amino groups in the dCM proteins. Results reveal a degree of amine functionalization of 59.5 ± 5.8 % and 66.5 ± 3.2 % for CMMA100 and CMMA250, was respectively. As expected, the volume of methacrylic anhydride added to CMMA250, increased the functionalization of the amines and, consequently, the degree of protein modification. However, for a more accurate evaluation of modification degree, and due to the complexity of the proteins in the samples, a posterior analysis by mass spectrometry will be performed.

3.3.Biochemical characterization of dCM and CMMA

As the ECM is mainly composed of proteins, proteoglycans, glycosaminoglycans and soluble factors, and each ECM component provides different functionalities to this complex network, the quantification of the major proteins and glycosaminoglycans in CMMA was performed [25,26] and compared to dCM. Total protein quantification was performed and some of the most abundant proteins in ECM were quantified (**Figure IV.4**) These proteins have fundamental functions at the structural level or in cell viability and proliferation.

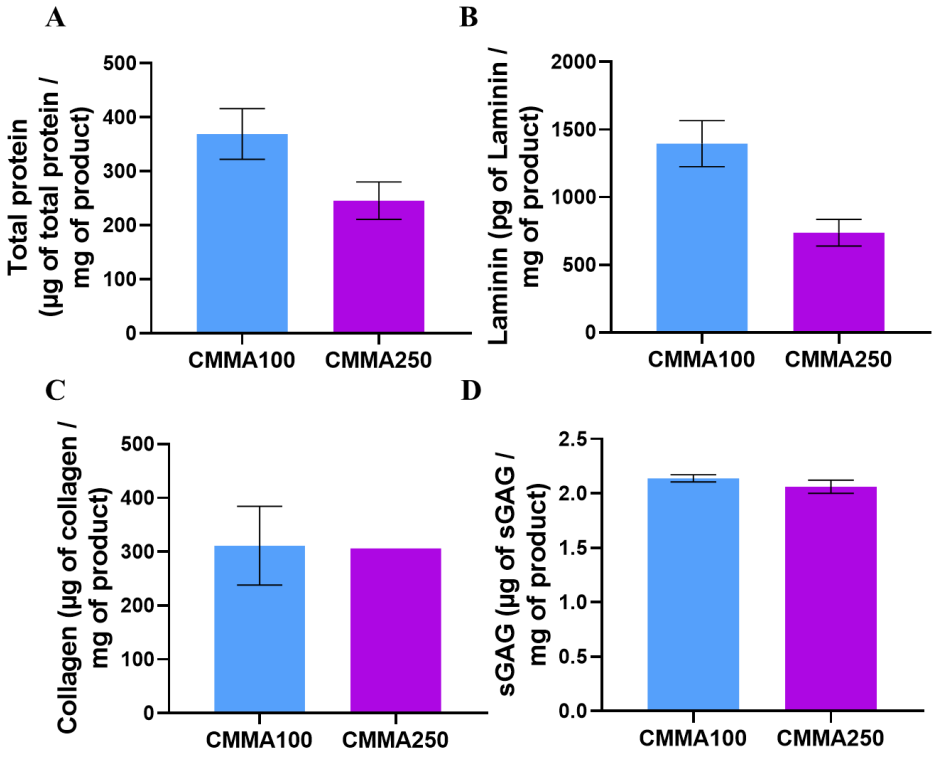

Figure IV.4: Biochemical characterization of processed CMMA from both modification degrees. A) Total protein quantification. B) Laminin quantification. C) Collagen quantification. D) Sulfated GAGs quantification.

3.3.1. Total protein quantification

Micro BCA assay was used for the total protein quantification. Results show a decrease from CMMA100 (369 ± 47 µg of proteins / mg of product) and CMMA250 (246 ± 35 µg of proteins / mg of product) (**Figure IV.4** A**)**. This decrease may be explained by the fact that this spectrophotometric assay is based on the reduction of Cu^{2+} in Cu^{+} by nitrogen atoms under alkaline conditions [27]. Since some amine groups of the proteins were modified, they are no longer available to bind to Cu^{2+} and allow reduction. The higher the degree of modification, the higher number of modified amines, and, therefore, the number of available nitrogen atoms to reduce copper, decreases.

3.3.2. Laminin quantification

Laminin is a structural basement membrane glycoprotein from ECM being the major non-collagenous component that is also present on the CM. It is essential in the morphogenesis process and interacts with cell surface receptors initiating intracellular signaling events that regulate cellular organization and differentiation [29]. The quantification of laminin (**Figure IV.4** B) demonstrates a decrease in this protein content in the higher degree of modification. This decrease could be explained by the chemical insertion of methacrylamide and methacrylate moieties in hydroxyl and amine groups from laminin, and consequent unrecognition by the antibodies used in this quantification. The ELISA kit utilized is specific for the subunits α1, β1 and γ1 from laminin. However, it is not possible to determine whether the chemical modification of this protein actually prevents it from being recognized by the antibodies and, consequently, from being quantified. The influence of methacrylation in the recognition of laminin may be performed by chemically modified pure laminin and analyze the effect using the same protocol for quantification.

3.3.3. Collagen quantification

Collagen is the most abundant protein in the ECM network. In the case of the CM, it has in its composition collagens type I, III, IV, V and VI. The collagen fibers provide principally tensile strength and elasticity, which, in turn, has a role in regulating cell adhesion, growth, proliferation, and differentiation [29,30]. The concentration of collagen, contrary to the laminin, increased after chemical modification (**Figure IV.4** C). In this quantification, all the samples were previously subjected to an ultrasonic treatment in order to homogenize the tissue. This step, in addition to dissolving the samples, also increase the yield of collagen extracted [31].

The quantification of CMMA100 and CMMA250 varied from 211 to 206 µg of collagen / mg of product, respectively, which is not a significant variation.

3.3.4. Sulphated GAGs quantification

Usually highly sulfated glycosaminoglycan (GAG) chains are coupled to core proteins to form proteoglycans. In fact, proteoglycans are structurally described as "filler" macromolecules from the ECM which adopt an amorphous structure. GAGs and proteoglycans are of huge importance since they are responsible for high water uptake, allowing the hydration of the ECM, due to their polar nature. Consequently, they are a supply of resistance to compressive forces, being partially a source of mechanical stability. Moreover, cell membrane-bound proteoglycans are responsible to binding collagen, fibronectin in the ECM and growth factors as well as having the role of protecting them from proteolysis or inhibiting factors [33,34]. In this quantification the dye 1,9-dimethylmethylene blue combines with repeating negative charges from sulphates on the GAGs resulting in the precipitation of the dye molecules and a shift in the absorption maximum [35]. Here, the concentration of sulphated GAGs has not significant variation, which means that methacrylation do not affect sulphate GAGs content (**Figure IV.4** D).

To a more accurate analysis for all the biochemical characterization, other characterization techniques, as for instance liquid chromatography and mass spectrometry, should be performed [28]. One way to understand the losses that occur in the chemical modification step due to handling and dialysis, would be to make a control with all the same steps, except the addition of methacrylic anhydride. This would allow a more reliable comparison.

3.4.Preparation of CMMA hydrogels

CMMA was subsequently processed into a photocrosslinkable hydrogel in the presence of a photoinitiator when irradiated with light. Compared with other stimuli (e.g., pH or temperature), a light stimulus is an interesting option as it can be easily controlled using defined power, times of crosslinking and distance from the light, in order to produce customized hydrogels. Furthermore, it is possible to produce hydrogels in mild conditions with very controlled shape and size [37–39]. In this work, CMMA derived hydrogels were polymerized very fast (20-40 seconds) using high-intensity light at 385-515 nm. **Figure IV.5.** A and B displays hydrogels prepared with low modification degree CMMA at two

concentrations and **Figure IV.5.** C-F displays hydrogels prepared high modified CMMA using concentrations from 0.25% until 2% (w/v). Although not represented here, it was possible to produce CMMA100 hydrogels with lower concentrations, as 0.25% and 0.5% (w/v) that were used in *in vitro* cell culture. The CMMA100 0.25% and 0.5% (w/v) photocrosslinking resulted in very soft hydrogels that were not able to withstand mechanical tests and are not here represented. The other hydrogels were characterized mechanically in terms of compression forces. Moreover, the water uptake and their biological response was also evaluated.

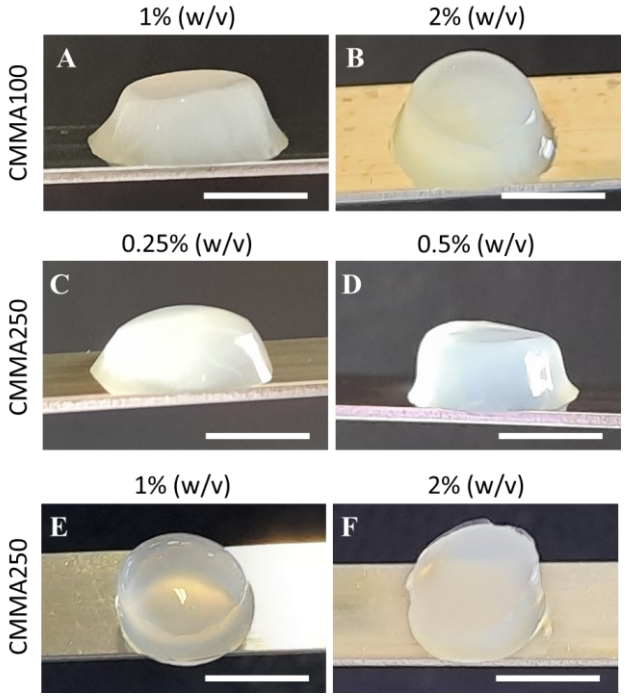

Figure IV.5. Hydrogels of CMMA. A) Low modification degree hydrogel with concentration of 1% (w/v) and B) Low modification degree hydrogel with concentration of 2% (w/v). High modification degree hydrogels with concentration of C) 0.25% (w/v), D) 0.5% (w/v), E) 1% (w/v) and F) 2% (w/v). Scale bar: 5 mm.

3.4.1. Characterization of CMMA hydrogels: mechanical properties and water content

Typically, ECM derived hydrogels are prepared by a process that combines decellularization of ECM, enzymatic solubilization and finally jellification at 37°C [20]. However, they have low mechanical properties, with values in the pascal range, while many human tissues are in the kPa range [40]. For example, human myocardium ECM has an elastic modulus between 10-20 kPa in the transverse direction (orthogonal to cardiomyocyte alignment) and 40-50 kPa in the longitudinal direction [41]. The **Figure IV.6** A, display the data obtained to the compressive mechanical tests.

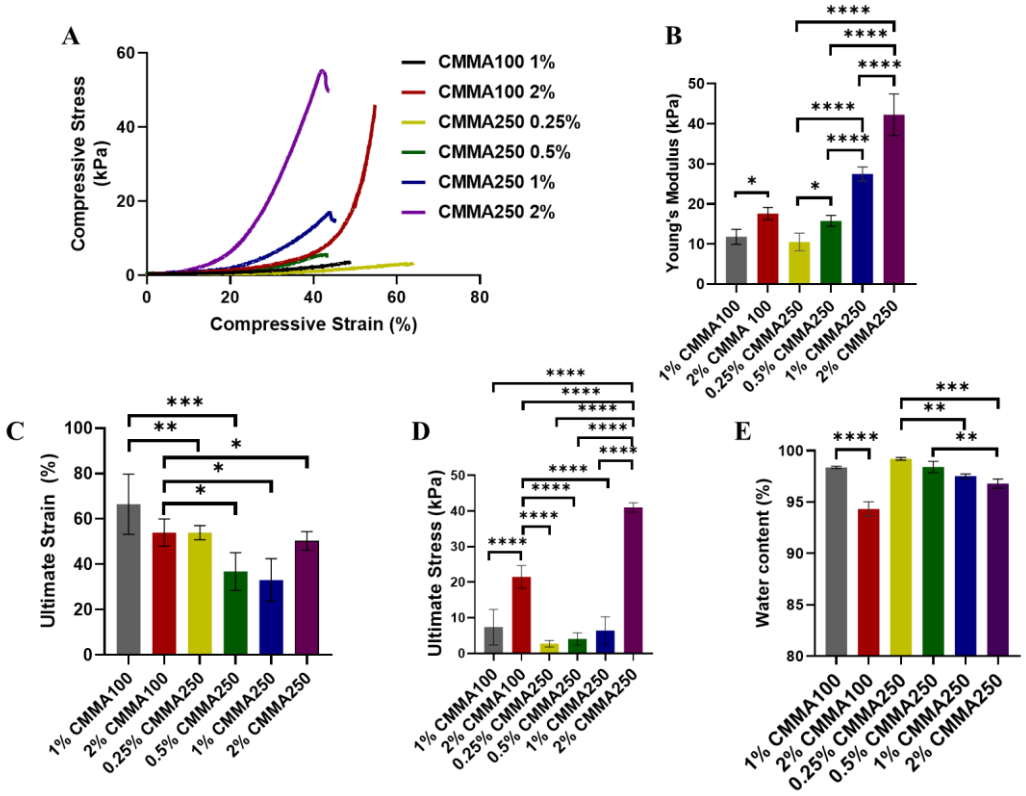

Figure IV.6. A) Representative compressive stress-strain curves, B) Young's modulus, C) ultimate strain, D) ultimate stress and E) water content obtained for CMMA100 and CMMA250 hydrogels.

The Young's modulus (**Figure IV.6** B) of all hydrogels were between 10-50 kPa, which proves that they have adequate stiffness to be used for the TE of multiple tissues (e.g., brain, heart, lung). It is also possible to verify that within each degree of modification, an increase in polymer concentration, is directly associated with an increase in the Young's modulus or, by other words, increases stiffness. Comparing the two degrees of modification, the hydrogels with the lowest degree of modification (CMMA100) but with the same concentration as the hydrogels of the highest degree, have the least Young's modulus. This would be expected, as the higher the degree of modification, the more covalent bonds are formed and stiffer the hydrogel will be. Other properties that can be determined through this mechanical test are the ultimate strain (**Figure IV.6** C) and ultimate stress (**Figure IV.6** D). It is possible to verify that more flexible hydrogels deform more, yet accumulate less energy, whereas stiffer hydrogels deform less, yet accumulate less energy. Except the ultimate strain of 2% CMMA250 hydrogel that is out of the expectable. The results of ultimate strain should be repeated for this concentration. The **Figure IV.6** E, demonstrate that all concentrations of both degrees of modification had water content superior to 90%. Moreover, it is possible

to verify a tendency to the amount of water retained in the polymeric network of the hydrogels decrease with the increase of their concentration.

3.5.Cell culture and hydrogels biological response

In this study, the biological properties of the CMMA hydrogels were tested using human bone marrow derived mesenchymal stem cells (hBM-MSCs). Cell viability using live/dead assay and cell morphology using DAPI/Phalloidin staining was performed after pre-determined time points up to 7 days in culture. hBM-MSCs cultured on the top of CMMA100 hydrogels clearly show that cells are able to adhere after 24h of culture and maintain their viability up to 7 days in culture (**Figure IV.7** A). Apparently, hBM-MSCs would prefer softer CMMA hydrogels and results in 0.25% (w/v) show high levels of cell proliferation. Nevertheless, for all the polymer concentrations, the cells are perfectly elongated and spread over the gels after 7 days of culture (**Figure IV.7** B).

CMMA250 hydrogels also show to support cell adhesion, proliferation and viability up to 7 days in culture (**Figure IV.8** A). Interestingly, in CMMA250 and contrary to the lower modified CM, apparently hBM-MSCs, proliferate better for higher polymer concentrations (1% w/v) (**Figure IV.8** B).

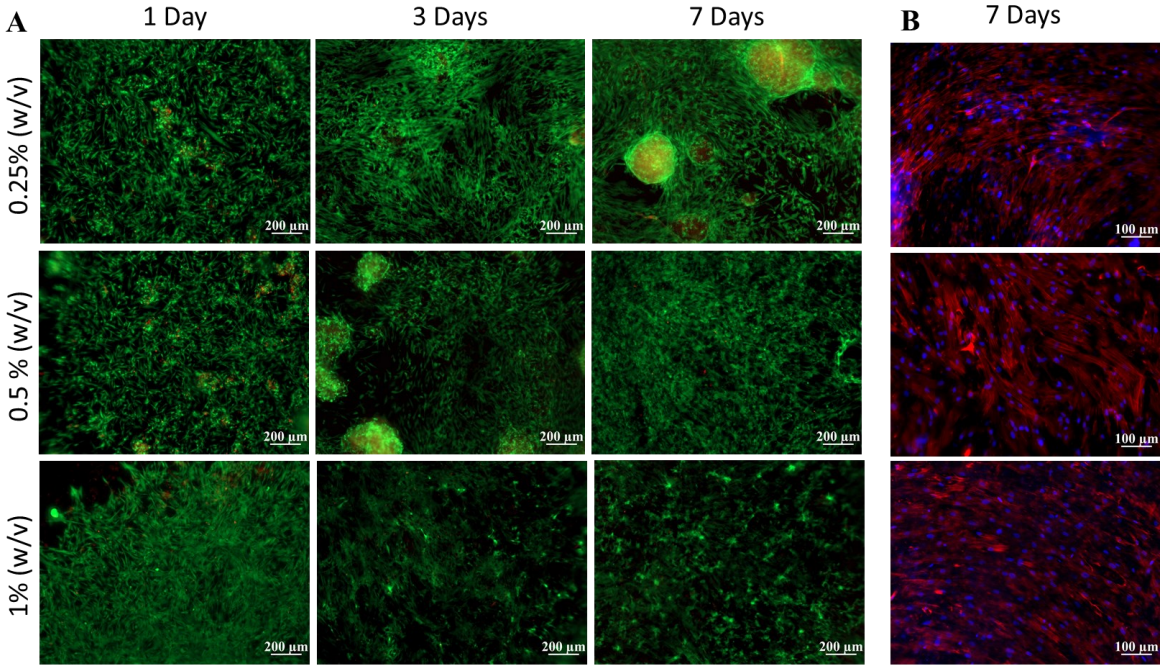

Figure IV.7. Top seeding of hBM-MSCs in CMMA100 hydrogels with 0.25% (w/v), 0.5% (w/v) and 1% (w/v) of concentration: A) Live-dead staining at 24 hours, 3 and 7 days of culture. B) DAPI / Phalloidin staining at 7 days.

When the cells are encapsulated within the 0.25% (w/v) and 0.5% (w/v) hydrogels, they show the capacity to spread and invade the gels, after 3 days of culture (**Figure IV.9** B). At day 7, cells are perfectly viable inside gel and invading the 3D network of CMMA matrix (**Figure IV.9** A). When the polymer concentration is increase to 1% (w/v), cells are not able to spread inside the gels, and after 3 days most of the cells are dead (data not shown). This may be explained by the highly compacted CMMA network that limits nutrient and oxygen diffusion, avoiding at the same time cell infiltration within the gels.

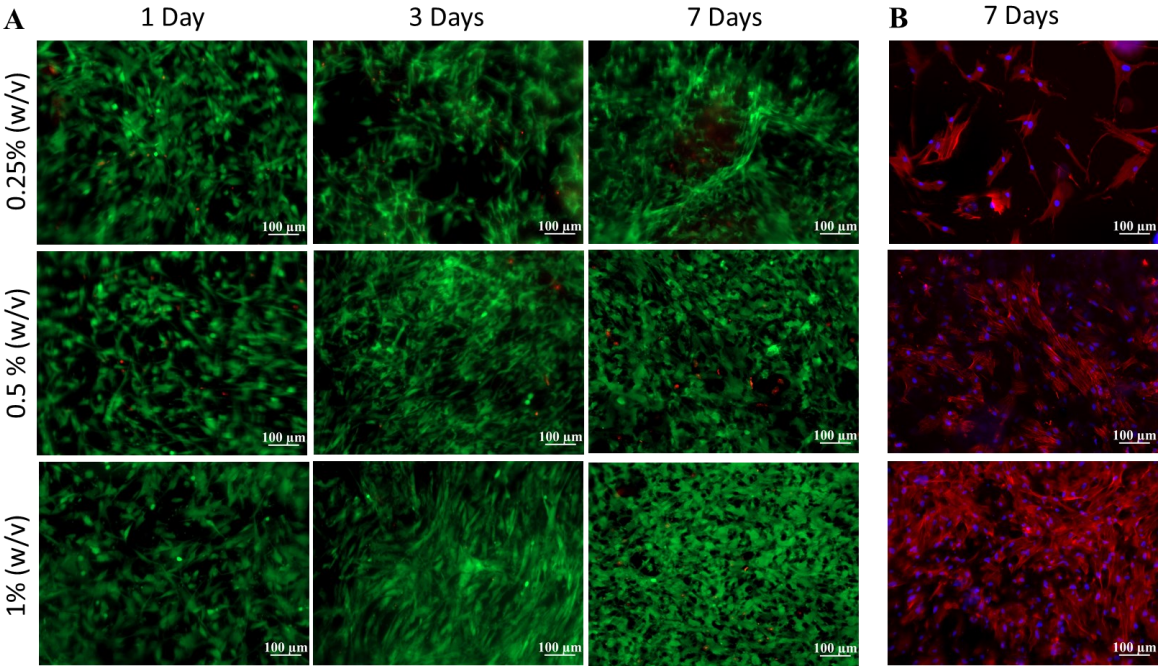

Figure IV.8. Top seeding of hBM-MSCs in 0.25% (w/v), 0.5% (w/v) and 1% (w/v) CMMA250 hydrogels: A) Live-dead staining at 24 hours, 3 and 7 days of culture. B) DAPI / Phalloidin staining at 7 days.

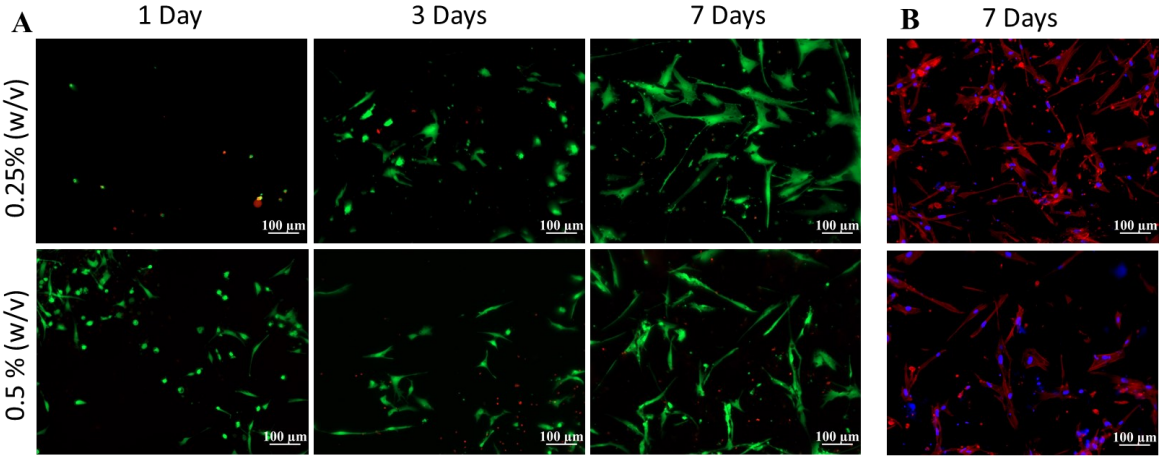

Figure IV.9. Encapsulation of hBM-MSCs in CMMA100 hydrogels with 0.25% (w/v) and 0.5% (w/v) of concentration: A) Live-dead staining at 24 hours, 3 and 7 days of culture. B) DAPI / Phalloidin staining at 7 days.

4. Conclusions and future perspectives

In this study, were produced CM prepolymers by the reaction of dCM with methacrylic anhydride using different volumes to produce two degrees of modification: a lower degree (CMMA100) and a higher degree of modification (CMMA250). By adding a photoinitiator to these prepolymers and in the presence of light with a specific wavelength it is possible to produce hydrogels with tunable mechanical properties. The quantifications of some of the most important ECM proteins allowed to verify their retention in the obtained material, however, for more reliable results and robust proteomic characterization, mass spectrometry analysis will be performed. The evaluation of the mechanical properties allowed to confirm that it was possible to produce robust hydrogels and whose properties vary with their concentration and which are in the range of most human tissue elastic modulus. In addition, the degree of modification also changes the physical properties such as the water absorption capacity. Moreover, it was possible to verify that both produced hydrogels allowed the culture of cells on the top, and, in the case of hydrogels produced from CMMA100, encapsulated cells also remained viable for at least 7 days. As future work, the cell proliferation should be evaluated quantitatively, quantifying as for instance metabolic activity of the cells and DNA increase during cell culture. In addition, the rheological properties of the CMMA solution will be evaluated. Nevertheless, the obtained results suggest that CMMA-based hydrogels have good potential to be used as 3D cell culture platforms. Due to the origin of the raw material (human source, free of charge, widely available) and its biochemical properties (ECM composition, highly vascularized) the hydrogels that herein studied for the first time may provide a good alternative for the currently used materials.

5. References

(1) Berthiaume, F.; Maguire, T. J.; Yarmush, M. L. Tissue Engineering and Regenerative Medicine: History, Progress, and Challenges. Annu. Rev. ofChemical Biomol. 2011, 2, 403–430. https://doi.org/10.1146/annurev-chembioeng-061010-114257.

(2) Faulk, D. M.; Johnson, S. A.; Zhang, L.; Badylak, S. F. Role of the Extracellular Matrix in Whole Organ Engineering. J. Cell. Physiol. 2014, 229 (8), 984–989.

(3) Hinderer, S.; Layland, S. L.; Schenke-Layland, K. ECM and ECM-like Materials—Biomaterials for Applications in Regenerative Medicine and Cancer Therapy. Adv. Drug Deliv. Rev. 2016, 97, 260–269.

(4) Gilbert, T. W.; Sellaro, T. L.; Badylak, S. F. Decellularization of Tissues and Organs. Biomaterials 2006, 27 (19), 3675–3683. https://doi.org/10.1016/j.biomaterials.2006.02.014.

(5) Deus, I. A.; Mano, J. F.; Custódio, C. A. Perinatal Tissues and Cells in Tissue Engineering and Regenerative Medicine. Acta Biomater. 2020, 110, 1–14.

(6) SABKLLA, N. Use of the Fetal Membranes in Skin Grafting. Med. Rec. 1913, 83 (11), 478.

(7) Suresh, D. K.; Gupta, A. Gingival Biotype Enhancement and Root Coverage Using Human Placental Chorion Membrane. Clin. Adv. Periodontics 2013, 3 (4), 237–242.

(8) Kothiwale, S. V. The Evaluation of Chorionic Membrane in Guided Tissue Regeneration for Periodontal Pocket Therapy: A Clinical and Radiographic Study. Cell Tissue Bank. 2014, 15 (1), 145–152.

(9) Esteves, J.; Bhat, K. M.; Thomas, B.; Varghese, J. M.; Jadhav, T. Efficacy of Human Chorion Membrane Allograft for Recession Coverage: A Case Series. J. Periodontol. 2015, 86 (8), 941–944.

(10) Hills, D. Evaluation of Demineralized Freeze-Dried Bone Allograft in Combination with Chorion Membrane in the Treatment of Grade II Furcation Defects: A Randomized Controlled Trial. Int. J. Periodontics Restor. Dent. 2019, 39, 659–667.

(11) Go, Y. Y.; Kim, S. E.; Cho, G. J.; Chae, S.-W.; Song, J.-J. Differential Effects of Amnion and Chorion Membrane Extracts on Osteoblast-like Cells Due to the Different Growth Factor Composition of the Extracts. PLoS One 2017, 12 (8), e0182716–e0182716.

(12) Mohr, S.; Portmann-Lanz, C. B.; Schoeberlein, A.; Sager, R.; Surbek, D. V. Generation of an Osteogenic Graft from Human Placenta and Placenta-Derived Mesenchymal Stem Cells. Reprod. Sci. 2010, 17 (11), 1006–1015.

(13) Ferreira, P.; Coelho, J. F. J.; Almeida, J. F.; Gil, M. H. Photocrosslinkable Polymers for Biomedical Applications. Biomed. Eng. Challenges 2011, 1, 55–74.

(14) Naahidi, S.; Jafari, M.; Logan, M.; Wang, Y.; Yuan, Y.; Bae, H.; Dixon, B.; Chen, P. Biocompatibility of Hydrogel-Based Scaffolds for Tissue Engineering Applications. Biotechnol. Adv. 2017, 35 (5), 530–544.

(15) Hoffman, A. S. Hydrogels for Biomedical Applications. Adv. Drug Deliv. Rev. 2012, 64, 18–23.

(16) Saldin, L. T.; Cramer, M. C.; Velankar, S. S.; White, L. J.; Badylak, S. F. Extracellular Matrix Hydrogels from Decellularized Tissues: Structure and Function. Acta Biomater. 2017, 49, 1–15.

(17) Handorf, A. M.; Zhou, Y.; Halanski, M. A.; Li, W.-J. Tissue Stiffness Dictates Development, Homeostasis, and Disease Progression. Organogenesis 2015, 11 (1), 1–15.

(18) Correia, C. R.; Santos, T. C.; Pirraco, R. P.; Cerqueira, M. T.; Marques, A. P.; Reis, R. L.; Mano, J. F. *In Vivo* Osteogenic Differentiation of Stem Cells inside Compartmentalized Capsules Loaded with Co-Cultured Endothelial Cells. Acta Biomater. 2017, 53, 483–494.

(19) Crapo, P. M.; Gilbert, T. W.; Badylak, S. F. An Overview of Tissue and Whole Organ Decellularization Processes. Biomaterials 2011, 32 (12), 3233–3243. https://doi.org/10.1016/j.biomaterials.2011.01.057.

(20) Ferreira, L. P.; Gaspar, V. M.; Mano, J. F. Decellularized Extracellular Matrix for Bioengineering Physiomimetic 3D *in vitro* Tumor Models. Trends Biotechnol. 2020, 38 (12), 1397–1414. https://doi.org/10.1016/j.tibtech.2020.04.006.

(21) Santos, S. C.; Custódio, C. A.; Mano, J. F. Photopolymerizable Platelet Lysate Hydrogels for Customizable 3D Cell Culture Platforms. Adv. Healthc. Mater. 2018, 7 (23), 1–12. https://doi.org/10.1002/adhm.201800849.

(22) Monteiro, C. F.; Santos, S. C.; Custódio, C. A.; Mano, J. F. Human Platelet Lysates-Based Hydrogels : A Novel Personalized 3D Platform for Spheroid Invasion Assessment. Adv. Sci. 2020, 7 (7), 1902398–1902411. https://doi.org/10.1002/advs.201902398.

(23) Ali, M.; Anil Kumar, P. R.; Yoo, J. J.; Zahran, F.; Atala, A.; Lee, S. J. A Photo-Crosslinkable Kidney ECM-Derived Bioink Accelerates Renal Tissue Formation. Adv. Healthc. Mater. 2019, 8 (7), 1–10. https://doi.org/10.1002/adhm.201800992.

(24) Visscher, D. O.; Lee, H.; van Zuijlen, P. P. M.; Helder, M. N.; Atala, A.; Yoo, J. J.; Lee, S. J. A Photo-Crosslinkable Cartilage-Derived Extracellular Matrix (ECM) Bioink for Auricular Cartilage Tissue Engineering. Acta Biomater. 2020. https://doi.org/https://doi.org/10.1016/j.actbio.2020.11.029.

(25) Hinderer, S.; Layland, S. L.; Schenke-Layland, K. ECM and ECM-like Materials - Biomaterials for Applications in Regenerative Medicine and Cancer Therapy. Adv. Drug Deliv. Rev. 2016, 97, 260–269. https://doi.org/10.1016/j.addr.2015.11.019.

(26) Hoshiba, T. Decellularized Extracellular Matrix for Cancer Research. Materials (Basel). 2019, 12 (8), 1311–1327.

(27) Scientific, T. F. Protein Assay Technical Handbook: Tools and Reagents for Improved Quantitation of Total or Specific Proteins; 2017.

(28) Karpievitch, Y. V; Polpitiya, A. D.; Anderson, G. A.; Smith, R. D.; Dabney, A. R. Liquid Chromatography Mass Spectrometry-Based Proteomics: Biological and Technological Aspects. Ann. Appl. Stat. 2010, 4 (4), 1797.

(29) D'Lima, C.; Samant, U.; Gajiwala, A. L.; Puri, A. Human Chorionic Membrane: A Novel and Efficient Alternative to Conventional Collagen Membrane. Trends Biomater. Artif. Organs 2020, 34 (1), 33–37.

(30) Klimek, K.; Ginalska, G. Proteins and Peptides as Important Modifiers of the Polymer Scaffolds for Tissue Engineering Applications—A Review. Polymers (Basel). 2020, 12 (4), 844–882.

(31) Kyung, H.; Young, K.; Kim, H. Effects of Ultrasonic Treatment on Collagen Extraction from Skins of the Sea Bass Lateolabrax Japonicus. Food Sci. Technol. 2012, 78, 485–490. https://doi.org/10.1007/s12562-012-0472-x.

(32) Zhu, M.; Wang, Y.; Ferracci, G.; Zheng, J.; Cho, N.-J.; Lee, B. H. Gelatin Methacryloyl and Its Hydrogels with an Exceptional Degree of Controllability and Batch-to-Batch Consistency. Sci. Rep. 2019, 9 (1), 1–13.

(33) Neves, M. I.; Araújo, M.; Moroni, L.; da Silva, R. M. P.; Barrias, C. C. Glycosaminoglycan-Inspired Biomaterials for the Development of Bioactive Hydrogel Networks. Molecules 2020, 25 (4), 978–1017.

(34) Han, W. M.; Jang, Y. C.; García, A. J. The Extracellular Matrix and Cell–Biomaterial Interactions. Biomaterials Science. 2020, pp 701–715. https://doi.org/10.1016/b978-0-12-816137-1.00045-3.

(35) Mort, J. S.; Roughley, P. J. Measurement of Glycosaminoglycan Release from Cartilage Explants. In Arthritis Research; Springer, 2007; pp 201–209.

(36) Lim, J. J.; Hammoudi, T. M.; Bratt-Leal, A. M.; Hamilton, S. K.; Kepple, K. L.; Bloodworth, N. C.; McDevitt, T. C.; Temenoff, S. J. Development of Nano-and Microscale Chondroitin Sulfate Particles for Controlled Growth Factor Delivery. Acta Biomater. 2012, 7 (3), 986–995. https://doi.org/10.1016/j.actbio.2010.10.009.Development.

(37) Choi, J. R.; Yong, K. W.; Choi, J. Y.; Cowie, A. C. Recent Advances in Photo-Crosslinkable Hydrogels for Biomedical Applications. Biotechniques 2019, 66 (1), 40–53.

(38) Ferreira, P.; Coelho, J. F. J.; Almeida, J. F.; Gil, M. H. Photocrosslinkable Polymers for Biomedical Applications. In Biomedical Engineering-Frontiers and Challenges; InTech, 2011; Vol. 1, pp 55–74.

(39) Custódio, C. A.; Reis, R. L.; Mano, J. F. Photo-Cross-Linked Laminarin-Based Hydrogels for Biomedical Applications. Biomacromolecules 2016, 17 (5), 1602–1609.

(40) Giobbe, G. G.; Crowley, C.; Luni, C.; Campinoti, S.; Khedr, M.; Kretzschmar, K.; Santis, M. M. De; Zambaiti, E.; Michielin, F.; Meran, L.; et al. Extracellular Matrix Hydrogel Derived from Decellularized Tissues Enables Endodermal Organoid Culture. Nat. Commun. 2019, 10 (1), 1–14. https://doi.org/10.1038/s41467-019-13605-4.

(41) Morrissette-mcalmon, J.; Ginn, B.; Somers, S.; Fukunishi, T.; Thanitcul, C.; Rindone, A.; Hibino, N.; Tung, L. Biomimetic Model of Contractile Cardiac Tissue with Endothelial Networks Stabilized by Adipose- Derived Stromal / Stem Cells. Sci. Rep. 2020, 10 (1), 1–12. https://doi.org/10.1038/s41598-020-65064-3.

(42) Naahidi, S.; Jafari, M.; Logan, M.; Wang, Y.; Yuan, Y.; Bae, H.; Dixon, B.; Chen, P. Biocompatibility of Hydrogel-Based Scaffolds for Tissue Engineering Applications. Biotechnol. Adv. 2017, 35 (5), 530–544. https://doi.org/10.1016/j.biotechadv.2017.05.006.

Chapter V

Conclusions and Future Perspectives

Conclusion and Future Perspectives

The aim of this thesis was to design and produce for the first time a CM-based hydrogel for 3D cell culture of human cells and TE. Due to the inherent properties of the CM ECM, rich in collagen and laminin and highly vascularized, conferring angiogenic properties, the proof of concept for validating these hydrogels will be performed for cardiac cell culture.

CM prepolymers were successfully produced by the reaction of dCM with methacrylic anhydride using different volumes to produce two degrees of modification: a lower degree (CMMA100) and a higher degree of modification (CMMA250). The quantification of DNA confirmed that the decellularization process was efficient and the quantifications of some of the most important ECM proteins allowed to verify their retention in the obtained material, nonetheless, for more reliable results and robust proteomic characterization, mass spectrometry analysis will be performed. By adding a photoinitiator to the synthesized prepolymers and in the presence of light with a specific wavelength it was possible to produce hydrogels with tunable mechanical properties. The evaluation of the mechanical properties allowed to confirm that it was possible to produce robust hydrogels and whose properties vary with their concentration and which are in the range of most human tissue elastic modulus. Moreover, it was possible to verify that the produced hydrogels allowed the culture of human cells, that remain viable and proliferate for at least 7 days.

As future work, DNA quantification and metabolic activity will be assessed for the cells cultured in CM derived hydrogels. The rheological properties of the CMMA prepolymer under a source of light will be evaluated. Finally, the culture of cardiomyocytes and endothelial cells will be performed.

Nevertheless, for the best of our knowledge, this is the first study that produced a robust tunable CM-derived hydrogel which may have several advantages due to the origin of the raw material (human source, free of charge, widely available) and its biochemical properties (ECM composition, highly vascularized) may provide a good alternative for the currently used materials.